TRW NO. 14671-6008-R0-00

Get DRA

the applications of satellites to

COMMUNICATIONS, NAVIGATION AND SURVEILLANCE

For Aircraft Operating Over the Contiguous United States

VOLUME II - APPENDICES

MALLINCKRODT, MILLER, EASLEY, CLARK, HARTE, WONG, ET AL.

DECEMBER 1970

NATIONAL AERONAUTICS AND SPACE ADMINISTRATION
GODDARD SPACE FLIGHT CENTER

Prepared Under Contract NAS 5-21535 by

TRW SYSTEMS GROUP

ONE SPACE PARK • REDONDO BEACH CALIFORNIA 90278

TRW NO. 14671-6008-R0-00

the applications of satellites to

COMMUNICATIONS, NAVIGATION AND SURVEILLANCE

For Aircraft Operating Over the Contiguous United States

VOLUME II - APPENDICES

MALLINCKRODT, MILLER, EASLEY, CLARK, HARTE, WONG, ET AL.

DECEMBER 1970

NATIONAL AERONAUTICS AND SPACE ADMINISTRATION
GODDARD SPACE FLIGHT CENTER

Prepared Under Contract NAS 5-21535 by

ONE SPACE PARK • REDONDO BEACH CALIFORNIA 90278

This report has been reviewed and approved:

J. H. Craigie
Principal Investigator

D. D. Otten
Advanced Systems Manager
Navigation/Control Satellites

ACKNOWLEDGEMENT

This study has been an extensive team effort. While numerous technical personnel made contributions to the study, the following TRW Systems people made significant contributions to this volume:

Appendix A - I. Zipper, R. R. Valleni
Appendix B - J. H. Craigie
Appendix C - R. R. Valleni
Appendix D - G. E. Clark, R. J. Harte
Appendix E - A. J. Mallinckrodt
Appendix F - C. S. Miller
Appendix G - A. J. Mallinckrodt
Appendix H - J. Wokurka
Appendix I - A. Garabedian, C. S. Miller
Appendix J - C. S. Easley
Appendix K - G. G. Wong
Appendix L - North American Rockwell
Appendix M - D. D. Morrison

In addition, valuable technical information was obtained during this study through discussions with the National Aeronautics and Space Administration, the Department of Transportation, the Federal Aviation Administration, the National Transportation Safety Board, the Air Transport Association, Aeronautical Radio Incorporated, the MITRE Corporation, Aerospace Corporation, North American Rockwell Corporation, the Aircraft Owners and Pilots Association, the Airline Pilots Association, and a number of U. S. air carriers. In addition, we gratefully acknowledge the significant contribution made by NARCO, King Radio, Bendix Avionics, Collins Radio, and Wilcox to the LIT pricing effort. Finally, a special acknowledgement is given for the assistance provided by the DOT/Transportation Systems Center who, as the NASA Electronics Research Center, initiated this study and to those individuals at Goddard Space Flight Center who assumed responsibility for and an interest in this study.

CONTENTS

APPENDIX A
FUTURE ATC LOADS

1. MEASURES OF ATC WORKLOAD

The workload on FAA air traffic controllers and facilities is generally given in terms of aircraft activity (Ref. A-1), which includes the following factors:

1. Number of flights
2. Number of operations
3. Number of hours flown
4. Nature of flight
   a. Itinerant
   b. Local
   c. VFR
   d. IFR
5. Time distribution of flights
6. Area distribution of flights

The accumulation of activity statistics on the first four items above permits the determination of activity relationships among these factors and between these and other factors, such as average numbers of operations per itinerant flight and average annual hours flown per (type of) aircraft.

Statistics for Items 5 and 6 above are used to determine total peak activity and peak instantaneous density of aircraft. The former, of course, has implications regarding the total required capacity of the ATC system and the latter relates to the capacity of a localized portion of the airspace and the local facilities.

Additional factors affecting the ATC load* are those which influence the complexity of the control procedures. Such factors are:

1. Types of aircraft
   a. Speed
   b. Optimum altitude
2. Aircraft Communication and Navigation Equipment
3. Pilot Experience

*Other than the available ground facilities themselves. However, projections of required ATC services are generally based upon "unconstrained" growth of activity.

An independent extrapolation of the future aircraft fleet and their activities is far beyond the scope of this study. Consequently, this appendix will describe some of the more prominent forecasting methods and the results given in other studies.

2. EXTRAPOLATION METHODS

Extrapolation of future activity starts first with the projection of numbers and types of aircraft. Then by the application of the above factors and their relationships, which may also be projected in a rational way, the future air traffic activities and their associated ATC loads can be predicted.

For obvious reasons a great deal of effort goes into the extrapolation of the (required) future (domestic) anticipated air carrier fleet size. This is a function of the number of passenger-miles traveling between major city-pairs in the U. S. The task is facilitated somewhat because of the amount of detailed statistics concerning air carrier activities and passenger behavior patterns which are collected on a continuing basis. Relationships between these factors and socio-economic conditions are established with the aid of survey data and these relationships are used in the extrapolation process.

Some of the methods used in predicting the future on carrier fleet are described in a prominant study (Ref. A-2) performed by Lockheed in 1965. A brief summary of the methods is given at the end of this Appendix. Similar studies are performed by the FAA (Ref. A-3). The principal technological assumptions made by the FAA are those which foresee no new scientific innovations which will seriously influence evolutionary growth and no constraint on aviation demand with specific anticipated improvements in the present system. With respect to air carrier fleet forecasts, FAA methodology is not described in so great detail as in Ref. A-2. However, the basic principal appears to be one of extrapolating total revenue and revenue yield per passenger mile based upon historical revenue vs. Gross National Product (GNP) trends, taking into account future fleet structure, performance and costs obtained from aircraft manufacturers.

It is of interest to see how the FAA forecast compared with the one made by Lockheed four years earlier. The comparison is shown in Table A-1 and it can be seen that a disparity of approximately 60 percent (relative to the earlier forecast) exists for the year 1980. Both results were obtained from a

Table A-1. Comparison of Domestic Air Carrier Travel Forecasts

Year	Billions of Passenger-Miles (Ref. A-2)	Billions of Passenger-Miles (Ref. A-5)
1964		41.3*
1965	51.5*	
1969		91.9*
1970	90	
1975	135	167
1980	185	295
1985	250	
1990		

*Actual.

relatively good (air carrier) data base and consistent projections of GNP and average trip length.

Projections of the general aviation aircraft fleet are more difficult due to the less disciplined data collection process. This situation is being rectified with the recent institution of more extensive collection of general aviation statistics by the FAA. This will undoubtedly produce higher confidence predictions in the near future; however, it is not surprising to find evidence in present predictions for general aviation (Ref. G-4, Appendix G1) that differ by as much as 70 percent for the year 1995.

With respect to military aircraft, it was not possible to obtain sufficient information regarding military planning to estimate the future fleet size. Consequently there is no questioning the assumption that this fleet will remain approximately constant through 1995.

Analysis performed by the FAA forecast the aircraft fleet size for air carrier, general aviation and military flying (Refs. A-4 and A-6). Even more importantly, these quantities are converted to the more usable parameters described earlier for the purpose of estimating loads on the National Airspace System. The projected aircraft fleet is first converted to annual flying hours. The conversion factor, in this case the average annual flying hours per aircraft (type), is derived from historical records which are appropriately modifi to reflect anticipated change (e.g., the annual average aircraft usage for general aviation as a whole is expected to increase from 201 hours in 1968 to 262 hours in 1995). After the hours are distributed between itinerant and local flying, they are converted to number of flights and operations, again using projected historical relationships of average hours per flight and operatio per flight. Numerous sources of data and surveys conducted by the FAA are used to establish factors which relate the peak airborne aircraft count to the average annual hours flown (for the various types of aircraft). Table A-2, A-3 and A-4 indicate the activity factors described above for the years 1968, 1980 and 1995.

Table A-2. 1968 Air Traffic Activity for Continental U.S. (Ref. A-4)

User class and aircraft type	Active fleet size (as of Jan 1)	Annual utilization (Hours)	Annual flying hours (thousands)			Annual flights (thousands)			Annual operations (thousands) [2]			Peak airborne aircraft count		
			Itinerant	Local	Total	Itinerant	Local	Total	Itinerant	Local	Total	Itinerant	Local	Total
Air carrier [1]														
Jet	1344	3230	4253	87	4340	2650	87	2737	5300	520	5820	870	.....	870
2- and 3-engine	638	2770	1735	35	1770	1670	35	1705	3340	210	3550	350	.....	350
4-engine	706	3640	2518	52	2570	980	52	1032	1960	310	2270	520	.....	520
Turbo-prop	444	2270	990	20	1010	1340	20	1360	2680	120	2800	200	.....	200
1- and 2-engine	248	2300	559	11	570	1020	11	1031	2040	70	2110	110	.....	110
4-engine	196	2240	431	9	440	320	9	329	640	50	690	90	.....	90
Piston	642	1360	853	17	870	1000	17	1017	2000	100	2100	170	.....	170
1- and 2-engine	377	1350	500	10	510	780	10	790	1560	60	1620	100	.....	100
4-engine	265	1360	353	7	360	220	7	227	440	40	480	70	.....	70
Helicopter	22	1400	29	1	30	170	1	171	340	10	350	10	.....	10
Total air carrier	2452	2550	6125	125	6250	5160	125	5285	10,320	750	11,070	1250	.....	1250
General aviation														
Turbine	1281	445	540	30	570	450	40	490	900	240	1140	190	10	200
Piston	109,910	197	16,190	5510	21,700	15,440	7420	22,860	30,880	44,520	75,400	5830	1820	7650
Multi-engine	13,439	269	3250	360	3610	2500	600	3100	5000	3800	8800	1170	120	1290
Single-engine	96,471	188	12,940	5150	18,090	12,940	6820	19,760	25,880	40,920	66,800	4660	1700	6360
1-3 place	39,675	193	4600	3060	7660	4600	3830	8430	9200	22,980	32,180	1650	1010	2670
4 place or more	56,796	184	8340	2090	10,430	8340	2990	11,330	16,680	17,940	34,620	3000	690	3690
Rotorcraft	1899	295	220	340	560	310	1130	1440	620	6780	7400	80	110	190
Other [3]	1096	64	.....	70	70	.....	140	140	.....	280	280	.....	20	20
Total general aviation	114,186	201	16,950	5950	22,900	16,200	8730	24,930	32,400	51,820	84,220	6100	1960	8060
Military														
Jet	9000	470	2115	2115	4230	1060	1410	2470	2120	11,280	13,400	680	890	1570
Turbo-prop	1000	500	350	150	500	140	75	215	280	600	380	110	60	170
Piston	5000	615	1860	1215	3075	930	810	1740	1860	6480	8340	590	510	1100
Single engine	2000	450	225	675	900	110	450	560	220	3600	3820	70	280	350
Multi-engine	3000	725	1635	540	2175	820	360	1180	1640	2880	4520	520	230	750
Helicopter	5000	325	160	1465	1625	100	980	1080	200	9800	10,000	50	620	670
Total military	20,000	470	4485	4945	9430	2230	3275	5505	4460	28,160	32,620	1430	2080	3510
All users														
Turbine	13,069	815	8248	2402	10,650	5640	1632	7272	11,280	12,760	24,040	2050	960	3010
Piston	115,552	222	18,903	6742	25,645	17,370	8247	25,617	34,740	51,500	85,840	6590	2330	8920
Rotorcraft	6921	320	409	1806	2215	680	2111	2691	1160	16,590	17,750	140	730	870
Other	1096	64	.....	70	70	.....	140	140	.....	280	280	.....	20	20
Total	136,638	282	27,560	11,020	38,580	23,590	12,130	35,720	47,180	80,730	127,910	8780	4040	12,820

[1] Includes aircraft and flying hours for both the domestic and the international/territorial U.S air carrier fleets Air carrier flying hours include 4 percent non-revenue hours.
[2] Based on two operations per itinerant flight, an average of six operations per civil aircraft local flight; eight operations per military fixed wing local flight, and 10 operations per military helicopter local flight
[3] The "other" category includes gliders (primarily), balloons and blimps Operationsestimated at two per flight

Table A-3. 1980 Air Traffic Activity for Continental U.S. (Ref. A-4)

User class and aircraft type	Active fleet size (as of Jan. 1)	Annual utilization (Hours)	Annual flying hours (thousands)			Annual flights (thousands)			Annual operations (thousands) [4]			Peak airborne aircraft count		
			Itinerant	Local	Total	Itinerant	Local	Total	Itinerant	Local	Total	Itinerant	Local	Total
Air carrier [1]														
Jet	3316	2940	9565	195	9760	8453	195	8648	16,906	1170	18,076	1950	.....	1950
2- and 3-engine	2574	2880	7260	150	7410	7260	150	7410	14,520	900	15,420	1480	.....	1480
4-engine	666	3150	2060	40	2100	1030	40	1070	2060	240	2300	420	.....	420
SST [2]	76	3300	245	5	250	163	5	168	326	30	356	50	.....	50
Turboprop	196	2500	480	10	490	914	10	924	1828	60	1888	100	.....	100
1- and 2-engine	176	2500	441	9	450	882	9	891	1764	54	1818	90	.....	90
4-engine	20	2000	39	1	40	32	1	33	64	6	70	10	.....	10
Piston	40	1000	39	1	40	65	1	66	130	6	136	10	.....	10
1- and 2-engine	30	1000	29	1	30	58	1	59	116	6	122	10	.....	10
4-engine	10	1000	10	..	10	7	.....	7	14	.....	14	.....	.....	.....
Rotorcraft	48	1450	69	1	70	345	1	346	690	6	696	15	.....	15
Total air carrier	3600	2880	10,153	207	10,360	9777	207	9984	19,554	1242	20,796	2075	.....	2075
General aviation														
Turbine	7800	500	3705	195	3900	3090	280	3370	6180	1680	7860	1330	60	1390
Piston	199,650	210	32,850	9050	41,900	30,920	12,580	43,500	61,840	75,480	137,320	11,830	2990	14,820
Multi-engine	26,650	350	8370	930	9300	6440	1550	7990	12,880	9300	22,180	3020	310	3330
Single-engine	173,000	190	24,480	8120	32,600	24,480	11,030	35,510	48,960	66,180	115,140	8810	2680	11,490
1-3 place	50,000	160	4800	3200	8000	4800	4000	8800	9600	24,000	33,600	1730	1060	2790
4 place or more	123,000	200	19,680	4920	24,600	19,680	7030	26,710	39,360	42,180	81,540	7060	1620	8700
Rotorcraft	4900	330	640	960	1600	910	3200	4110	1820	19,200	21,020	230	320	550
Other [3]	1750	100	.....	200	200	.....	400	400	.....	800	800	.....	70	70
Total general aviation	214,000	220	37,195	10,405	47,600	34,920	16,460	51,380	69,840	97,160	167,000	13,390	3440	16,830
Military														
Turbine	10,000	480	2400	2400	4800	1200	1600	2800	2400	12,800	15,200	770	1010	1780
Piston	2000	600	720	480	1200	360	320	680	720	2560	3280	230	200	430
Rotorcraft	8000	325	260	2340	2600	170	1560	1730	340	15,600	15,940	80	980	1060
Total military	20,000	430	3380	5220	8600	1730	3480	5210	3460	30,960	34,420	1080	2190	3270
All users														
Turbine	21,312	890	16,150	2800	18,950	13,657	2085	15,742	27,314	15,710	43,024	4150	1070	5220
Piston	201,890	210	33,609	9531	43,140	31,345	12,901	44,246	62,690	78,046	140,736	12,070	3190	15,260
Rotorcraft	12,848	330	969	3301	4270	1425	4761	6186	2850	34,806	37,656	325	1300	1625
Other	1750	100	.....	200	200	.....	400	400	.....	800	800	.....	70	70
Total all users	237,600	280	50,728	15,832	66,560	46,427	20,147	66,574	92,854	129,362	222,216	16,545	5630	22,175

[1] Includes aircraft and flying hours for both the domestic and the international/territorial U S air carrier fleets Air carrier flying hours include 4 percent non-revenue hours
[2] SST aircraft are assumed to fly at subsonic speeds over populated land areas (CONUS).
[3] The "other" category includes gliders (primarily), balloons and blimps. Operations estimated at two per flight
[4] Based on two operations per itinerant flight; an average of six operations per civil aircraft local flight, eight operations for military fixed wing local flight; and 10 operations per military rotorcraft flight

Table A-4. 1995 Air Traffic Activity for Continental U. S. (Ref. A-4)

User class and aircraft type	Active fleet size (as of Jan. 1)	Annual utilization (Hours)	Annual flying hours (thousands)			Annual flights (thousands)			Annual operations (thousands)[3]			Peak airborne aircraft count		
			Itinerant	Local	Total	Itinerant	Local	Total	Itinerant	Local	Total	Itinerant	Local	Total
Air carrier [1]:														
Long-haul type	3000	3600	10,580	220	10,800	3530	220	3750	7060	1320	8380	2200	-------	2200
Medium-haul type	3000	3300	9700	200	9900	6470	200	6670	12,940	1200	14,140	2000	-------	2000
Short-haul type	700	3000	2060	40	2100	4120	40	4160	8240	240	8480	400	-------	400
Total air carrier	6700	3400	22,340	460	22,800	14,120	460	14,580	28,240	2760	31,000	4600	-------	4600
General aviation:														
Turbine	70,000	500	33,250	1750	35,000	27,700	2500	30,200	55,400	15,000	70,400	12,000	600	12,600
Piston	415,000	218	66,850	23,650	90,500	63,200	30,300	93,500	126,400	181,800	308,200	24,100	7800	31,900
Multi-engine	50,000	350	15,750	1750	17,500	12,100	2900	15,000	24,200	17,400	41,600	5700	600	6300
Single-engine [2]	365,000	200	51,100	21,900	73,000	51,100	27,400	78,500	102,200	164,400	266,600	18,400	7200	25,600
VTOL	15,000	350	2100	3150	5250	3000	10,500	13,500	6000	63,000	69,000	800	1000	1800
Total general aviation	500,000	262	102,200	28,550	103,750	93,900	43,300	137,200	187,800	259,800	447,600	36,900	9400	46,300
Military														
Turbine	10,000	500	2500	2500	5000	1250	1670	2920	2500	13,360	15,860	800	1100	1900
V/STOL	10,000	400	400	3600	4000	270	2400	2670	540	24,000	24,540	100	1500	1600
Total military	20,000	450	2900	6100	9000	1520	4070	5590	3040	37,360	40,400	900	2600	3500
All users:														
Turbine	86,700	724	58,090	4710	62,800	43,070	4630	47,700	86,140	31,120	117,260	17,400	1700	19,100
Piston	415,000	218	66,850	23,650	90,500	63,200	30,300	93,500	126,400	181,800	308,200	24,100	7800	31,900
VTOL	25,000	370	2500	6750	9250	3270	12,900	16,170	6540	87,000	93,540	900	2500	3400
Total all users	526,700	309	127,440	35,110	162,550	109,540	47,830	157,370	219,080	299,920	519,000	42,400	12,000	54,400

[1] Includes aircraft and flying hours for both the domestic and the international/territorial U S. air carrier fleets, Air carrier aircraft types categorized as (1) designed primarily for short haul, up to 500 miles; (2) medium haul, 500 to 1500 miles; or (3) long haul, over 1500 miles. Air carrier flying hours include 4 percent non-revenue hours.

[2] Includes an estimated 3,000 "other" aircraft (gliders, blimps and balloons).

[3] Based on two operations per itinerant flight; and average of six operations per civil aircraft local flight; eight operations per military fixed wing aircraft local flight; and ten operations for military V/STOL local flight.

The ATC services rendered to IFR flights are much more extensive than those afforded VFR flights. The total future load will then depend upon the regulatory changes which may bring large numbers of VFR flights under positive control. Disregarding such changes, future IFR activity may be estimated using the assumptions given in Table A-5.

Table A-5. Assumed IFR Activities in 1995 (Ref. A-6)

User Category	Percent IFR	
	Itinerant	Local
Air Carrier	100	0
General Aviation		
Multiengine Piston	60	0
Single Engine Piston	5	0
Military	100	50*

* Jet types only.

Applying these percentages to the annual operations and peak airborne aircraft count in Table A-4 gives the IFR activity for 1995 as shown in Table A-6.

Table A-6. 1995 IFR Air Traffic Activity for Continental U. S.

User Category	IFR Operations (Millions)	Peak Airborne IFR Aircraft Count (Thousands)
Air Carrier	28.2	4.6
General Aviation	75	16.2
Military	9.2	1.3
Total	112.4	22.1*

*This peak IFR load, which is in approximate agreement with that shown in Table 3-5, should not be construed as the total load on the ATC system. In an environment involving some form of IPC the total load must also include the peak instantaneous count of VFR traffic.

The analysis of future air carrier aircraft requirements performed by Lockheed in 1965 is described below. Three different approaches, termed the market analysis method, the city analysis method, and the gross national product method were used. A measure of confidence in the three methods was established by cross checking the results with correlation and linear programming methods. In these forecasting techniques as well as in others performed by various organizations, certain basic assumptions, such as the absence of a major war or major recession are made explicit in order to keep the process simple. One can speculate on many other influential factors such as population control or technological advances in competitive transportation modes which would have a significant effect on future air travel, but, for the purpose of this study, to expand on such speculation would only complicate an already difficult forecasting process.

The market analysis method utilizes basic forecast data of population growth, labor force and industry make-up, unemployment rate, GNP, productivity and family income. The basic steps in converting these to forecast air travel is as follows:

a. The U.S. population at a particular time is divided into socio-economic groups for personal and business travel. Distinguishing characteristics of these groups are such things as family income "... the single most important factor affecting business as well as personal air travel ...", occupation, industry affiliation, age, and education. Survey data is used to aid in the proper allocation of business travel to these groups.

b. Actual travel characteristics of these groups are determined from survey data. In addition to distribution by income, the survey population is classified as to previous flying experience to obtain a measure of the relative acceptance of flying with increasing income.

c. The travel behavior values as determined from statistical sampling are applied to each group of the population at the time of the study in order to estimate the total number of trips made. (The result of this process was compared to the actual number of trips reported by air carriers to the CAB, and was found to agree extremely well.)

d. Estimates are then made of the distribution of future (1975 and 1985 population in the socio-economic groups described previously. Groups distributed by income are adjusted for the appropriate increases of per capita income for those times.

e. The behavior values, properly adjusted, are then again applied to the 1975 and 1985 groups to estimate the number of trips for those future years.

The results of this extrapolation are shown in Table A-7. Lines 3 and 7 were added to account for the fact that minors and military personnel were not included in the population groups of the above survey. The adjustment of Line 10 makes it possible to compare these results directly with CAB format. Total passenger miles are determined from the indicated trips and a forecast of average trip length, which is discussed later.

The city analysis method of forecasting future air carrier traffic is based upon the historical evidence that major air traffic hubs maintain a relatively constant share of the total domestic originating passengers. Between 1950 and 1964 this share increased only slightly from 66 to 69 percent.* Under the assumption that this share would steadily increase to 70 percent by 1985, the historical ratios of originating passengers to population for each area are projected to 1975 and 1985. These ratios are applied to population forecasts for those years to obtain numbers of originating passengers at the hubs, and ultimately, the total for the nation. The values are given in Table A-8.

The Gross National Product method is based on the historical relationship between total domestic air travel and gross national product. Between 1949 and 1966 the ratio of passenger miles to GNP showed an upward trend through 1959, a level period for the next few years during a slowdown in economic activity rate, and subsequently an upsurge in which the ratio was reestablished. The results of this forecast also are presented in Table A-8.

*This value disagrees slightly with other data (Ref. A-5), which indicate that the hubs accounted for 68 percent of U.S. emplaned passengers in 1968. This may be explained by the fact that the 1964 list contained 23 hubs while Reference 4 has 21. (The later lists does not contain Buffalo, Cincinnati, and Tamps; Los Vegas is a new addition.)

Table A-7. Market Analysis Method - Estimated Total Trips and Passenger Miles (Ref. A-2)

Trip Types	1975 (Millions)	1985 (Millions)
1. Adult Round Trips - Business	48.7	89.7
2. Adult One-Way Trips - Business	97.5	179.4
3. Trips by Minors and Armed Forces[1]	3.9	8.1
4. Total Business Trips	101.4	187.5
5. Adult Round Trips - Personal	28.7	46.3
6. Adult One-Way Trips - Personal	57.5	92.5
7. Trips by Minors and Armed Forces[2]	10.4	18.5
8. Total Personal Trips	67.9	111.0
9. Total U.S. Domestic Trips - Unduplicated	169.3	298.5
10. Adjustment for Duplication by Reporting Carriers[3]	16.9	30.0
11. Total Duplicated Trips[4]	186.2	328.5
12. Average Length of Trip (Statute Miles)	687.0	725.0
13. Total U.S. Passenger Miles (billions)	127,900	238,200

1 3% in 1963, 4% in 1975, and 4.5% in 1985

2 15% in 1963, 18% in 1975, and 20% in 1985

3 11% in 1963, 10% in 1975, and 10% in 1985

4 Conforms to originated passengers in CAB Form 41

Table A-8. Final Forecast Domestic Originating Air Passengers Major Metropolitan Areas (Ref. A-2)

Air Traffic Hub	1975	1985
Atlanta	5,965	10,470
Boston	5,918	10,390
Buffalo	1,614	2,835
Chicago*	18,927	33,225
Cincinnati	2,048	3,595
Cleveland	3,366	5,910
Dallas	5,874	10,310
Denver	3,616	6,350
Detroit	4,600	8,075
Houston	3,425	6,010
Kansas City	2,858	5,015
Los Angeles	13,192	23,155
Miami/Ft. Lauderdale	3,942	6,920
Minneapolis	3,274	5,745
New Orleans	2,658	4,665
New York*	22,074	38,750
Philadelphia	4,508	7,910
Pittsburgh	3,361	5,900
St. Louis	3,402	5,970
San Francisco	7,969	13,990
Seattle/Tacoma	2,398	4,210
Tampa/St. Petersburg	1,311	2,300
Washington D.C./Baltimore	11,301	19,835
Total Major Hubs	137,600	241,450
U.S. Total	197,000	345,000
Percent of U.S.	70%	70%

*Consolidated metropolitan area

Multiple correlation analysis were used in the Lockheed study to investigate the effects of GNP and other factors, such as air fares and speed, on domestic travel demand. (Between 1946 and 1965 real air fares decreased from 6.79 to 5.29 cents per passenger mile and average speed increased from 160 to 320 mph.) Although there was high correlation with all factors, GNP was significantly dominant. Analysis tends to confirm this correlation (Ref. A-7), except that in connection with that study it was impossible to distinguish between the effect of travel speed and GNP on air travel demand. The results of the first two analysis methods (market analysis and city analysis) are plotted in Figure A-1 in terms of passenger miles per $100 of GNP. It can be seen that the methods differ by only about 10 percent. However it will become apparent later that the comparison with other forecasts is considerably less consistent.

In order to determine the future number and types of air carrier aircraft required, a method similar to the city analysis method, but using city-pairs, is used to determine the distribution of air travelers over the various routes. The historical portion of each city pair's share of the total U.S. originating passengers is applied to the future populations.

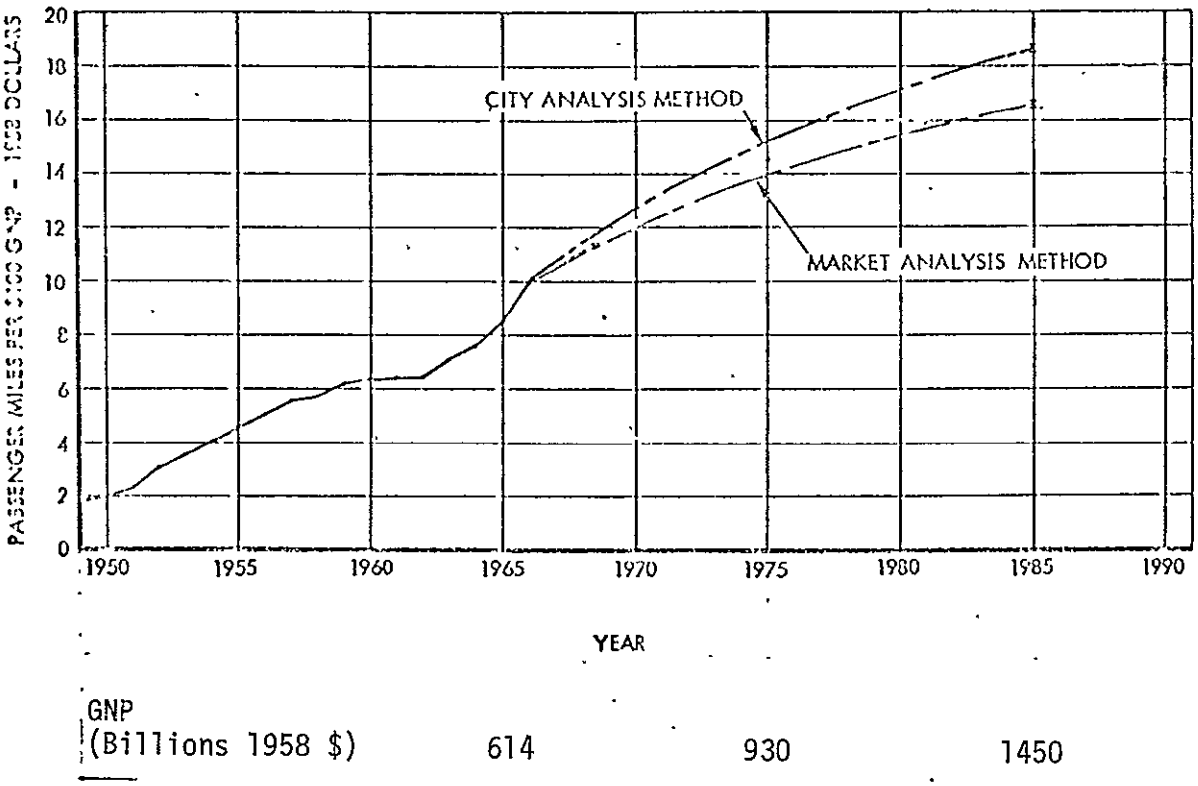

GNP (Billions 1958 $)	614	930	1450

Figure A-1. Air Carrier Travel Forecasts (Ref. A-2)

REFERENCES

A-1 "FAA Air Traffic Activity, Fiscal Year 1968", Department of Transportation, Federal Aviation Administration, Office of Management System (August 1968).

A-2 "Air Traffic Forecasts", Lockheed California Co.

A-3 "National Aviation System Policy Summary", Dept. of Transportation, Federal Aviation Administration (March 1970).

A-4 Dept. of Transportation Air Traffic Control Advisory Committee Report, Vol. 2 - Appendices (December 1969).

A-5 "National Aviation System Plan - 1971-1980", Dept. of Transportation, Federal Aviation Administration (March 1970).

A-6 The Institute of Electrical and Electronics Engineers, Special Issue on Air Traffic Control Proc. IEEE 58 (3) (March 1970) pp. 289-518.

A-7 United Research Corporation Study.

APPENDIX B

AIR TRAFFIC SYSTEM ORGANIZATION AND MANAGEMENT

This appendix will treat the way aircrews and air traffic controllers function together in order to make the air transportation system work.

1. FLIGHT RULES AND PROCEDURES

1.1 Background. As aviation grew from its infancy during the first half of this century, "rules of the air" evolved which were in large part three-dimensional adaptations of the centuries old "rules of the sea"; but as the air space became more highly populated, better organization was required. Long before World War II a number of United States airlines formed a private corporation called Air Traffic Control, Inc., which performed minimal air traffic control functions during bad weather in some of the major cities of the country. By 1936, however, even this did not suffice and the Department of Commerce took over this function in the United States (Ref. B-1).

During the mid-forties it became clear that there would be a large scale expansion of national and international air transport following the end of World War II. In 1944 an international conference on aviation was held in Chicago to deal with civil aviation as it related to international air transportation. As a result of the Chicago conference, the Provisional International Civil Aviation Organization was established, and then in 1947 the International Civil Aviation Organization (ICAO) was established in Montreal, Canada. ICAO became a specialized United Nations function dealing with aviation matters. The vast majority of the members of the United Nations are likewise members of ICAO and subscribe to ICAO flight rules and procedures which are defined in Annex 2 (Rules of the Air) to the Convention on Civil Aviation.

Member nations, for the most part, pattern their national rules and procedures (which of course represent laws) after the ICAO procedures. Although ICAO rules are not binding on military aircraft, the United States' and most other member nations' military aircraft are required by their own regulations to comply as far as possible with the ICAO procedures. In general, nations maintain the prerogative of making their national pro-

cedures more restrictive than the ICAO procedures if they desire to. Likewise, organizations such as the Dept. of Defense can choose to be more restrictive in their regulations than the Federal Air Regulations. For example, the U. S. Air Force requires better weather conditions for an approach at a particular airport for a new pilot then the civil regulations and company practices would require for a senior airline pilot. However, Air Force or Navy flying regulations may not be less restrictive than the Federal Air Regulations. Since national air regulations everywhere are patterned after ICAO flight rules and regulations, an American pilot can for all major air routes around the world follow similar rules of the air. In places where air regulations are in conflict, a logical hierarchy prevails, (i. e., Federal Air Regulations over DOD or company practices and procedures, ICAO regulations over national regulations in international areas but more restrictive national regulations over ICAO Regulations in the country of interest) (Ref. B-2).

1.2 Highlights of Flight Rules. The ICAO Rules and Procedures, the United States Federal Air Regulations, and the Department of Defense General Flight Rules are all much too detailed to repeat here, but some of the most significant items contained in the ICAO Rules and Procedures merit consideration. Item 9b of Table B-1 is important, and states:

> "IFR flights operating in controlled airspace are provided by Air Traffic Control with separation from other IFR flights, except during specified portions of such flights cleared to maintain operation in visual meteorological conditions (VMC), in which case it is the direct responsibility of the pilot to avoid collision with other aircraft. Note: It is important to realize that the direct responsibility of the pilot to avoid collision with other aircraft when flying in VMC applies not only when an IFR flight has been specifically cleared to climb, descend, cruise, or hold, subject to maintaining VMC, but also when the flight is not operating on a VMC clearance. Indeed, when meteorological conditions exist in a given area, the VFR flights, as well as other IFR operating on a VMC clearance, may be flying in the area, and no separation from such aircraft is provided by air traffic control. Information will be given, however, with respect to those known aircraft which are separated from the IFR flight in question by less than the minima prescribed for IFR traffic."

Table B-1. Selected Items from ICAO Rules and Procedures

1) Responsibility for compliance with rules of the air
2) Authority of pilot in command of an aircraft
3) Protection of persons and property
4) Avoidance of collisions, negligence, airspace restrictions, proximity, right of way
5) Flight plan information
6) Air traffic control clearances
7) Control of Aerodrome traffic
8) Visual flight rules (VFR)
   a) Flight visibility requirements
   b) Distance from clouds
9) Instrument flight rules (IFR)
   a) Required aircraft equipment
   b) Required pilot rating
   c) Required minimum weather conditions
   d) Air traffic control service
   e) Separation of aircraft
   f) Flight plan and ATC clearance
   g) Air/ground ATC communications
   h) Departure, holding, and approach procedures

Item 9g is very important. It includes the requirement that an aircraft shall maintain a continuous listening watch on an appropriate assigned radio frequency and contains the following instructions in the event of communications failure:

"5. 4. 4. 4. 1. If a radio failure precludes compliance with 5. 4. 4. 1. 1, the pilot must:

1) If in visual meteorological conditions

   a) Continue to fly in visual meteorological conditions;

   b) Land at the most suitable aerodrome.

2) If in instrument meteorological conditions or when weather conditions are such that it does not appear feasible to complete the flight in accordance with 1):

a) Proceed according to the current flight plan, maintaining the last acknowledged assigned cruising level (or levels) to the point specified in the clearance to which the cruising level(s) apply, if different from those of the flight plan, and thereafter at the cruising level (or levels) indicated in the current flight plan;

b) Arrange the flight so as to arrive as closely as possible to the estimated time of arrival;

c) Commence descent as nearly as possible to the expected approach time last received and acknowledged; or, if no expected approach time has been received and acknowledged, as nearly as possible to the estimated time of arrival specified in the flight plan."

1.3 Fundamental Principles. Examination of various flight rules, regulations, and procedures brings out several fundamental points:

1) Safety. Air safety is paramount. There are standards which separate aircraft from the ground, from each other, and even from clouds; and that prohibit dangerous operations in the air above populated areas. This fundamental principle will not change.

2) Flight Rules and Services. There are basically two types of services which can be provided a pilot in flight. He may travel on a fairly unrestricted basis and receive only minimal support from ground stations. This, of course, corresponds to visual flight rules operation. The pilot may elect (or be compelled) to fly a much more regulated and restricted flight path, obtaining in the process much greater aid in the form of protection from other aircraft, position fixing help, and the like. This latter case, of course, corresponds to instrument flight rules operation. Although there is a trend toward more and more IFR operation, this fundamental principle will remain. The pilot may elect to receive varying degrees of service from ATC, but his equipment requirements and legal obligations to conform to the instructions given by ATC will increase with an increase in services provided.

3) Legal Implications. A flight plan which has been proved by Air Traffic Control in the form of a granted and acknowledged clearance is in effect a binding contract. Air crews and air traffic controllers can find themselves in legal jeopardy if through negligence they violate that contract and the result involves fatalities. For this reason in the past, both by regulation and by practice, personnel have gone to great length to make sure that an

aircraft clearance was clearly understood and understood in the same way by both the ground and air parties. The full and complete readback of long and complicated air traffic control clearances remains a common occurrence and a clearance is not considered valid unless it has been acknowledged. This acknowledgment has in the past occurred over a voice link such that there was clearly a meeting of the minds between the pilot and the air traffic controller or at least the radio relay man on the ground. In the future when many air traffic control commands are given via data link, it will be important to take this factor into account. An agreement between a computer on the ground and an airborne computer in flight may or may not be an operationally acceptable solution. In summary, as hardware mechanizations and procedures change, the legal implications must not be ignored or forgotten in the synthesis of a new system.

4) Pilot-Controller Relationship. There is a division of responsibility and authority in the planning and execution of air traffic control. This fundamental point, too, is not likely to change. It is unlikely that the following ICAO Rule of the Air will change: "The Pilot-in-command of an aircraft shall have final authority as to disposition of the aircraft while he is in command." Although the ultimate responsibility for his aircraft and the lives of the people aboard rests with the aircraft commander or pilot-in-charge, this responsibility does not entitle him to complete freedom of action. There are times when he must follow the instructions of an air traffic controller, even though they may involve changes in his flight plan which are inconvenient to him. One of the primary reasons that the air traffic control system works as well as it does, especially during peak traffic hours, is the high degree of teamwork and cooperation between pilots and air traffic controllers, which for the most part is born of mutual respect. The psychological factors are not entirely understood, and are certainly not quantified, but they are by no means trivial or imaginary.

5) Fail Safe Operation. The air traffic control system must continue to operate in the presence of emergencies and failures. In-flight emergencies, which involve rapid, large, and unavoidable variations from the nominal and predicted flight path for an aircraft in distress, will continue to occur. An air traffic control system that cannot respond flexibly to situations such as this is not a viable one. Furthermore this system must be capable of operating in the presence of failures or anomalies in both ground and airborne hardware.

6) Flight Requirements. Air traffic regulations, especially for flight under instrument conditions, has in the past imposed requirements on both pilot and equipment. Indications are that they can be expected to do so to an even greater degree in the future.

A combination of two fundamentals treated thus far; namely, that 1) a clearance is a contract and 2) that the system must function in the presence of failures, led to the extremely explicit and detailed "Radio out" or "Communication Failure" regulation quote earlier. The reason for this emphasis was simply that the failure of a radio in flight was a relatively common occurrence and adequate provisions had to be made to protect all aircraft when there was an aircraft operating in the clouds with a radio failure. Clearly, however, if technology alters the situation enough, reducing the likelihood of failure of communications, surveillance transmitter, navigation or other equipment to a very small value, then it is likely that flight rules and procedures will be altered accordingly. It is the implementation, however, which will change. The fundamental points -- the need for some form of fail-soft operation and the fact that all flights in the National Airspace System involve legal implications and responsibilities -- will not change.

2. AIRSPACE ORGANIZATION

2.1 Domestic Regions

One of the more significant features of the ICAO and U.S. Flight Rules and Procedures is that there are two significantly different sets of rules — visual flight rules and instrument flight rules — which may be used under varying weather conditions. Although not spelled out in the same way, there are different sets of rules which apply when aircraft fly into different geographical regions. The airspace itself is organized in such a way that a pilot flying into a given region, say in the vicinity of a high-density air terminal, knows that he is under far stricter control than if he were out over sparsely populated terrain. The airspace over the United States is considered a national resource and use of portions of it may be granted unconditionally; conditionally, or not at all. The airspace over the United States, then, has been mapped out in three dimensions, with different sets of rules applying in different regions and under different conditions. For obvious reasons, the rules of flight

governing aircraft crossing international borders during times of formal or informal hostilities will be different than for peacetime operation. The remainder of this section will treat the peacetime airspace organization over the contiguous United States.

Table B-2 contains a number of listings of airspace categories which have been suggested or designated by various interested and responsible organizations. Although space does not permit a detailed discussion of each of these points of view, several points should be made:

- There is unanimous agreement that airspace organization is required, and that the degree of organization or control must become quite high in densely populated regions.

- Most of the listings allow for the existence of mixed airspace, i.e., airspace wherein controlled aircraft are provided separation from one another, but are not necessarily provided separation from uncontrolled aircraft. The Air Transport Association listing specifically excludes this possibility, although their Type 3 Controlled Airspace would not provide separation service between two unregulated aircraft.

- It can be seen from these listings (and it is even more obvious when the source documents are studied) that the legitimate but different points of view of the air carrier and general aviation communities produce different recommended flight rules and regulations. Any meaningful system synthesis must not, in an attempt to appear palatable to all users, ignore or equivocate on this issue.

- Although the RTCA listing is the only one that calls it out, all organizations recognize the existence of Special Use Airspace.* As the airspace itself becomes more and more precious, it can be expected that more and more pressure will be brought to bear (primarily on the Department of Defense) to shrink up this Special Use Airspace. Again, however, the synthesis of an ATC system requires recognition that such airspace will continue to exist to some degree, probably indefinitely.

*Special Use Airspaces are identified on aeronautical charts and in aeronautical planning data and procedures documents, and are divided into four categories (Ref. B-3).

- Prohibited Areas, where flights are prohibited except by special permission
- Restricted Areas, where flights are prohibited during published periods of use, unless permission is obtained from controlling authorities
- Warning Areas, where flights are not restricted but avoidance is advised during use
- Caution Areas, where flights are not restricted but the pilots are warned to exercise extreme vigilance.

Data given on Special Use Airspace includes, in addition to its location: airspace number, area name, effective altitudes, times used (days of week, hours of day, weather conditions), and the controlling authority.

Table B-2. Airspace Categories as Designated by Several Authoritative and Representative Sources

FAA (Ref. B-4)

1. Positive control area (PCA)
2. PC terminal access corridor
3. Terminal PCA (TPCA)
4. Control area (mixed airspace)
5. Controlled airway (mixed airspace)
6. Uncontrolled

FAA (Ref. B-5)

1. PCA
2. TPCA
3. Control zones
4. High density terminal area airspace (initially mixed airspace, going TPCA)

General Aviation (Ref. B-1)

1. Controlled
2. Mixed airspace
3. Uncontrolled

Air Transport Association (Ref. B-6)

1. Controlled:
   - Type (1): Positive control of aircraft
   - Type (2): AFR/IFR control
IFR/VFR control
VFR/VFR advisory
   - Type (3): IFR/IFR control
IFR/VFR control
VFR/VFR-no service
2. Uncontrolled: No service.

Radio Technical Commision for Aeronautics (Ref. B-7)

1. Controlled
2. Uncontrolled
3. Special use

Alexander Committee (Ref. B-8)

1. High density airspace
2. Positive controlled airspace
3. Mixed airspace (with IPC)
4. Uncontrolled airspace

2.2 Oceanic and Transition Regions

There are certain fundamental differences, in the present environment, between the requirements of an oceanic system and those of a domestic system as affecting airspace organization. Furthermore, the requirements may differ between the Atlantic and Pacific Ocean areas, since the optimum system for the Atlantic must satisfy high traffic density in the North Atlantic corridor, while comparable densities may not be reached in the Pacific for many years due to the dispersion of air routes. Most of these differences arise from the modes and methods of communication available to present day aircraft.

When SST flights become a significant proportion of the overall traffic, some of these differences will begin to disappear. Reduced transit time may dictate the use of common data bases for the computational systems for domestic and oceanic control, thus simplifying the interface between the systems and in fact forcing the system toward the concept of an integrated ATCS for the domestic/oceanic transition regions.

The congestion in the North Atlantic corridor, as the problem is currently experienced, is caused by two factors:

1) The need for aircraft to utilize a "minimum time track" over the great circle route between North America and Europe

2) The peaking of East/West and West/East traffic at certain hours to provide for passenger convenience.

As aircraft speed increases, both constraints will assume different weighting factors. The velocity of winds aloft will become a much smaller percentage of aircraft speed and meteorological effects on the minimum time track will be less important. However, fuel consumption will become a more critical parameter. The greatly reduced intercontinental transit times will also permit more flexibility in arrival and departure times. These factors will result in changes to the physical airspace assignments in the North Atlantic corridor and modify requirements for aircraft separation distances. Smoothing the peak traffic curves for East/West and West/East departures should be possible as a result of shorter transit times. This in turn will impact the requirement for corridor density.

In addressing the question of compatibility between oceanic and domestic systems in the study, the following observations can be made:

- Oceanic users, while fewer in number than domestic users, can, by their nature, afford somewhat more sophisticated equipment on their aircraft; and the trade-off between aircraft costs and satellite/ground system costs may differ from a domestic system.

- It follows that oceanic users should in general be required to be compatible with domestic systems to the extent necessary rather than attempting to force compatibility with ocean systems on domestic users. However, both systems should be co-existent so that ocean users are not forced to pay an unacceptable penalty for entry into the domestic system. Ideally, little or no penalty would be paid.

Thus, at this time, there appear to be no difficult hurdles to be encountered since a number of satisfactory solutions to the transition area are readily apparent. If the over-ocean CNS System is very similar to that used for the contiguous United States, then functionally there is no real interface. If the over-ocean system resembles that studied for NASA/ERC in the Navigation Traffic Control Satellite Mission Study (Ref. B-9), then the interface between say CNS surveillance and NAVSTAR/AUTOREP surveillance (discussion in Reference B-9) could simply take place during the approach or departure phase, since the satellite service capabilities will overlap. Likewise, in the event that no satellite-based over-ocean capability exists, the interface will be much as it is today. Today, surveillance and communications capabilities simply cease when the aircraft is no longer within line of sight of the ground station to which it reports. The system reverts to HF communications and whatever navigation aids are available. In the future, the same thing would happen when the aircraft flew out of the field of view of the Satellite CNS System.

2.3 Effect on Airspace Organization of the Use of Collision Avoidance Systems/Proximity Warning Indicators

Many collision avoidance system (CAS) and proximity warning indicators (PSI) employing airborne electronic equipment have been proposed and developed as experimental hardware. Their use could affect airspace organization and management procedures. The CAS, in providing not

only an indication of a collision threat but also an escape maneuver, requires a rapid and precise solution of a complex dynamic problem which implicitly requires the cooperation of all participants. As generally proposed, the hardware that satisfies this need can be complex and costly. The currently considered PWI functions as an attention-getter and would probably be useful only in visual systems in weather conditions where traffic is relatively light and closing speeds relatively low.

The FAA is understood to regard CAS and PWI as optional equipment supplementing the existing ATC service. However, if such hardware designs as the present candidates are adopted, the FAA would be expected to provide any ground reference stations that are needed. An experimental station is now being procured for the ATA-sponsored CAS.

The CAS technique now being seriously considered could have a broader application since precision time standards can also provide a reference for surveillance, navigation, and communications frequency control. Also, if a practicable system were available that includes the quantative distance and rate information needed for air-derived station-keeping, some of the positive control burden could be shifted from the controller to the pilot. Ground-based monitoring would continue and intervention would be provided only as needed. This would go beyond the ATCAC IPC concept in that the pilot - on his own initiative - would be able to overtake and pass a slower aircraft - still, of course, maintaining safe separation. Collision tracks on other than the overtake situation would probably require ground intervention or CAS-indicated emergency procedures because a timely and orderly response would be much more difficult to determine and to indicate in the aircraft. Clearly, if a significant increase in cockpit capability (represented by the implementation of effective CAS/PWI systems) is implemented, airspace management would become more flexible and would involve less ground control. More of the responsibility and authority would revert to the pilot. Any decision to dramatically alter air traffic control philosophy in this direction, however, would hinge on a clearly demonstrated and widely accepted CAS/PWI capability. At the time of this report, this situation does not exist and the issues are not sufficiently well established to predict the eventual outcome.

3. CONCLUSIONS

The following conclusions are drawn from the foregoing discussions and from the related analyses performed on this study.

- The Satellite CNS System implementation must be synthesized using a consistent and viable airspace organization and management strategy.

- This strategy must be capable of accepting a wide range of aircraft, air crews, and flight plans.

- Mixed airspace in the terminal environment is the single most critical problem. At the outset of this study, TRW felt that a probable ultimate goal should be the elimination of mixed airspace. We now feel that this may not be necessary; and if it is not necessary, it is certainly not desirable. Elimination of mixed airspace would substantially constrain the freedom of a large fraction of the aircraft population. The key to this question is the satisfactory implementation of a short access time collision warning system that would adequately serve the needs of the total aircraft population.

- Although the Satellite CNS System described in Volume 1 does not represent an optimum system design, it is clear that this system concept could be implemented without constraining ATC rules and procedures. Further, no ATC organization and management issues have been identified that would inhibit adoption of the Satellite CNS System concept.

REFERENCES

B-1 "Air Traffic Control", Part 1, "Air Traffic Out of Control", Part 2, "Air Traffic, The Clearing Skies", Flying (January and February 1969).

B-2 "International Rules and Procedures", DOD Flight Information Publication on Flight Planning, USAF Aeronautical Chart and Information Center, St. Louis, Mo. (Published Semiannually).

B-3 "Planning Data and Procedures", DOD Flight Information Publication on Flight Planning, USAF Aeronautical Chart and Information Service, St. Louis, Mo. (Published every eight weeks).

B-4 The National Aviation System Plan 1970-1979, Book 1, Federal Aviation Administration, Dept. of Transportation (January 1969).

B-5 "Approval of Area Navigation Systems for Use in the U.S. National Airspace System", Federal Aviation Administration, Dept. of Transportation (14 June 1969).

B-6 "Recommendations for a National Air Traffic Management System", ATA Air Traffic Control System Planning Group (15 May 1969).

B-7 "Long Range Planning for the Traffic System", Radio Technical Commission for Aeronautics, Doc. No. DO-135 (March 17, 1967).

B-8 Appendixes to Report of Air Traffic Control Advisory Committee, Dept. of Transportation (December 1969).

B-9 "Navigation/Traffic Control Satellite Mission Study", TRW Report No. 09778-6008-RO-00 (June 1969).

APPENDIX C

ESTIMATE OF FILTERED POSITION AND VELOCITY ERRORS

1 INTRODUCTION

A simple analysis is described which estimates the position and velocity errors associated with the use of a steady state Kalman Filter for the determination of aircraft position and velocity. The errors can be conveniently considered to be composed of two parts. The first part, the noise term, is the error caused by the noisy (non-deterministic) measurements which are used by the filter. The second part, the lag term, is the error produced because the aircraft is accelerating. These two parts are determined separately and then are combined to produce the total filtered output error. For this study it was convenient to work with Z transforms (Ref. C-1), and therefore, a knowledge of this transform is necessary to thoroughly understand the analysis.

2. DESCRIPTION OF THE FILTER

The steady state Kalman Filter is described by the following difference equations:

$$\bar{x}_k = x_{pk} + \alpha(x_k - x_{pk})$$

$$\bar{\dot{x}}_k = \bar{\dot{x}}_{k-1} + \frac{\beta}{T}(x_k - x_{pk})$$

$$x_{pk+1} = \bar{x}_k + T\,\bar{\dot{x}}_k$$

where:

$x_k \equiv$ Noisy input measurement data at the k^{th} time instant.

$\bar{x}_k \equiv$ Estimated position at the k^{th} time instant.

$\bar{\dot{x}}_k \equiv$ Estimated velocity at the k^{th} time instant.

x_{pk+1} ≡ Predicted position at the $k+1^{th}$ time instant.

T ≡ Sampling time.

α, β ≡ Filter constant.

A Z transform signal flow diagram of the filter can be drawn from the above equations:

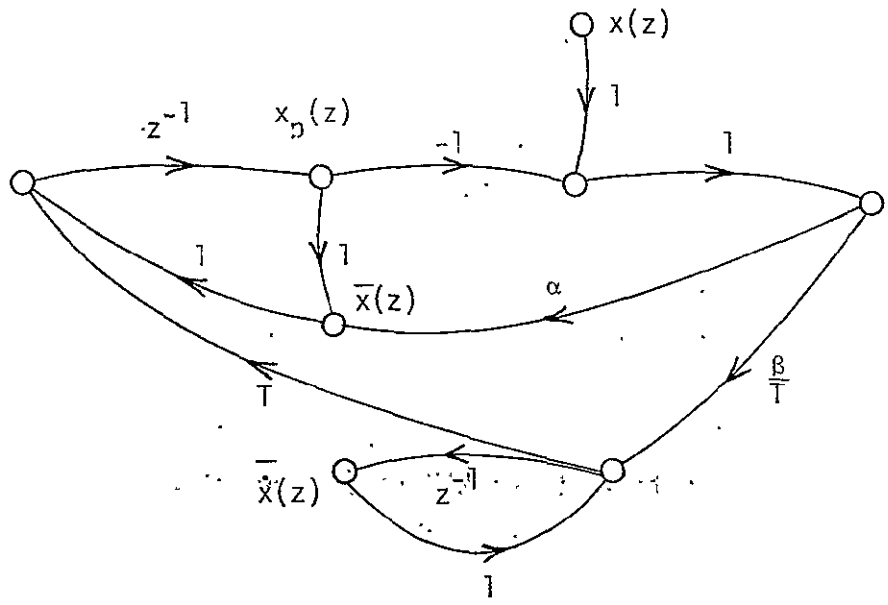

where:

z ≡ Z transform variable.

f(z) ≡ Z transform of the function f_k; that is,

$$f(z) = \sum_{k=0}^{\infty} f_k \, z^{-k}.$$

Using the signal flow diagram and Mason's gain formula, the following transfer functions can be obtained:

$$T_x(z) \equiv \frac{\bar{x}(z)}{x(z)} = \frac{z(\beta - \alpha + \alpha z)}{z^2 + z(\alpha + \beta - 2) + (1 - \alpha)}$$

$$T_{\dot{x}}(z) \equiv \frac{\dot{\bar{x}}(z)}{x(z)} = \frac{\frac{\beta}{T} z(z - 1)}{z^2 + z(\alpha + \beta - 2) + (1 - \alpha)}$$

3. NOISE TERM OF THE FILTER ERROR

The noise term of the filter error was evaluated by determining the steady state variance of the outputs of the filter caused by a gaussian, independent noise input, having a zero mean and known constant variance, σ_x^2. The filter is linear and therefore the output-input relationship is given by the convolution equation:

$$y_k = \sum_{j=0}^{k} H_{k-j}\, x_j$$

where:

$y_k \equiv$ Output variable at the k^{th} time instant.
$x_k \equiv$ Input variable at the k^{th} time instant.
$H_{k-j} \equiv$ Impulse response of the filter from time instant j to k.

The variance of the output at the k^{th} instant of time, $\sigma_{y_k}^2$, is given as,

$$\sigma_{y_k}^2 \equiv E\{y_k^2\} = E\left\{\left[\sum_{j=0}^{k} H_{k-j}\, x_j\right]\left[\sum_{i=0}^{k} H_{k-i}\, x_i\right]\right\}$$

Using the statistical properties of the input signal, the expression for the output variance can be reduced to,

$$\sigma_{y_k}^2 = \sigma_x^2 \sum_{j=0}^{k} H_{k-j}^2$$

The steady state output variance, σ_y^2, is therefore given by:

$$\sigma_y^2 \equiv \lim_{k\to\infty} \sigma_{y_k}^2 = \sigma_x^2 \sum_{j=0}^{\infty} H_j^2$$

A convenient method of evaluating the infinite sum can be obtained by using the Ergodic Hypothesis which results in the fact that the sum

is equal to the mean-square value of the filter output to a pure white noise input. In turn, this mean-square value of the output is equal to the autocorrelation function at $\tau = 0$ which can be obtained from the Z transform of the impulse response, $H(z)$. Using these facts, one can write:

$$\sum_{j=0}^{\infty} H_j^2 = \text{Inverse Z transform of } H(z)\, H(z^{-1}) \text{ with } n = 0$$

$$= \frac{1}{2\pi j} \oint_{\Gamma} H(z)\, H(z^{-1})\, z^{n-1}\, dz, \text{ for } n = 0.$$

The above expression can be determined by the use of residues:

$$\frac{1}{2\pi j} \oint_{\Gamma} H(z)\, H(z^{-1})\, z^{-1}\, dz = \sum_{\substack{\text{All poles} \\ \text{inside the} \\ \text{unit circle}}} \text{Residues of } H(z)\, H(z^{-1})\, z^{-1}$$

Using the above scheme, the steady state variance of the filter velocity error, $\sigma_{\dot{\bar{x}}}^2$, can be determined. The Z transform of an impulse response is equal to the transfer function; therefore

$$H(z) = T_{\dot{x}}(z)$$

and the poles of $T_{\dot{x}}(z)\, T_{\dot{x}}(z^{-1})\, z^{-1}$ inside the unit circle are $z = 0$, z_1, z_2

$$z_{1,2} = \frac{2 - \alpha - \beta \pm j\sqrt{4\beta - (\alpha-\beta)^2}}{2}$$

Let $z_{1,2} = R \pm jc$, then after algebraic manipulations the residues of the above three poles are found to be:

$$\text{for } z = 0: \quad \text{Residue} = R_0 = 0$$

$$\text{for } z = z_1: \quad \text{Residue} = R_{z_1} = \frac{(1 - R - jc)}{(1 + R + jc)(1 - R^2 - c^2)(2\,jc)}$$

$$\text{for } z = z_2: \quad \text{Residue} = R_{z_2} = \text{Complex conjugate of } R_{z_1}.$$

The variance is then obtained as:

$$\sigma_{\dot{\bar{x}}}^2 = \sigma_x^2 [R_0 + R_{z_1} + R_{z_2}],$$

which after more algebra becomes:

$$\boxed{\sigma_{\dot{\bar{x}}}^2 = \sigma_x^2 \left[\frac{2\beta^2}{T^2 \alpha(4 - 2\alpha - \beta)}\right]}$$

For the noise term of the filter position error one used:

$$H(z) = T_x(z).$$

The poles of $T_x(z)\, T_x(z^{-1})\, z^{-1}$ inside the unit circle are also $z = 0, z_1, z_2$. By proceeding in similar manner, one arrives at the following result for the steady state variance of the filter position error, $\sigma_{\bar{x}}^2$:

$$\boxed{\sigma_{\bar{x}}^2 = \sigma_x^2 \left[\frac{2\alpha^2 - 3\beta\alpha + 2\beta}{\alpha(4 - 2\alpha - \beta)}\right]}.$$

4. LAG TERM OF THE FILTER ERROR

The Lag term of the filter error was estimated by determining the steady state filter output error when the input measurement is equal

to a parabolic function of time; that is,

$$x_k = \frac{A(kT)^2}{2}$$

A was chosen to be equal to the maximum acceleration of the aircraft. This input is equivalent to the aircraft having a constant maximum acceleration, which in terms of filter lag error, corresponds to the "worst case". The steady state error can be evaluated by using the method of error coefficients. (Ref. C-1).

If the error is given by the following Z transform;

$$e(z) = W(z)\, x(z)$$

where:

$e(z) \equiv$ Z transform of the error,

$x(z) \equiv$ Z transform of the input, and

$W(z) \equiv$ error transfer function

then the steady state error, e_k, is given by the following equation:

$$e_k = c_0 x_k + c_1 \frac{d\, x_k}{dt} + \frac{c_2}{2!} \frac{d^2 x_k}{d\, t^2}$$

$$+ \ldots + \frac{c_n}{n!} \frac{d^n x_k}{dt^n} + \ldots$$

where:

$$c_n = \left. \frac{d^n W^*(s)}{d\, s^n} \right|_{s = 0}$$

$$W^*(s) = \left. W(z) \right|_{z = e^{Ts}}$$

For our case, x_k is a parabolic function of time, and therefore,

$$x_k = \frac{A(kT)^2}{2}$$

$$\frac{d\,x_k}{dt} = A\,kT$$

$$\frac{d^2\,x_k}{dt^2} = A$$

$$\frac{d^n\,x_k}{dt^n} = 0 \text{ for } k \geq 3$$

and one needs only to evaluate c_0, c_1, c_2.

Using the above method, the steady state filter position error, $e_{\overline{x}_k}$, can be determined. The position error transfer function is given as

$$W_x(z) = \frac{e_{\overline{x}}(z)}{x(z)} = \frac{x(z) - \overline{x}(z)}{x(z)} = 1 - T_x(z)$$

$$= \frac{(1 - \alpha)(z^2 - 2z + 1)}{z^2 + z(\alpha + \beta - 2) + (1 - \alpha)}$$

The corresponding c_n's are determined to be:

$$c_0 = 0$$

$$c_1 = 0$$

$$c_2 = \frac{2T^2(1 - \alpha)}{\beta}$$

Finally, the steady state filter position error is:

$$\boxed{e_{\bar{x}_k} = \frac{T^2(1 - \alpha)A}{\beta}}$$

Similarly the steady state filter velocity error, $e_{\bar{\dot{x}}_k}$, can be determined. The velocity error transfer function is given as:

$$W_{\dot{x}}(z) = \frac{e_{\dot{x}}(z)}{x(z)} = \frac{\dot{x}(z) - \bar{\dot{x}}(z)}{x(z)} = \frac{\dot{x}(z)}{x(z)} - T_{\dot{x}}(z)$$

$$= \frac{2(z - 1)}{T(z + 1)} - \frac{\frac{\beta z}{T}(z - 1)}{z^2 + z(\alpha + \beta - 2) + (1 - \alpha)}$$

The corresponding c_n's are:

$$C_0 = 0$$

$$C_1 = 0$$

$$C_2 = T(1 - 2\frac{\alpha}{\beta}):$$

The steady state filter velocity error is,

$$\boxed{e_{\dot{x}_k} = \frac{T}{2}(1 - 2\frac{\alpha}{\beta})A}$$

These errors correspond to one aircraft. The collision hazard determination scheme uses the relative position and velocity betwen two aircraft; therefore, assuming independence and equal maximum acceleration, A, the lag terms of the filter are estimated to be twice the steady state errors, or,

$$\boxed{\begin{aligned}&\text{Lag position error} = \frac{2AT^2}{\beta}(1-\alpha)\\ &\text{Lag velocity error} = AT(1 - 2\frac{\alpha}{\beta}).\end{aligned}}$$

5. TOTAL FILTER OUTPUT ERRORS

The total filter output errors are evaluated by using the results of Sections 3 and 4. This total error, "3σ + worst case number," is determined as:

$$\text{filtered position error} \equiv |\Delta R| = [3\sigma_{\dot{X}}] + [\text{lag position error}]$$

$$= \left[3\sigma_{\dot{X}} \sqrt{\frac{2\alpha^2 - 3\beta\alpha + 2\beta}{\alpha(4 - 2\alpha - \beta)}}\right] + \left[\frac{2AT^2}{\beta}(1 - \alpha)\right]$$

$$\text{filtered velocity error} \equiv |\Delta V| = [3\sigma_{\dot{X}}] + [\text{lag velocity error}]$$

$$= \left[3\sigma_{\dot{X}} \frac{\beta}{T} \sqrt{\frac{2}{\alpha(4 - 2\alpha - \beta)}}\right] + \left[AT(1 - 2\frac{\alpha}{\beta})\right]$$

Obtained results (Ref. C-2) indicate that the parameter β can be selected to minimize both the position and velocity errors. A performance criterion was used which compromises between the transient and steady state characteristics of the filter. This optimum value of β is given as:

$$\beta = \frac{\alpha^2}{(2 - \alpha)}.$$

k

The selection of α is dependent on the practical application of the filter. For the case of determining aircraft collision hazard regions, the value of α was selected to minimize the half width of the hazard region.

REFERENCES

C-1 B. C. Kus,"Analysis and Synthesis of Sampled-Data Control Systems", Prentice-Hall, Inc., New Jersey (1963).

C-2 T. R. Benedict and G. W. Bardner, "Synthesis of Optimum Set of Radar Track-While-Scan Smoothing Equations", IRE Trans. Automatic Controls AC-7 (July 1962) pp.27-32.

APPENDIX D

LIT PRICING QUOTATIONS

This appendix contains the LIT Request For Quotation, two of its attachments, and the written responses received from four vendors.

1. LIT REQUEST FOR QUOTATION

Subject: Request for Quotation 70-2376-RS-047
Location/Identification Transmitter

Gentlemen:

TRW Systems Group presently holds a contract with NASA Goddard Space Flight Center to study the application of satellites to communications, navigation, and surveillance, for aircraft operations within the contiguous United States. As a part of this study, we are engaged in the concept design of a satellite-based air traffic control system. The single most important element of the total system is a satellite-based surveillance system concept, which appears to offer the following significant advantages to a domestic ATC application:

- All airborne aircraft will be precisely known in 3 dimensions (50 - 300 ft.) with updating about once per second.
- All airborne aircraft will be identified.
- The system saturation point can be kept well above projected traffic forecasts for this century with a relatively modest use of the R. F. spectrum.
- Very low cost avionics (target price of $400).

Although the satellite approach is clearly not a close-in solution to today's air transportation problems in the United States, satellites will almost certainly be providing aeronautical services for over-ocean use within 3 to 5 years. There is good reason to believe that significant research and development efforts for satellite-based United States ATC services will take place in the same time frame. This could lead to operational usage in the late 1970's or early 1980's. A significant element for judgment as to when satellites should replace ground-based radar and augment ground-based navigation and communication aids is, of course, economics. Thus, cost estimates are necessary at this initial feasibility study stage.

We recognize that when a system like this comes into being, the people who will build the LIT transmitter will be the people who are presently building ATC radar transponders.

Although it seems clear that the LIT transmitter, like today's radar transponder, will come in a number of versions with a fairly wide range of prices, in this feasibility study, we are emphasizing the general aviation user rather than the commercial air carrier or the military. Thus, it is this "model" that we seek to price out since to a large extent the ultimate practicality of the system will depend on its bringing into the air traffic control system the vast majority of the general aviation fleet.

We hope to obtain a pricing input from you. Your participation will be acknowledged in our final report to NASA which is expected to receive wide distribution within DOT, FAA, DOD, and other Government agencies, as well as the aviation industry itself.

Your response to this RFQ is requested by 28 August 1970. Should you have questions of a technical nature, you may contact Mr. Cecil Easley at (213) 536-7706. Other questions concerning this RFP may be directed to the undersigned at (213) 536-1755.

Very truly yours,
TRW SYSTEMS GROUP
TRW, INC.

C. T. Gibson
Subcontracts Manager
Electronics Systems Division

Attachments:
(1) AIAA PAPER (NOT INCLUDED IN THIS REPORT)
(2) LIT TRANSMITTER CONCEPTS AND DESCRIPTION
(3) LIT RFP GROUNDRULES

2. LIT TRANSMITTER CONCEPTS AND DESCRIPTION

This document describes a design approach for the development of a Location/Identification Transmitter (LIT). Although there are other approaches which can be applied, the approach described is straightforward and is well within existing technology.

Three configurations are proposed. The salient characteristics of the three configurations are shown in Table D-1 below.

Model Number	Frequency, MHz	Pulse Burst Length, sec	Peak Power Watts
A	1600	51	2500
B	900	51	890
C	900	204	240

Table D-1. LIT Configurations

The application of this transmitter is described in the AIAA paper.

The specification for the LIT is indicated below:

	Model A	Model B	Model C
Carrier Frequency	1600 MH ± 2 ppm	900 MHz ± 2 ppm	900 MHz ± 2 ppm
Output Peak Power (watts)	2500	890	240
Pulse Width (μs)	51.1	51.1	204
Pulse Rep. Period	1 Sec ± 2 ppm	1 Sec ± 2 ppm	1 Sec ± 2 ppm

Common requirements for all configurations:

Pulse Modulation - 511 bit biphase ($\pm 90^{o}$) code at 10 Megabits/Sec

Code - First 511 bits of a $2^{13} - 1$ maximal length shift register sequence

Oscillator Long Term Accuracy - 2 ppm or better per year

Power Supply - Compatible with DC source on general aviation aircraft (12V)

Logic Design - The code sequence and pulse repetition period should be fix wired into the unit, however, the logic design should be such that simple factory modifications can change the pulse repetition period in 10 μsec increments in the range between 1.0 and 1.1 seconds per pulse and the code sequence from the first 511 bits of the $2^{13} - 1$ sequence to the 2nd 511 bits or the 3rd 511 bits all the way up to the 16th 511 bits. NOTE: There are 16 disjoint or nonoverlapping 511 bit subsequences in a $2^{13} - 1$ or 8191 bit length code sequence.

2.1 Detail Description of Configuration A Amplifier Multiplier Chain

For the following discussion refer to the LIT Transmitter Model A block diagram shown in Figure D-1.

2.1.1 10-MHz Oscillator

It is a relatively simple matter to show that temperature compensation for what is hopefully a relatively low cost oscillator radically increases the cost of the circuitry, primarily due to the additional labor required to obtain adequate compensation. Consequently, a technique suggested is quite inexpensive and yet adequate to obtain the desired stability. A simple thermal blanket will be wrapped about either the crystal or the entire oscillator depending upon the physical configurations selected for the final design. This thermal blanket will be controlled by a small silicon controlled rectifier which will be caused to fire by a thermistor sensing a lower temperature

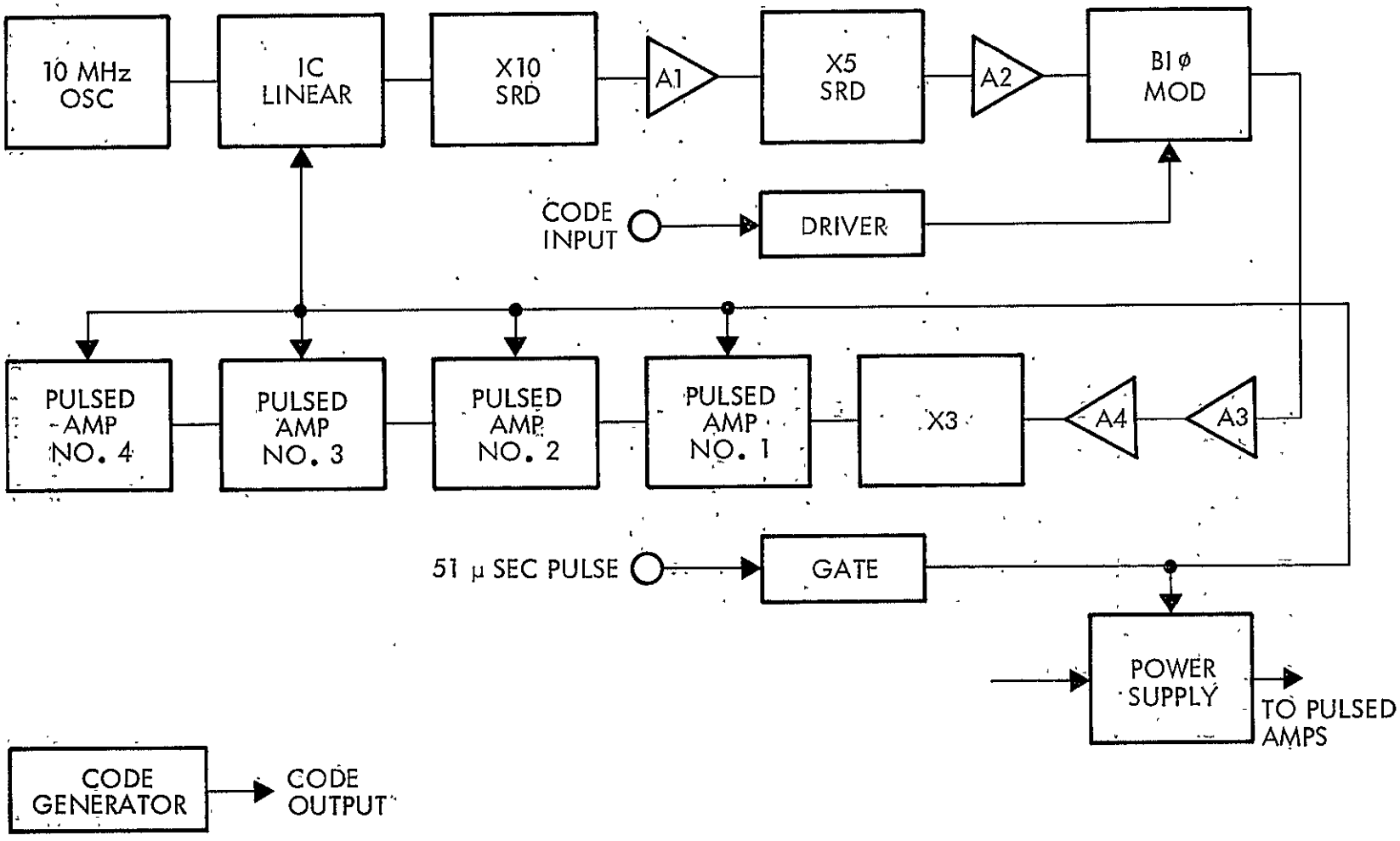

Figure D-1. LIT Transmitter Model A

extreme which will be arbitrarily selected upon test of the design prototype circuit. Thus the temperature excursion of the oscillator will be limited to a range much less than the ambient excursions anticipated for an aircraft environment. By so doing, the basic stability of the oscillator will thus be limited to less than the requisite two parts per million frequency deviation. Although the thermal blanket described appears attractive a self contained crystal oven should be investigated.

2.1.2 Linear IC Amplifier

Following the 10 MHz oscillator is a linear integrated circuit designed to act both as a buffer between the oscillator and the balance of the transmitter circuitry, and also to provide approximately 30 db gain for the low powered oscillator. Of course, it is possible to increase oscillator power and delete the integrated circuit, but in general the crystal oscillator configuration precludes large output if the required stability is to be maintained.

2.1.3 X10 Multiplier

Following the linear integrated circuit is a times ten multiplier consisting of a snap recovery diode and a few passive components. This simple circuit allows the frequency to be translated upward by a large order of magnitude, and although the loss incurred in this circuit is on the order of 10 dB, this is a small price to pay for obtaining a decade increase in the basic oscillator frequency.

2.1.4 A-1 Amplifier, S-5 Multiplier, and A-2 Amplifier

Following the times ten multiplier is an amplifier designated A-1 which more than recovers the power lost through the multiplication process. And again, immediately following this amplifier is a times five multiplier nearly identical to the times ten circuitry. And, once again, following this multiplier is an amplifier designated A-2 which amplifies the CW RF to a level sufficient to drive a biphase modulator circuit.

2.1.5 Biphase Modulator and Amplifiers A-3 and A-4

The biphase modulator consists of a simple diode quadrature ring of relatively conventional design. Ordinarily, one can expect 180° phase shift ± 1° from this simple phase flipping circuit. After the biphase modulator two amplifiers designated A-3 and A-4 provide high level drive to the final multiplier designated times three. The output from this multiplier will be on the order of 3-1/2 watts at the final output frequency (1.6 GHz). This level is sufficient to drive the pulsed amplifier chain to a final output at the antenna connector of 2500 watts at a frequency of 1,600 MHz.

2.1.6 Pulse Power Amplifiers

The power amplifiers which are gated on only during the desired pulse transmission duration consists of ceramic triode tubes in a strip-line configuration. These amplifiers are extremely rugged and capable of producing more than the indicated output power levels. The electron tube generic type tentatively selected for this application is the type Y1537, for the lower level stages and the type Y1536 for the output stage; however, lower price units should be investigated.

2.1.7 Power Supply

It should be noted that due to the extremely low duty cycle imposed upon the pulsed amplifiers the power supply need only deliver its maximum current during a very small portion of the operating time. Consequently, the power supply may be very inexpensively constructed utilizing a capacitive discharge output to maintain the necessary current level during the very short burst of pseudorandom pulse sequences. The proposed power supply is designed to convert a nominal 12 volt DC level to several isolated DC outputs required by the LIT transmitter system. These outputs are:

Vout (V)	Iout (ma)	Ipulse (A)	Pave (W)	
+1200	0.1	1.5	.48	
+ 600	0.1	0.3	.096	
- 50	1	0.8	.058	
- 5	1	0.05	.001	
+ 28	20	1.12	.594	
+ 5	500	0	4.000	(Including Regulator Loss)
			5.253 = Ptotal	

The power supply will utilize a standard DC-DC converter configuration (magnetic inverter-rectifier-filter). The +5V output (for the digital circuitry) is regulated and an additional 24 volt regulated output is derived from the +28V output for the crystal oscillator. These regulators will use integrated circuit techniques. The expected 12V input power is 6.6 watts for a nominal average input current drain of approximately 0.55A for Configuration "B". The power supply for all configurations is similar except designed for the higher or lower power requirements.

The high pulse current requirements are handled through capacitor energy storage techniques. The expected voltage drop during the pulse duration is less than 10%.

2.1.8 Code Generator

The following describes a possible design for the code generator. The LIT code generator produces sequence bursts of 511 bits at a rate of 10 MB/s. The bursts are repeated every one to 1.1 seconds. The repetition rate is selected between one and 1.1 seconds with a resolution of 10μs, thus providing 10,000 distinguishable rates (Frame Identification). The Timing Diagram of Figure 3 illustrates the process. Generation of the code burst is implemented by the micro-programmer and code generator illustrated by Figure 4.

The run rates of the micro-programmer are derived from a divider chain which is driven by a 10 MHz TCXO. Resettable decimal dividers are used to produce the desired frequencies of 100 kHz and 1 kHz. 10 MHz is available from the TCXO whose output is also delivered to the transmitter. (Note that the multiplier-amplifier indicates an oscillator in the chain; however, only one oscillator is required.)

At Reset Time all counters are reset to zero. The mode counter, now in 00 mode (compare Figure D-2), selects the 10 MHz clock and produces a Transmit Enable pulse which lasts for the duration of the code burst (51.1μs). This pulse also opens the clock gate for the PN generator which produces the 511 bit sequence starting with a vector which was loaded previously. During the 00 mode, the program counter counts to 512. This count is decoded and steps the mode counter to 01. Simultaneously, the PN generator is reset. In the 01 mode, the 1-kHz clock is selected by the clock commutator. The programmer counts to 1512 - the 01 mode lasts one second - then steps the

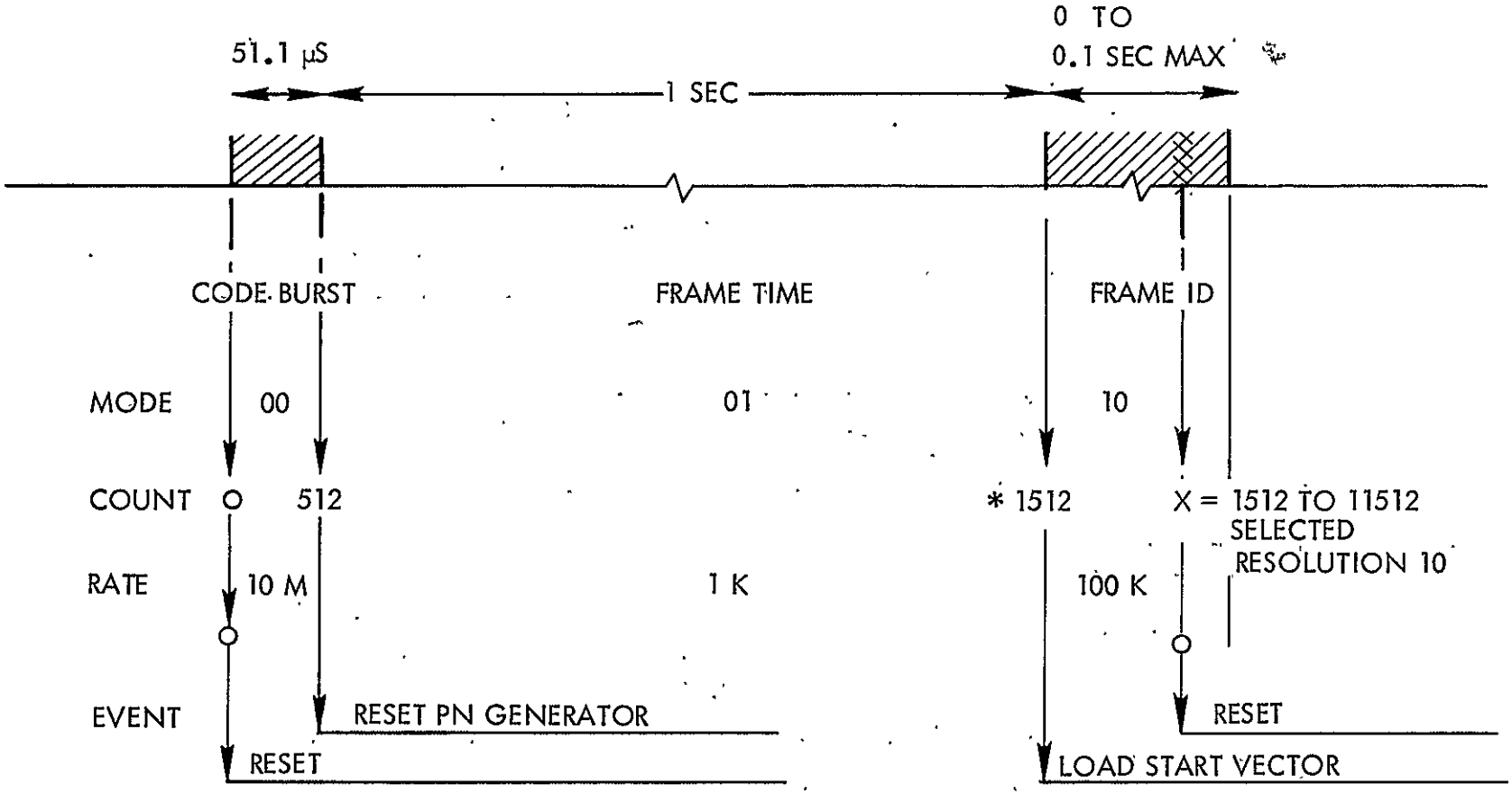

* NOTE: PRP'S ARE ACTUALLY BETWEEN 1.0 SEC +51.1 μSEC AND 1.1 SEC +51.1 μSEC

Figure D-2. LIT Code Generator Timing Diagram and Microprogrammer Mode Table

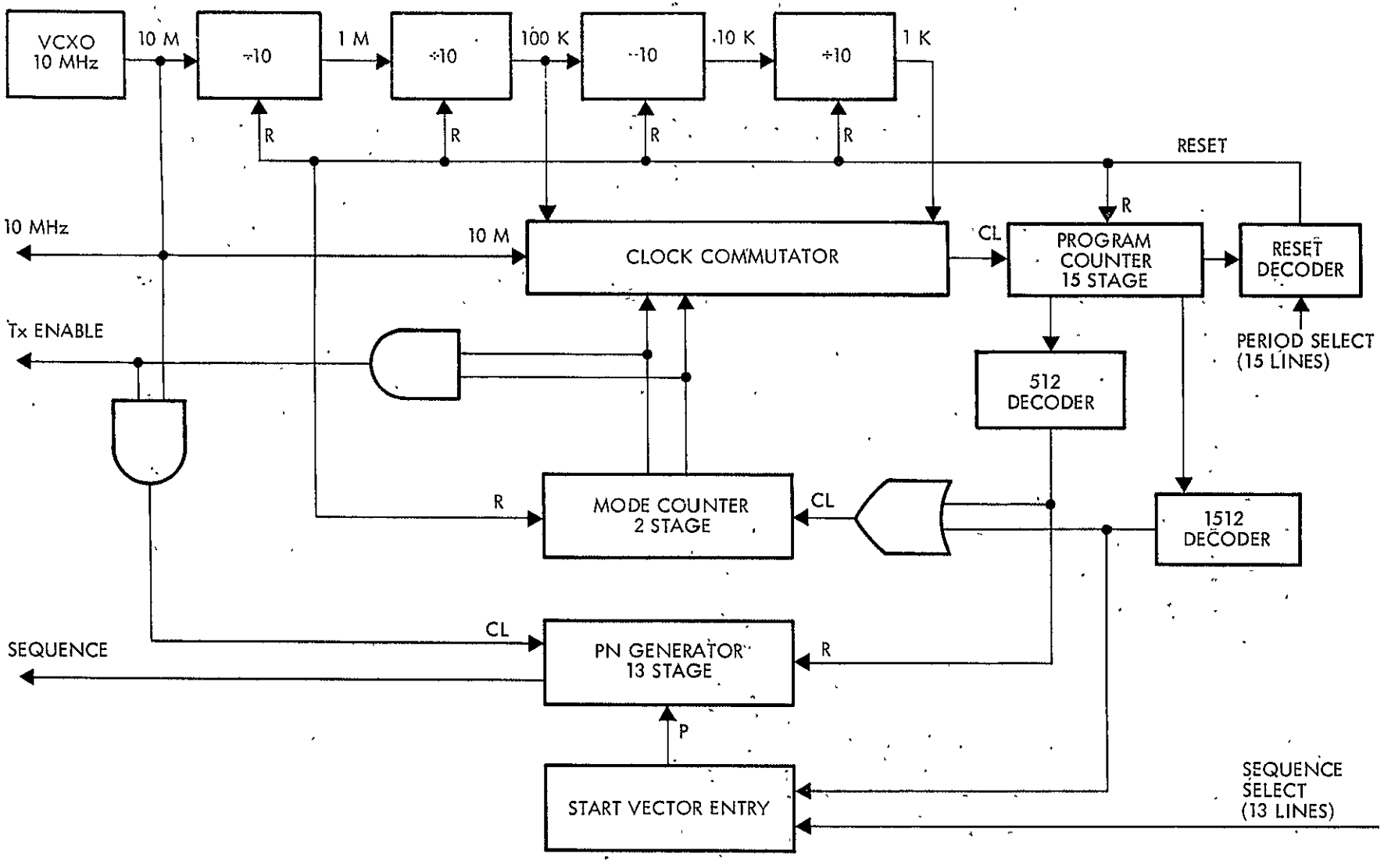

Figure D-3. LIT Code Generator Block Diagram

mode counter to 10 via the 1512 decoder. Simultaneously, the desired start vector is loaded into the PN generator. In the 10 mode the program counter is clocked at 100 kHz until the Reset Decoder detects coincidence with a selected number between 1512 and 11512. Fourteen binary lines are necessary for this selection (Period Selection).

The code is generated by a 13-stage maximum linear code generator. 16 non-overlapping segments of the $2^{13} - 1$ bit sequence are selected by loading appropriate start vectors. Thirteen binary lines are needed for this selection.

It is expected that the code generator will be LSI technology. Its implementation is facilitated by using many identical elements, thereby reducing the mask generation effort considerably.

2. CONFIGURATIONS B AND C

Configurations B and C are shown in Figure D-4. (Note: No block diagram is shown for Configuration D, which is similar to Figure D-4 except that is has one less pulse amplifier.) In many respects these two configurations are similar to Configuration A. The differences are primarily an X-3 multiplier in place of an X-5 multiplier and a lower power level required from the amplifier/multiplier chain.

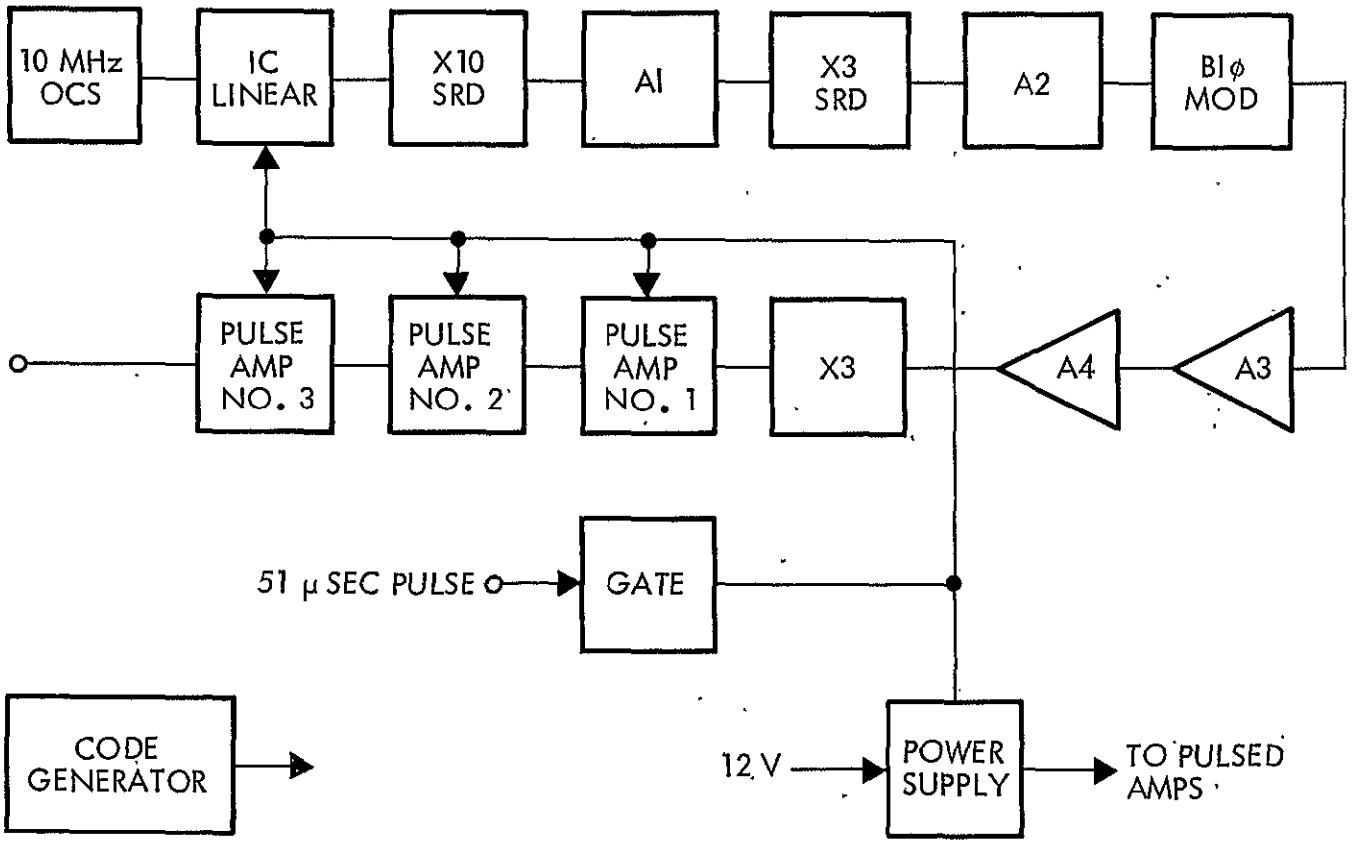

NOTE: CONFIGURATION D
IS SIMILAR TO CONFIGURATION C
BUT HAS ONE LESS PULSE AMPLIFIER

Figure D-4. LIT Transmitter Model C

3. LIT RFP GROUNDRULES

You are requested to observe the following groundrules in the preparation of your quotation to TRW:

1) We wish to have pricing on Models A. B. and C. If you should chose to price only one model, we desire that it be Model B.

2) Assume commercial avionics quality standards and component reliability.

3) Assume a fixed design and released manufacturing drawings will be available from a previous government sponsored development program.

4) Transmitter units consist of:

   One (1) R.F./Digital black box 6" x 10" x 3 1/2" (R.F. sealed), which is made of one (1) double sided PCB which requires R.F. stage separation. Gaskets required between top and bottom covers.

5) The installation kit is to consist of:

   One (1) appropriate antenna, interconnecting cable of nominal length, and installation hardware (mountings, brackets, etc.) for transmitter and antenna.

6) Automatic conformal coating is suggested.

7) End item acceptance testing should consist of functional tests at room temperature for transmitter and antenna. The units may be tested separately or together; however, the transmitter and antenna are not to be considered as "matched pairs".

8) You should assume in-line tuning and testing during the assembly operation.

9) The costing is to be based on continuous production runs in the quantities of 2,500 units and 10,000 units. Unit cost summary

sheets are provided, as Attachment 4 to this RFQ, for your convenience.

10) Costing should be based on today's dollars. We do not wish economic inflation factors to be considered at this time.

11) An unpriced parts list for each model is requested.

12) Define your optimum build time span for production runs of 2,500 and 10,000 units.

13) Your total selling prices should be stated FOB point of manufacture.

14) Realizing that this program is in the concept stage, we request that your pricing be your best budgetary and planning estimate.

15) Should, after your review of the attached technical documents, you wish to propose an alternate model of your design, please feel free to do so. We wish to note we have utilized a multiplexer/amplifier approach as illustrated in the typical block diagram in the technical discussion. Any alternate design proposal rational should have as its target an ultimate low cost unit ($400 or less).

4. RESPONSES

4.1 Bendix Avionics Division

Bendix

Avionics Division

Mr. C. T. Gibson
Subcontracts Manager
Electronic Systems Division
TRW Systems Group
TRW Inc.
One Space Park
Redondo Beach, California 90278

August 27, 1970

Reference: Request for Quotation 70-2376-RS-047
Location/Identification Transmitter
Dated 7 August 1970

Dear Mr. Gibson:

The general parameters of the RFQ represent an interesting industry challenge.

A preliminary review of the proposal indicates that the normal ATC transponder concept would not be applicable to this satellite program.

On an educated guess basis, pricing for the Location/Identification Transmitter (L.I.T.) meeting your requirements and designed for the general aviation market could be expected to sell in the price range of $3,000 to $4,000 in a quantity of 2,500 units and an increase to 10,000 units could reduce the price to the range of about $2,500 to $3,000 each. These prices would be in the category of that paid by the normal end user in the general aviation market.

We well realize prices indicated above are considerably higher than the $400 target you had indicated. We can foresee substantial cost reduction becoming possible in the future as the state-of-the-art develops and low cost, high power, solid state devices become available which could replace today's requirement for vacuum tubes.

Bendix

Avionics Division

Mr. C. T. Gibson
Page two
August 27, 1970

Bendix certainly would be willing to work further with TRW in developing the airborne equipment for the satellite concepts you are interested in.

Sincerely yours,

Herb Sawinski
General Sales Manager
General Aviation Sales

HS:gs

cc: R. M. Winston
E. D. Hart
L. R. Yates

4.2 Collins Radio Company

COLLINS RADIO COMPANY • CEDAR RAPIDS

COLLINS

Cedar Rapids, Iowa 52406 Area Code 319 395-1000 Cable: COLINRAD

4 September 1970

TRW
Systems Group of TRW Inc.
One Space Park
Redondo Beach, California
90278

Attention: Mr. C. T. Gibson
Subcontracts Manager
Electronic Systems Division

Subject: Request for Quotation 70-2376-RS-047
Location/Identification Transmitter

Reference: (a) TRW Letter dated 18 August 1970

Gentlemen:

Collins Radio Company is pleased to have the opportunity to review the operational and hardware requirements for the proposed Location/Identification Transmitter (LIT) for air traffic control application. We recognize the criticality of this problem and realize, as you, that general aviation must be included in the ATC scheme. Based on the specification that you outlined for the LIT models A, B, and C and realizing that these specifications may change considerably over the next few years before an operational system exists, we arrived at an estimated "ball park" sell price of these equipments. These prices do exceed your desired $400.00 price by a considerable amount, however, the specified frequency of operation, stability, power output, and pulse length necessitated a more costly design. We realize the importance of each of these parameters in achieving an adequate aircraft-to-satellite power budget however, if these parameters could be relaxed, the system price would decrease. Additionally, you must consider that our design methods and manufacturing processes are more geared to the commercial and business aviation class market rather than the light, private aircraft market. Thus, our estimate may be more appropriate for former class of market.

The following are our price estimates for the three LIT models, A, B, and C.

	Model A	Model B	Model C
Qty. 2,500	$3,000 - $4,000	$2,000 - $3,000	$2,000 - $3,000
Qty. 10,000	$2,500 - $3,500	$1,500 - $2,500	$1,500 - $2,500

The above prices do not include the aircraft antenna or installation kit.

I hope that this information is useful to TRW in your study. Collins Radio Company would certainly appreciate a copy of your report if that would be possible.

If additional information is desired, please contact the undersigned at Area Code 319, 395-2044.

Very truly yours,

Richard A. Albinger

Richard A. Albinger
Manager, Space Systems Sales

RAA:mld

4.3 King Radio Corporation

KING RADIO CORPORATION

400 N ROGERS ROAD • OLATHE, KANSAS 66061 • (913) 782-0400 • TELEX CODE 4-2299

August 20, 1970

TRW Systems Group
TRW Inc.
One Space Park
Redondo Beach, California 90278

Attention: Mr. C. T. Gibson
Subcontracts Manager
Electronic Systems Division

Subject: RFQ 70-2376-RS-047
Location/Identification Transmitter

Reference: (1) Your Mr. J. H. Craigie's telecon of August 19 with R. C. Christie, King Radio Corporation Vice President of Marketing

(2) Your letter of 7 August 1970

Dear Mr. Gibson:

As indicated to Mr. Craigie by Mr. Christie in the reference telecon, King Radio Corporation has been unable to allocate extensive effort toward responding to the subject RFQ. We have, however, undertaken an abbreviated investigation, the results of which may be of interest to TRW.

In considering LIT Model B, and thinking in terms of a 10,000 production quantity in an approximate two year production run, we would estimate an FOB factory price of $555.00 per LIT for the transmitter mechanical parts and case, plus an estimated $90.00 for the LIT code generator subassembly which would encompass two large scale integrated chips, plus an estimated $45.00 for an appropriate installation kit and antenna; yielding a total Model B price of $690.00 per unit. For your reference, our current factory FOB price for a TSO'd ATC transponder system, including installation kit and antenna, is approximately $550.00, this price applicable to a production rate on the order of 100 units per month with perhaps 5,000 units as a production base. We would further note for your reference that general aviation transponders of non-TSO'd configuration are presently on the market with an FOB factory price on the order of $250.00; the

⊕2

production and projected build quantities of these devices is not known to us.

In summary, it would appear, based on our estimates, that the LIT unit of the Model B configuration can be reasonably expected to cost 1.5 to 3 times as much as envisioned ATC transponder units which might be offered in a similar time frame and in like quantities.

We trust the foregoing information will be of some assistance to you. We regret that sufficient engineering time could not be allocated to prepare a complete and detailed response to the subject RFQ.

Very truly yours,

KING RADIO CORPORATION

J. E. Rosenlieb
Manager, Airline Sales

JER/ceh

4.4 Wilcox

WILCOX

AN AMERICAN-STANDARD COMPANY

28 August 1970

TRW Systems Group
TRW Incorporated
One Space Park
Redondo Beach, California 90278

Attention: C. T. Gibson
Subcontracts Manager

Subject: RFQ 70-2376-RS-047 LIT

Gentlemen:

This is in response to your letter of 7 August 1970 requesting cost estimates for a low cost Location/Identification Transmitter. After reviewing the description of the LIT, it is our opinion that $400.00 per unit is unrealistic at the present "State of the Art" of the industry.

From our preliminary estimates, it appears that Model "A" could sell for $950.00 and Model "B" for approximately $850.00. These prices would be direct to consumer prices and do not include any distributor fees.

The above estimates are naturally very preliminary and are based on our experience with this type of equipment.

We are very interested in this program and would appreciate the opportunity for a more "in depth" study as this program progresses.

Very truly yours,

AMERICAN-STANDARD, INCORPORATED

D. B. Hickman
Marketing
Wilcox Division

DBH/11

14TH AND CHESTNUT KANSAS CITY, MISSOURI 64127 816 231-0700 TELEX: 042251 • CABLE: WILCOLEC

APPENDIX E

PULSE DETECTION AND FALSE ALARM RATES DUE TO THERMAL NOISE AND CROSSTALK

The idealized LIT ground receiver is shown in Figure E-1. This consists first of a simple zero loss IF delay line, of total length T_l, with N_b taps at intervals τ, and tap polarities corresponding to the code structure to which it is matched. The delay line output then ideally consists of a single square IF pulse having duration τ. This is filtered in an IF bit matched filter with impulsive response matched to the τ pulse. The bit filter output is envelope detected and a received pulse is recorded whenever the envelope detector output exceeds a prescribed threshold, E_t.

The following parameters are defined for this analysis:

N_b = code length bits (e.g., 511)
τ = chip time (e.g., 10^{-7} sec)
N_u = number of other users (e.g., 10^5)
T = average repetition period (e.g., 1 sec)
T_l = signal pulse length = $N_b\tau$
D = duty cycle = T_l/T (e.g., $5.1 \cdot 10^{-5}$)
S_i = rms input signal
n_i = input noise power spectral density
C_i = rms crosstalk signal level

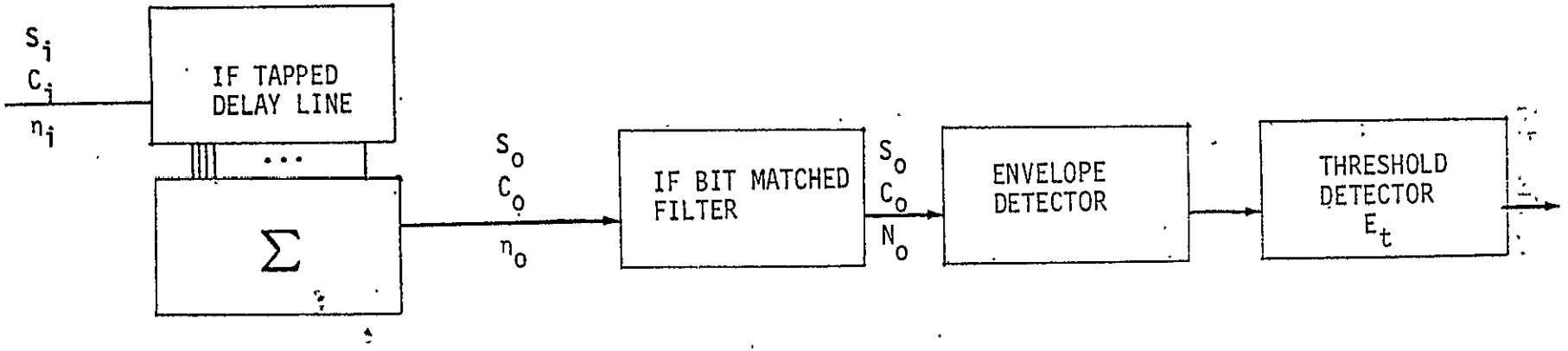

Figure E-1. Idealized Digital Pulse Compression Receiver

Signal, Noise and Crosstalk Response

For a signal matched to a particular delay line, the rms output signal is

$$S_o = N_b S_i$$

The various noise elements, on the other hand, are independent and add incoherently, yielding an output noise density.

$$n_o = N_b n_i$$

The effective IF bandwidth of the bit matched filter is just $1/\tau$ so the mean square noise at the bit filter output is

$$N_o^2 = n_o/\tau$$

$$= N_b n_i/\tau$$

For an interfering signal that just happens to be overlapped n bits, ($0 < n < N_b$, n not necessarily integral) into the delay line, the conditional variance of the crosstalk output if the interfering signal was uncorrelated with the desired signal would be

$$\text{var}_{ind}\ (C_o|n) = n\ C_i^2$$

n itself is a random variate which may coveniently be considered as the product of

1) the conditional probability of n given that there is any overlap and

2) the probability of any overlap.

The former is taken as a uniform distribution over 0 to N_b, or,

$$P\ (n|\text{overlap}) = \frac{1}{N_b}$$

The corresponding conditional variance is

$$\text{var}_{ind}(C_o|\text{overlap}) = \int_o^{N_b} \text{var}_{ind}(C_o|n) \cdot P(n|\text{overlap})\ dn$$

$$= \frac{N_b\ C_i^2}{2}$$

The above holds only for independent binary modulation sequences as if chosen from random number tables. This result may be generalized slightly to allow for some degree of average systematic correlation (positive or negative) between signals by defining a factor M (unity for independent sequences) such that

$$\text{var}\,(C_o|\text{overlap}) = M^2\,\text{var}_{ind}(C_o|\text{overlap})$$

$$= \frac{M^2 N_b\, C_i^2}{2}$$

or

$$\text{var}\,(C_o|\text{overlap}) = F^2\, C_i^2$$

The quantity

$$F = \frac{\sqrt{\text{var}\,(C_o|\text{overlap})}}{C_i}$$

$$= \sqrt{\frac{M^2 N_b}{2}}$$

is the "rms code correlation" commonly used in published studies of the aperiodic correlation properties of radar pulse code sequences. M is a figure of merit expressing how much better or worse the code is than random independent sequences. Peak correlations can also be conveniently normalized by the same factor by expressing

$$\max\,(C_i|\text{overlap}) = \hat{M}\sqrt{\frac{N_b}{2}}$$

2. Effective Signal/Noise Ratio

The probability of any overlap for any particular interferer is

$$\text{prob}\,(\text{overlap}) = 2D$$

where D is the duty cycle so the variance of crosstalk due to any particular interferer is

$$\text{var}\,(C_o) = \text{var}\,(C_o|\text{overlap}) \cdot \text{prob}\,(\text{overlap})$$

$$= M^2 N_b\, D\, C_i^2$$

and for all other users, the total crosstalk power is

$$C_o^2 = N_u\, \text{Var}\,(C_o)$$

$$= M^2 N_u\, N_b\, D\, C_i^2$$

Thus, the total (signal)/(noise + crosstalk) ratio is

$$R = \frac{S_o^2}{N_o^2 + C_o^2}$$

$$= \frac{N_b^2 S_i^2}{N_b \eta_i / \tau + M^2 N_u N_b D C_i^2}$$

$$= \frac{1}{\left(\frac{\eta_i}{N_b \tau S_i^2}\right) + \left(\frac{M^2 D N_u C_i^2}{N_b S_i^2}\right)}$$

Noting that

$$N_b \tau S_i^2 = E$$

the total signal energy

we define

$$R_s = \frac{\text{signal energy}}{\text{noise density}}$$

$$\boxed{R_s = \frac{E}{\eta_i}}$$

$$R_c = \frac{\text{signal power}}{\text{crosstalk power}}$$

$$= \frac{N_b S_i^2}{M^2 D N_u C_i^2}$$

$$\boxed{R_c = \frac{T S_i^2}{M^2 \tau N_u C_i^2}}$$

Then, the effective output signal/(noise + crosstalk) ratio becomes

$$R = \frac{1}{\frac{1}{R_s} + \frac{1}{R_c}}$$

Notice that R is less than the smaller of either R_s or R_c. For present parameters and assuming pessimistically

$$M = 1$$
$$T = 1 \text{ sec}$$
$$\tau = 10^{-7} \text{ sec}$$
$$N_u = 10^5$$

and

$$S_i^2 = C_i^2$$

then

$$R_c = 20 \text{ db}$$

which is the limiting effective signal/noise ratio.

3. False and Missed Alarms for Gausian Noise

If we assume that the distribution of effective noise (real noise plus crosstalk) is Gaussian like that of the thermal noise, then the results of the classical radar pulse detection analysis are applicable to the problem of missed and false alarms. This proceeds as follows:
In general, the detection probability of a signal S, (rms) with noise N, and threshold E is given by Marcums Q function

$$P_d = Q(R,\beta) = \int_{\beta}^{\infty} x\, e^{-(R + \frac{x^2}{2})} I_o(\sqrt{2R}\,x)\, dx$$

where

$$R = \frac{S^2}{N^2} = (E/\eta_i) \qquad \text{(energy ratio)}$$

N = rms noise ,

$$\beta = E_t/N \qquad \text{(normalized threshold setting)}$$

For False Alarms, i.e., when no signal is actually present, we have simply

$$P_{fa} = Q(0,\beta)$$

$$= \int_{\beta}^{\infty} x\, e^{-x^2/2}\, dx$$

$$\boxed{P_{fa} = e^{-\beta^2/2}}$$

Independent opportunities for such false alarms occur at the rate of the bandwidth of the noise which, for the matched filter is $1/\tau$. Thus, the number of false alarms per second is

$$N_{fa} = P_{fa}/\tau$$

$$\boxed{N_{fa} = \frac{1}{\tau} e^{-\beta^2/2}}$$

The probability of missing a particular pulse is

$$P_m = 1 - P_d$$

$$= 1 - Q(R,\beta)$$

However, the coast mode operates so that a track is not given up for lost until N_t (= 2 or 3) pulses in a row are lost. Thus, the probability of losing track of a particular aircraft in a particular frame period is

$$P_{\ell t} = (P_m)^{N_t}$$

or the probability of losing track of a particular aircraft in a particular second is

$$P'_{\ell t} = P_{\ell t}/(N_t T)$$

Finally, if the total number of users, N_u is divided uniformly into N_c code sets, so that a particular receiver is handling just N_u/N_c aircraft, the expected number of lost tracks in that receiver per second is

$$N_{\ell t} = (N_u/N_c)\, P'_{\ell t}$$

$$\boxed{N_{\ell t} = \frac{N_u}{N_t N_c T}\, (1 - Q(R,\beta))^{N_t}}$$

Finally, note that each false alarm automatically enters the sort mode and each lost track signal eventually reenters via the sort mode, so that the number of new signals entering the sort mode per second, N_s (i.e., not counting repetition of lost track signals which have already entered the sort mode) is

$$N_s = N_{\ell t} + N_{fa}$$

$$\boxed{N_s = \frac{1}{\tau} e^{-\beta^2/2} + \frac{N_u}{N_t N_c T} \left(1 - Q(R,\beta)\right)^{N_t}}$$

where

R = effective $S/(C + N)$ ratio (equation 23) $= \dfrac{1}{\frac{1}{R_s} + \frac{1}{R_c}}$

$R_s = E/n_i$

$R_c = \dfrac{T}{M^2 \tau N_u} \left(\dfrac{S_i}{C_i}\right)^2$

E = total signal energy

n_i = input noise spectral density

T = total pulse length (≈ 51 μsec)

τ = chip length ($\approx .1$ μsec)

M = code correlation figure of merit (≈ 1)

$(S_i/C_i)^2$ = signal/crosstalk input power ratio

N_u = number of users

N_c = number of codes

β = normalized threshold setting $= E_t(\tau/\eta_i)^{1/2}$

N_t = number of tracks in coast mode before giving up for lost

$Q(R,\beta)$ = Marcums Q function

$$= \int_{\beta}^{\infty} x e^{-\left(R + \frac{x^2}{2}\right)} I_o\left(\sqrt{2R}\, x\right) dx$$

N_s is the most important single criterion of system performance since it is estimated that N_s must be held to something between 10 and 100 per second in order to avoid saturation of the pulse sort computer. It should be pointed out that

1) this formulation assumes most pessimistically, that <u>all</u> pulses are of strength S_i for the purposes of detection, but are C_i/S_i greater for the calculation of interference
2) direct interference of pulses on the same code is ignored
3) β should ideally be chosen to minimize N_s.

Computations of N_s as a function of the parameters effecting it were made. The optimum threshold setting was computed to minimize N_s. Some of the results are shown in Figures 27 and 28 in Section 4.2.3 for various combinations of parameters and the threshold β optimized for minimum N_s. For the purpose of interference or crosstalk calculation, the signal was in all these cases taken 7 db greater. All results are for T = 1 sec (frame).

APPENDIX F
BIPHASE CODING STUDY

In the LIT system aircraft transmit coded pulses which are relayed by satellites to the ground where aircraft position is computed. Since no synchronization is assumed to exist it is possible for several pulses to arrive simultaneously at the receiver. A set of codes was obtained which possess good aperiodic auto and crosscorrelation properties so that the interference will be minimized for signals fully or partially overlapping the desired signal. The three types of binary codes which were evaluated were m-sequence codes, subsequences of long m-sequence codes, and codes formed by concatenating short sequences. Best performance was obtained with a set of sixteen 511 bit disjoint subsequences of an 8191 bit m-sequence which provide peak aperiodic auto and crosscorrelation sidelobes of $47/511 = 0.092$. Histograms for the aperiodic auto and crosscorrelation were computed and partial Doppler performance results obtained.

1. EVALUATED BINARY CODES

1.1 M-Sequence Codes

M-sequences, or maximal length shift register sequences, are known to have ideal periodic autocorrelation functions. Certain M-sequences of lenghts up to 255 bits are also known to have good aperiodic autocorrelation functions (Refs. F-1 and F-2.) To determine the aperiodic crosscorrelation between pairs of 511 bit m-sequences, several polynomials were selected from Peterson's tabulation (Ref. F-3 arbitrary initial conditions were assigned, and the correlations were computed. The results are shown in Table F-1. The peak crosscorrelation is seen to be relatively high with a considerable variation between the different pairs of sequences. The aperiodic autocorrelation for polynomial 01617* with initial state -1, 1,-1, 1,-1,-1, 1, 1,-1 was computed and the peak sidelobe found to be $\frac{25}{511} = 0.0489$, or $1.1\sqrt{511}$ which exceeds the estimated optimum $0.6\sqrt{L}$ (L being the sequence length in bits) relationship found by Boehmer (Ref. F-4.)

The performance of the set of 511 bit M-sequences was disappointing. It is likely that the crosscorrelation between pairs of sequences could be minimized by a judicious choice of initial conditions. However, there is no known method for choosing initial conditions for sequences to minimize the mutual aperiodic crosscorrelation between all pairs of a given set of 511 bit m-sequences, and a brute force exhaustive computation is out of the question. It is of interest to note that although the sequences generated by polynomials 1131 and 1617 exhibit a periodic crosscorrelation of $\frac{33}{511}$ with reference sequence 1021 (Ref. F-5), the aperiodic absolute peak crosscorrelation between the two for the initial states indicated in Table F-1 is seen to be $\frac{77}{511}$. This indicates that low periodic crosscorrelation between certain pairs of m-sequences does not imply mutually low aperiodic crosscorrelation.

*Polynomials are specified in octal notation

Table F-1. Results of Aperiodic Crosscorrelation Between Pairs of 511-Bit M-Sequences

Polynomial	Initial State	Peak Crosscorrelation With the Reference	
		Positive	Negative
01131 (Reference Polynomial)			
01743	-1 1 -1-1 1 1-1 1 1	61	-83
01617	-1 1 -1 1-1-1 1 1-1	71	-77
01563	-1-1 -1-1-1-1-1 -1-1	78	-54
01713	-1-1 -1-1-1-1-1 -1-1	52	-45
01533	-1-1 -1-1-1-1-1 -1-1	51	-56

1.2 Subsequence Codes - Codes Which are Disjoint Subsequences of Long M-Sequences

In the study of the synchronization of long m-sequences, Gold has tabulated the maximum crosscorrelation between all subsequences of a given length with the periodic full m-sequence for all possible alignments (i.e., shift positions). Although the aperiodic crosscorrelation can be as much as twice the maximum periodic crosscorrelation (Ref. F-4), it was conjectured that a set of codes with mutually low aperiodic crosscorrelation could be obtained by splitting the m-sequence into all possible disjoint subsequences of length 511 bits.

The experimental verification of this conjecture was obtained by computing the aperiodic crosscorrelation between two 511 bits disjoint subsequences of a m-sequence. The result revealed the surprising fact that the maximum aperiodic crosscorrelation is equal to the maximum periodic crosscorrelation tabulated by Gold (Ref. F-6).

As the length of the subsequences is made a larger fraction of the parent m-sequence the maximum crosscorrelation among the disjoint subsequences decreases. However, the number of disjoint subsequences available also decreases. There appears to exist a sphere packing type of relationship where the maximum aperiodic crosscorrelation among the disjoint subsequences of fixed length must increase as the number of subsequences, or codes, is increased For example, the two disjoint 511 bit subsequences of the parent 1023 bit sequence generated by polynomial 02157 were found to have a maximum aperiodic crosscorrelation of 35. To obtain 16 disjoint subsequences (or codes) of length 511, a parent m-sequence of length 8191 is required; the maximum aperiodic crosscorrelation in this case is 47.

The procedure for obtaining subsequence codes is to first choose the length of the code (constrained to 2^n-1) and the number of codes desired. Multiplying the number of codes times the length of the subsequence gives the length of the parent m-sequence. With the length of the m-sequence and the length of the subsequence code enter Gold's tabulation (Ref. F-6) to find the optimum polynomial. The initial state for each subsequence code is obtained by computing the state of the parent m-sequence at multiples of the subsequence length. To what extent the correlation properties can be improved by selecting the initial states is unknown. A study of the weight distribution of the sequences would shed light on this question.

It should be emphasized that different polynomials are optimum for different code lengths and different numbers of codes. The longest m-sequence in Gold's tabulation is $2^{13}-1 = 8191$; if a longer code length is desired, all polynomials of the required degree would have to be searched to find the optimum. If, for example, 32 disjoint 511 bit subsequences are desired, the 376 primitive polynomials of 14^{th} degree (length = $2^{14}-1$ bits) would have to be searched to find the best one. Thus, Gold's work on the synchronization of m-sequences has provided valuable data used for constructing sets of codes with mutually low aperiodic crosscorrelation. However, because of the limitation on Gold's tabulation of optimum polynomials the maximum m-sequence investigated was $2^{13}-1$ bits long, resulting in a maximum of 16 subsequence codes of 511 bits.

It can be shown using Gold's results that for any two fully overlapped codes (i.e., the interfering signal extends over all 511 bits) the cross-correlation cannot exceed $\frac{47^*}{511}$. The question arises if when the codes are partially overlapped whether the maximum crosscorrelation is still less than or equal to $\frac{47}{511}$. The actual calculation of the aperiodic crosscorrelation for all values of overlap showed the peak correlation to be less than or equal to $\frac{47}{511}$ for all of the four codes tested. The autocorrelation was also found to have peak sidelobes slightly less than $\frac{47}{511}$. To verify that the unnormalized correlation remains at or below 47 for all of the 120 possible pairs of the sixteen 511 bit subsequences by direct computation would require excessive computer time. A more efficient computation procedure is to analyze the maximum and minimum Hamming weights for all subsequence lengths.

In the correlation operation two codes are multiplied and the product integrated over an interval corresponding to the aperiodic overlap. For binary codes multiplication is equivalent to modulo two addition. Since the different codes are subsequences of the same m-sequence, the modulo two addition of any two subsequences of any length results in a subsequence of the parent m-sequence by the well-known shift and add property of m-sequences (Ref. F-7). The integration over the subsequence is equivalent to subtracting the number of zeros in the sequence from the number of 1's (or if +1, and -1's are used, summing the +1's and -1's algebraically). Consequently, the integral can be bounded by computing the maximum and minimum Hamming weight.

If $W_{1\ max}$ is the maximum number of 1's (i.e., the maximum weight) in any subsequence of length L, then the minimum number of zeros is,

---

*For the 16 disjoint subsequences of a 2^{13}-1 m-sequence.

$W_{0\ min} = L - W_{1\ max}$, and the maximum aperiodic crosscorrelation for any pair of disjoint subsequences with overlap of L bits is

$$\rho_{max} \leq W_{1\ max} - W_{0\ min} = 2\,W_{1\ max} - L \quad .$$

Similarly, the minimum (or maximum negative) aperiodic crosscorrelation can be obtained from knowledge of the minimum Hamming weight. If $W_{1\ min}$ is the minimum number of 1's in any subsequence of length L, then the minimum crosscorrelation is

$$\rho_{min} \leq 2\,W_{1\ min} - L \quad .$$

For the LIT application where the absolute phase of the signal carrier frequency is unknown, the positive and negative peak aperiodic crosscorrelation (ρ_{max} and ρ_{min}, respectively) are equally important performance characteristics. It is of interest to note that for subsequence lengths of 2^n-1 bits, the bounds on ρ_{max} and ρ_{min} were equal in Gold's tabulation, indicating for these lengths the worst case always occurs.

Verification that the maximum aperiodic crosscorrelation between any two pairs of 511 bit subsequences is $\frac{47}{511}$ using the Hamming weight concept was not completed for the study due to some unforseen computer problems. Partial results obtained indicate that the peak (unnormalized) crosscorrelation for any overlap from 46 to 81 bits is less than or equal to 27.

In an effort to increase the number of code words to more than 16, the code words provided by disjoint subsequences of the parent subsequence run backwards

in time (i.e., generated by the reciprocal polynomial) were evaluated. For sixteen disjoint 511 bit subsequences the best parent 8191 bit m-sequence polynomial listed by Gold was 27537. The reciprocal polynomial 37275 was found (as expected) to provide subsequences which, among themselves, provide equivalent performance. Crosscorrelation between subsequences from the original and the reciprocal polynomials, however, was substantially higher ($\frac{58}{511}$) vs $\frac{47}{511}$. Thus, to increase the number of code words by this means, it is apparently necessary to accept a higher crosscorrelation.

A method for increasing the number of code words without increasing the peak crosscorrelation is to use subsequences which are not disjoint. If the initial state of each subsequence is chosen so that there is a 40 bit overlap between the tail end of one sequence and the beginning of the next, the number of sequences can be increased from 16 to 19. When two adjacent sequences are received with a time shift such that the head of one sequence is aligned with the tail of the other the unnormalized crosscorrelation will be 40. For other time shifts the crosscorrelation will be no worse than usual. The introduction of these few conditions when the crosscorrelation reaches 40, still below the peak value of 47, should have only a slight effect on the detection and false alarm probabilities associated with the codes.

1.3 Codes from Concatenating Short Sequences

To obtain a set of codes with mutually low aperiodic crosscorrelation one procedure might be to select a group of short sequences or words and then construct the codes by concatenating the words in different order. Although we are interested in the unsynchronized case, it is possible for an interfering code to have a time delay such that the words in the reference and in the interfering code are exactly aligned; consequently, a necessary

(but not sufficient) condition for low crosscorrelation is that all pairs of dissimilar words exhibit low crosscorrelation. The next problem is to find a way to choose sequences of words to form the codes such that for any integer number of words overlapping the crosscorrelation remains low. Finally, and most difficult, insure that for any partial overlap (i.e., a non-integer number of words) the crosscorrelation is low. An additional constraint is that the code words also have a low sidelobe autocorrelation function so that the user aircraft position can be accurately and unambiguously determined.

Minimum crosscorrelation between fully overlapped word pairs can be achieved by choosing the words from an orthogonal set. The Walsh functions (Ref. F-8) are an obvious choice. To insure that crosscorrelation remains low for an integer number of word shifts, the Reed-Solomon (Ref. F-9) procedure can be used to insure that for codes composed of NW words, the crosscorrelation will not exceed $\frac{1}{NW}$. When the delay or shift between two codes is not an integer number of words the Walsh functions are no longer orthogonal for partial overlap, and the crosscorrelation of the codes cannot be predicted from theory.

Initial attempts to construct a set of codes indicated that it was advisable to limit the choice of Walsh functions to only the sal function (or alternatively, only the cal function) since in the unsynchronized case cal and sal functions can exhibit a crosscorrelation of as high as 0.75.

Preliminary results obtained for 32 bit codes (4 words of 8 bits each) showed a maximum aperiodic crosscorrelation of 9/32 could be obtained; thus, it appeared that the Reed-Solomon limit of 1/NW (equal to 8/32 in this case) could be closely approached.

Subsequent computations for 512 bit codes (16 words of 32 bits each) yielded a crosscorrelation of $\frac{63}{512}$, considerably worse than the limit value of $\frac{32}{512}$. This disappointing result indicated that it is essential to choose the code parameters so that the correlation sidelobes are minimized for shifts not integer multiples of the word length.

In forming codes composed of Walsh function concatenated according to Reed-Solomon codes there are a great many degrees of freedom. With N symbols there are N^2 first order Reed-Solomon codes. However, since N codes are cyclic shifts of a certain sequence, only N out of the N^2 possible codes are usable in the unsynchronized case. The phase or permuted order of each word also can be changed in order to minimize the sidelobes. With sixteen 512 bit codes, each made up of sixteen 32 bit words, there are 120 pairs of codes. The word order in each code can have 16 different initial conditions and each word can have up to 32 different phases. For each pair of codes there are 1023 possible alignment positions (delays). Thus, with billions of possible conditions the selection of word orders and phases to minimize the crosscorrelatior for all code pairs and delays presents a formidable problem.

In order to ascertain the characteristics of the codes a number of experimental computations were made. Reed-Solomon sequences of words were obtained by accumulating integers modulo 32.

It should be noted that this procedure only works for integers relatively prime to 32; generally, operations with polynomials are required. Arbitrarily selecting the integers 3 and 6, two codes were constructed. A computer search over initial conditions indicated that the lowest peak cross-correlation was obtained using the following two word sequences:

Code 3: 4,7,10,13,16,2,5,8,11,14, 1,3,6,9,12, 15

Code 6: 11,6,12,1,7,13,2,8,14,3,9,15,4,10,16,5

The Walsh functions indicated by the numbers are shown in Figure F-1. With the phases as indicated in Figure F-1 the peak unnormalized aperiodic cross-correlation found for the two 512 bit codes was -55 and +63. Since these values are substantially greater than that obtainable with the subsequence codes a further search was made varying the phases of the words. Each of the sixteen words was cyclicly shifted to the left the following number of bits starting with word number 1:

0,3,7,10,14,17,21,24,28,21, 4,8,11,15,18,22 .

This sequence of shifts also has the appearance of a Reed-Solomon sequence. The resulting unnormalized peak crosscorrelation values were found to be -50 and +49, an improvement over the case with no phase perturbations, but still slightly inferior to the subsequence codes which have peaks of 47.

These results for an arbitrary pair of codes, although encouraging, left the question of how to choose the word sequences or phases to minimize the crosscorrelation between all pairs of codes unanswered. Because of the vast

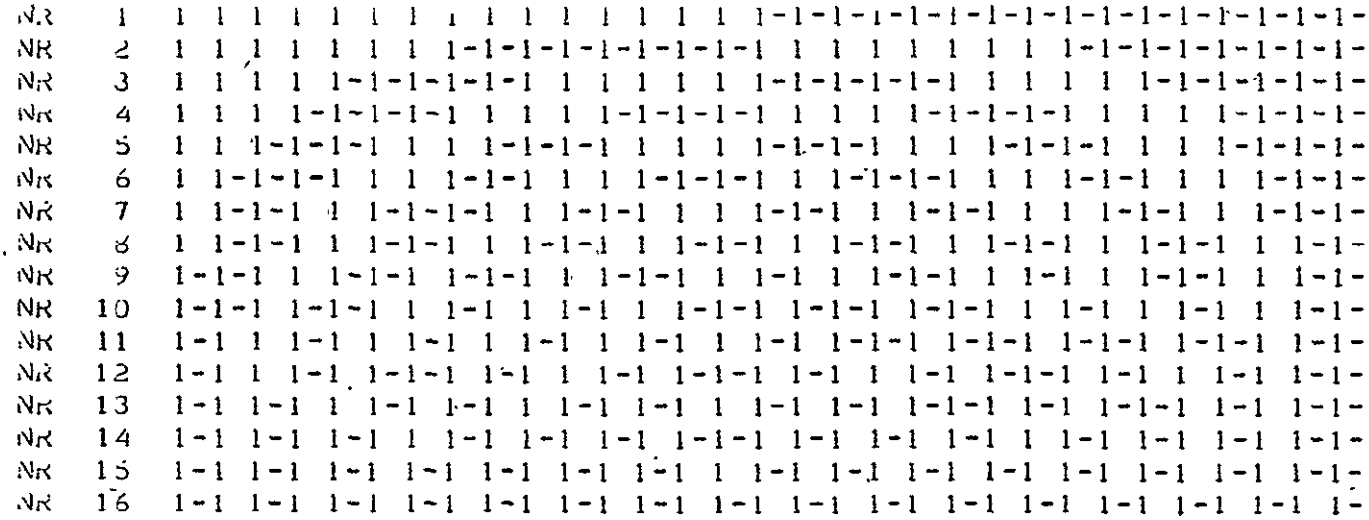

Figure F-1. Walsh Functions

number of possible arrangements it was decided to make a computer search of all the 120 pairs of the sixteen words to find the phases which would minimize the maximum aperiodic peak sidelobes and print the phases corresponding to the eight best values. The result of this minimax calculation showed that it is impossible to choose a set of phase values which will provide the minimum peak aperiodic crosscorrelation for all pairs of words. Although the average minimax unnormalized crosscorrelation was roughly equal to $\sqrt{32}$, certain word pairs showed values as high as 15. These high values occurred for certain pairs of words listed in Figure F-1 with word numbers differing by 8.

To eliminate the high peak crosscorrelation values caused by the periodicities inherent in the 32 bit words, the number of bits in the words was reduced to 31, a prime number, and the minimax calculation repeated. Although a computer failure terminated the run prematurely, sufficient data was obtained to see that it is still impossible to choose phases which will achieve the minimax sidelobe level for all pairs of words. With 31 bit words the peak values were more uniform, as expected, with the average value somewhat less than $\sqrt{31}$.

The minimax sidelobe computations showed the difficulty in achieving the limiting crosscorrelation value of 1/NW for all possible time shifts. It appears that the concatenation of Walsh functions according to Reed-Solomon codes can provide a constructive method for synthesizing a set of codes with relatively low aperiodic crosscorrelation; however, the crosscorrelation still is higher than that obtained with the subsequence codes. Efforts to reduce the crosscorrelation below that provided by the subsequence codes were unsuccessful. The autocorrelation of these codes was not thoroughly examined but is believed to have sidelobes roughly equal to the crosscorrelation.

The problem of reducing crosscorrelation sidelobes is simplified if the codes are constructed by repeating the same short sequence many times with some of the short sequences inverted. Different codes are formed from different short sequences of the same length with different patterns for inverting the short sequences. As a simplified example, consider two 16 bit codes, one constructed from the short sequence 1100 and the other from 1010.

Code 1:	1100	1100	0011	0011
Code 2:	1010	0101	1010	0101

It is seen that the last two short sequences in code 1 are inverted while the second and fourth short sequences are inverted in code 2. The peak values of aperiodic crosscorrelation between the two codes are +1 and -1. Unfortunately, this technique for suppressing the crosscorrelation sidelobes causes high sidelobes in the autocorrelation function for the individual codes.

In an attempt to improve the autocorrelation function of the codes the same m-sequence was mod-two added to each code. A number of computations were made using codes made up of fifteen short sequences consisting of Walsh functions of 33 bits. For computational ease the first 15 bits of the short sequence were taken as the pattern for inverting or not inverting the short sequences. Although this choice of patterns could be improved upon, the crosscorrelation performance of pairs of codes selected at random was very good. Initially, the 511 bit m-sequence generated by polynomial 1617 was mod-two added to the Walsh function sequences. Better results were obtained using the 127 bit m-sequence generated by polynomial 211. In this case the

m-sequence repeated almost four times, but since the m-sequence and the sequence of Walsh functions are relatively prime, the crosscorrelation remained low.

The results of the computation showed that in almost every case the crosscorrelation performance of these codes was better than the codes obtained from subsequences of long m-sequences. The autocorrelation, however, was much worse. The effect of mod-two adding the m-sequence was to degrade the cross-correlation performance over that with the sequence of Walsh functions alone, but, also, the autocorrelation was improved. For a typical code of length 495 bits the unnormalized autocorrelation exceeded 58 in approximately 30 alignment positions. With a matched filter receiver the central peak could be reliably detected with, say, a 10 dB signal-to-noise ratio; however, it is felt that the sidelobe peaks would so complicate the post detection processing that the moderate improvement in crosscorrelation would not justify choosing the Walsh function sequences over the subsequences of long m-sequences.

2. Performance of Subsequence Codes

To provide a basis for the system design the performance characteristics of 511 bit disjoint subsequences of the 8191 bit m-sequence generated by polynomial 27537 were studied. As the signal passes through the receiver matched filter a sequence of values appear at the output which correspond to the autocorrelation function of the signal if the correct signal (i.e., the signal to which the filter is matched) is received or to the crosscorrelation function if an interfering signal is received. The statistics of the output, obviously, are non-stationary. To characterize the output two calculations were made. The histogram of the output values for all possible alignments or delays was computed. Although this suppresses the time varying

nature of the output, it provides a good measure of the ensemble characteristics from which average detection and false alarm probabilities can be calculated. The second calculation computed the crosscorrelation of a reference subsequence and a Doppler shifted version of another subsequence. This was done to note possible degradation of the correlation levels with doppler shift.

The histogram of the aperiodic autocorrelation and crosscorrelation for typical 511 bit subsequences of the 8191 bit parent m-sequence generated by polynomial 27537 are given in Tables F-2 and F-3. The autocorrelation for this sequence shows a peak sidelobe of $\frac{44}{511}$; however, autocorrelation sidelobe peaks of $\frac{47}{511}$ have been found for other subsequences. The largest sidelobes occur with low probability. From the distributions in Tables F-2 and F-3 it is seen that there is about a one percent probability that the un-normalized aperiodic correlation, either auto or cross, has either a negative value less than -36 or a positive value greater than +36. The ten percent points on the distribution occur at about plus and minus 23 which is approximately equal to the square root of the subsequence length. From Lindholm's work (Ref. F-10) we know that the average RMS correlation of all 511 bit subsequences with the full 8191 bit sequence is about 23. Thus, the maximum correlation is only about twice the average RMS for full overlap. These remarks hold for both the aperiodic auto and cross correlation since the histograms of both are nearly the same.

Table F-2. Autocorrelation Histogram

Polynomial 27537
Initial State: -1,-1,-1,-1,-1,-1,-1,-1,-1,-1,-1,-1,-1,-1,-1,
Subsequence Length 511 bits

Unnormalized Correlation Value	Density	Distribution
-44	.001959	.0019588639
-43	.001959	.0039177277
-42	.001959	.0058765916
-36	.005877	.0117531832
-36	.003918	.0156709109
-35	.009794	.0254652302
-33	.003918	.0293829579
-32	.001959	.0313418217
-31	.001959	.0333006856
-30	.005877	.0391774772
-29	.005877	.0450538688
-28	.005877	.0509304603
-27	.007835	.0587659158
-26	.013712	.0724777628
-25	.007835	.0803134182
-24	.013712	.0940254652
-23	.005877	.0999020568
-22	.007835	.1077375122
-21	.011753	.1194906954
-20	.009794	.1292850147
-19	.011753	.1410381978
-18	.009794	.1508325171
-17	.013712	.1645445642
-16	.015671	.1802154750
-15	.007835	.1880507305
-14	.015671	.2037214413
-13	.019589	.2233104799
-12	.019589	.2428991185
-11	.017630	.2605288932
-10	.007835	.2683643467
-9	.011753	.2801175318
-8	.017630	.2977473066
-7	.017630	.3153770813
-6	.019589	.3349657199
-5	.019589	.3545543585
-4	.031342	.3858960802
-3	.021548	.4074436627
-2	.025465	.4329088128
-1	.037218	.4701273262
0	.027424	.4975514202
1	.039177	.5367286974
2	.035260	.5719882468
3	.013712	.5857002938
4	.033301	.6190009794
5	.021548	.6405484619
6	.017630	.6581782566
7	.027424	.6856023506
8	.023506	.7091067169
9	.025465	.7345739471
10	.025465	.7600391773
11	.023506	.7835455436
12	.007835	.7913809990
13	.009794	.8011753183
14	.015671	.8168462292
15	.029383	.8462291671
16	.019589	.8658178257
17	.023506	.8893241920
18	.009794	.8991185113
19	.011753	.9108716944
20	.011753	.9226248776
21	.001959	.9245837414
22	.003918	.9285014691
23	.009794	.9382957884
24	.001959	.9402546523
25	.007835	.9480901077
26	.005877	.9539666993
27	.007835	.9618021548
28	.003918	.9657196825
29	.001959	.9676787463
30	.005877	.9735553379
31	.001959	.9755142018
32	.007835	.9833496572
33	.001959	.9853085211
34	.001959	.9872673849
35	.005877	.9931439765
36	.001959	.9951028404
40	.001959	.9970617042
42	.001959	.9990205681
511	.000979	1.0000000000

Table F-3. Crosscorrelation Histogram

Polynomial 27537
Initial States NR1:-1,-1,-1,-1,-1,-1,-1,-1,-1,-1,-1,-1,-1,-1,-1,
NR2: 1, 1,-1, 1,-1,-1, 1, 1, 1, 1,-1,-1, 1
Subsequence Length 511 bits

Unnormalized Correlation Value	Density	Distribution
-47	.000979	.0009794319
-43	.000979	.0019586639
-40	.000979	.0029382958
-39	.000979	.0039177277
-38	.000979	.0048971596
-37	.000979	.0058765916
-36	.000979	.0068560235
-35	.002938	.0097943193
-34	.003918	.0137120470
-33	.004897	.0186092067
-32	.004897	.0235063663
-31	.007835	.0313416217
-30	.003918	.0352595495
-29	.004897	.0401567091
-28	.009794	.0499510284
-27	.006856	.0568070519
-26	.009794	.0666013712
-25	.012733	.0793339863
-24	.009794	.0891283056
-23	.006856	.0959843291
-22	.009794	.1057786484
-21	.006856	.1126346719
-20	.007835	.1204701273
-19	.007835	.1283055828
-18	.011753	.1400587659
-17	.011753	.1518119491
-16	.014691	.1665034280
-15	.019589	.1860920666
-14	.008815	.1949069540
-13	.013712	.2086190010
-12	.013712	.2223310480
-11	.023506	.2458374143
-10	.021548	.2673849167
-9	.014691	.2820763957
-8	.024486	.3065621939
-7	.015671	.3222331048
-6	.020568	.3426011753
-5	.021548	.3643486778
-4	.026445	.3907933399
-3	.018609	.4094025465
-2	.017630	.4270323913
-1	.026445	.4534769833
0	.032321	.4857962370
1	.028404	.5142017530
2	.034280	.5484618805
3	.028404	.5768854065
4	.023506	.6003917728
5	.026445	.6268364349
6	.022527	.6493633692
7	.022527	.6718903036
8	.022527	.6944172380
9	.023506	.7179236043
10	.029383	.7473065622
11	.024486	.7717923604
12	.019589	.7913809990
13	.015671	.8070519089
14	.014691	.8217433668
15	.016650	.8383937316
16	.012733	.8511263467
17	.016650	.8677768895
18	.015671	.8834476004
19	.011753	.8952007835
20	.007835	.9030342390
21	.009794	.9128305583
22	.006856	.9196865816
23	.010774	.9304603330
24	.003918	.9343780607
25	.007835	.9422135162
26	.011753	.9539666993
27	.010774	.9647404505
28	.005877	.9706170421
29	.003918	.9745347698
30	.002938	.9774730656
31	.001959	.9794319295
32	.005877	.9853085211
33	.002938	.9882468168
34	.001959	.9902056807
35	.001959	.9921645446
36	.001959	.9941234084
37	.003918	.9980411361
40	.000979	.9990205681
43	.000979	1.0000000000

When two signals experience different Doppler shifts the cross-correlation may reach a peak for some time displacement, τ, which is not an integer multiple of the bit duration, T_B. To evaluate the Doppler performance it is necessary to compute

$$R_{12}(\tau) = \frac{1}{L}\int_{\tau}^{NT_B} a(t) \sin \omega_1 t \; b(t-\tau) \sin \omega_2 t \; dt$$

where

$R_{12}(\tau)$ is the crosscorrelation function. $a(t)$ and $b(t)$ are the code sequences of +1 and -1 modulating the carrier frequencies ω_1 and ω_2, respectively,

N = number of bits in the code.

$L = NT_B - \tau$

Let $\tau = MT_B - \tau_o$ with M an integer and $0 \leq \tau_o \leq T_B$. Splitting the integral into segments in which the modulation is constant we have

$$R_{12}(\tau) = \frac{1}{L}\sum_{n=1}^{N-M+1} a_{n+M-1}\, b_n \int_{(n-1)T_B}^{(n-1)T_B+\tau_0} \sin \omega_1 t \sin \omega_2 t \; dt$$

$$+ \frac{1}{L}\sum_{n=1}^{N-M} a_{n+M}\, b_n \int_{(n-1)T_B+\tau_0}^{nT_B} \sin \omega_1 t \sin \omega_2 t \; dt$$

Integrating,

$$R_{12}(\tau) = \frac{1}{2L}\sum_{n=1}^{N-M+1} a_{n+M-1}\, b_n \left[\left(\frac{\sin[(\omega_1-\omega_2)((n-1)T_B+\tau_0)] - \sin[(\omega_1-\omega_2)(n-1)T_B]}{\omega_1-\omega_2}\right)\right.$$

$$\left. - \left(\frac{\sin[(\omega_1+\omega_2)((n-1)T_B+\tau_0)] - \sin[(\omega_1+\omega_2)(n-1)T_B]}{\omega_1+\omega_2}\right)\right]$$

$$+ \frac{1}{2L}\sum_{n=1}^{N-M} a_{n+M}\, b_n \left[\left(\frac{\sin[(\omega_1-\omega_2)nT_B] - \sin[(\omega_1-\omega_2)((n-1)T_B+\tau_0)]}{\omega_1-\omega_2}\right)\right.$$

$$\left. - \left(\frac{\sin[(\omega_1+\omega_2)nT_B] - \sin[(\omega_1+\omega_2)((n-1)T_B+\tau_0)]}{\omega_1+\omega_2}\right)\right]$$

For the LIT system operating at a carrier frequency of 1600 MHz and a maximum Doppler shift of 6 KHz the terms divided by $\omega_1+\omega_2$ are considered negligible since they contribute less than 10^{-5} of the normalized correlation. Dropping these terms and combining gives

$$R_{12}(\tau) = \frac{1}{2L(\omega_1-\omega_2)}\sum_{n=1}^{N-M} b_n\left[-a_{n+M-1}\sin[(\omega_1-\omega_2)(n-1)T_B]\right.$$

$$+ (a_{n+M-1} - a_{n+M})\sin[(\omega_1-\omega_2)((n-1)T_B+\tau_0)]$$

$$\left. + a_{n+M}\sin[(\omega_1-\omega_2)nT_B]\right]$$

$$+ \frac{a_N b_{N-M-1}}{2L(\omega_1-\omega_2)}\left(\sin[(\omega_1-\omega_2)((N-M)T_B+\tau_0)]\right.$$

$$\left. -\sin[(\omega_1-\omega_2)(N-M)T_B]\right)$$

The valve of $R_{12}(\tau)$ was computed for ten time shifts between each integer multiple of T_B. Unfortunately, because of computer problems, only 720 out of the 1021 integer bit time shifts were computed; consequently, the histogram was not obtained.

The partial results indicate a maximum aperiodic peak crosscorrelation with a 6 KHz Doppler shift of 28 as compared to the zero Doppler worst case of 47. Since only every twentieth value was printed it is likely the peak value printed is less than the actual peak. Based on a $\frac{\sin \pi fT}{\pi fT}$ assumed frequency response one would predict a peak value of .852 times the zero Doppler peak or $.852 \times 47 \doteq 40$. Since the Doppler shifted aperiodic cross-correlation function was sampled at every twentieth point one would expect the sampled values to indicate roughly the 97.5% point on the distribution. For the zero Doppler case the 97.5% point on the unnormalized distribution is 32. When this is multipled by the assumed 0.852 factor due to Doppler we obtain 27 as an estimate of the 97.5% point which is close to the computed value of 28. Thus, the $\frac{\sin x}{x}$ estimate of the Doppler performance appears plausible, but there is insufficient data to obtain a very great statistical confidence.

The partial results available indicate that the sidelobes decrease with the moderate Doppler expected for the LIT system. For codes structured to provide minimum zero Doppler autocorrelation sidelobes which are well below the average in the time-frequency ambiguity plane (e.g., Barker codes), Doppler shifts can produce a substantial degradation in performance compared to the zero Doppler case. Such sensitivity to Doppler would not be expected for the subsequence codes because the peak sidelobes, roughly twice the full overlap RMS value, are greater than the average sidelobes in the time-frequency ambiguity plane.

REFERENCES

F-1 Nathanson, Fred E., Radar Design Principles, McGraw-Hill, New York, N.Y., (1969).

F-2 Taylor, S. A., and J. L. MacAruthur, "Digital Pulse Compression Radar Receiver," Appl. Phys. Lab. Tech. Digest 6 (4) (1962).

F-3 Peterson, W. Wesley, Error Correcting Codes, M.I.T. Press, Cambridge, Mass. (1961).

F-4 Boehmer, A. B., "Binary Pulse Compression Codes," IEEE Trans. Info. Th. IT-13 (April 1967).

F-5 Gold, Robert, Technical Communication, "Algebraic Spectra of Correlation Functions for Linear Sequences of Periods to 8191."

F-6 Gold, Robert, "Study of Correlation Properties of Binary Sequences," Air Force Avionics Laboratory Technical Report AFAL-TR-67-311, Wright-Patterson Air Force Base, Ohio (November 1967).

F-7 Zierler, N., "Linear Recurring Sequences," J. SIAM, 7 (March 1967)

F-8 Harmuth, Henning F., "A Generalized Concept of Frequency and Some Applications," IEEE Trans. Info. Th. IT-14 (May 1968).

F-9 Reed, I.S. and G. Solomon, "Polynomial Codes Over Certain Finite Fields," J. SIAM, 8, (2) (June 1960).

F-10 Lindholm, James H., "An Analysis of the Pseudo-Randomness Properties of Subsequences of Long M-Sequences," IEEE Trans. on Info. Th., IT-14 (4) (July 1968).

APPENDIX G

GROUND MULTIPATH

This Appendix examines the three main factors which determine the strength of the multipath signals relative to the direct signals at the LIT ground receivers. These three factors are:

1) Ground specular reflection coefficient

2) Aircraft antenna directivity

3) Time and frequency spread due to diffuse return.

In addition, data was examined on both backscatter measurements from pulse altimeters and on errors in ILS installations due to multipath reflections. This data helped to infer the multipath that can be expected for the LIT system.

1.0 Ground Specular Reflection Coefficient

The smooth earth ground reflection coefficient is plotted in Figures G-1 and G-2 for cases of interest over land and sea. At frequencies of 450 to 1550 MHz and over the range of expected earth conductivity (10^{-2} to 10^{-4} mho/meter), the land reflection coefficient is essentially independent of both frequency and conductivity. The earth behaves essentially as a perfect dielectric and the reflection coefficient depends only on the relative dielectric constant. The curves in Figure G-1 are for $\varepsilon = 5$ and $\varepsilon = 10$ which generally cover the range of expected variation of land under various conditions of moisture and vegetation. Figure G-3 (Ref. G-1), shows measured data on asphalt and grass and generally confirms the agreement

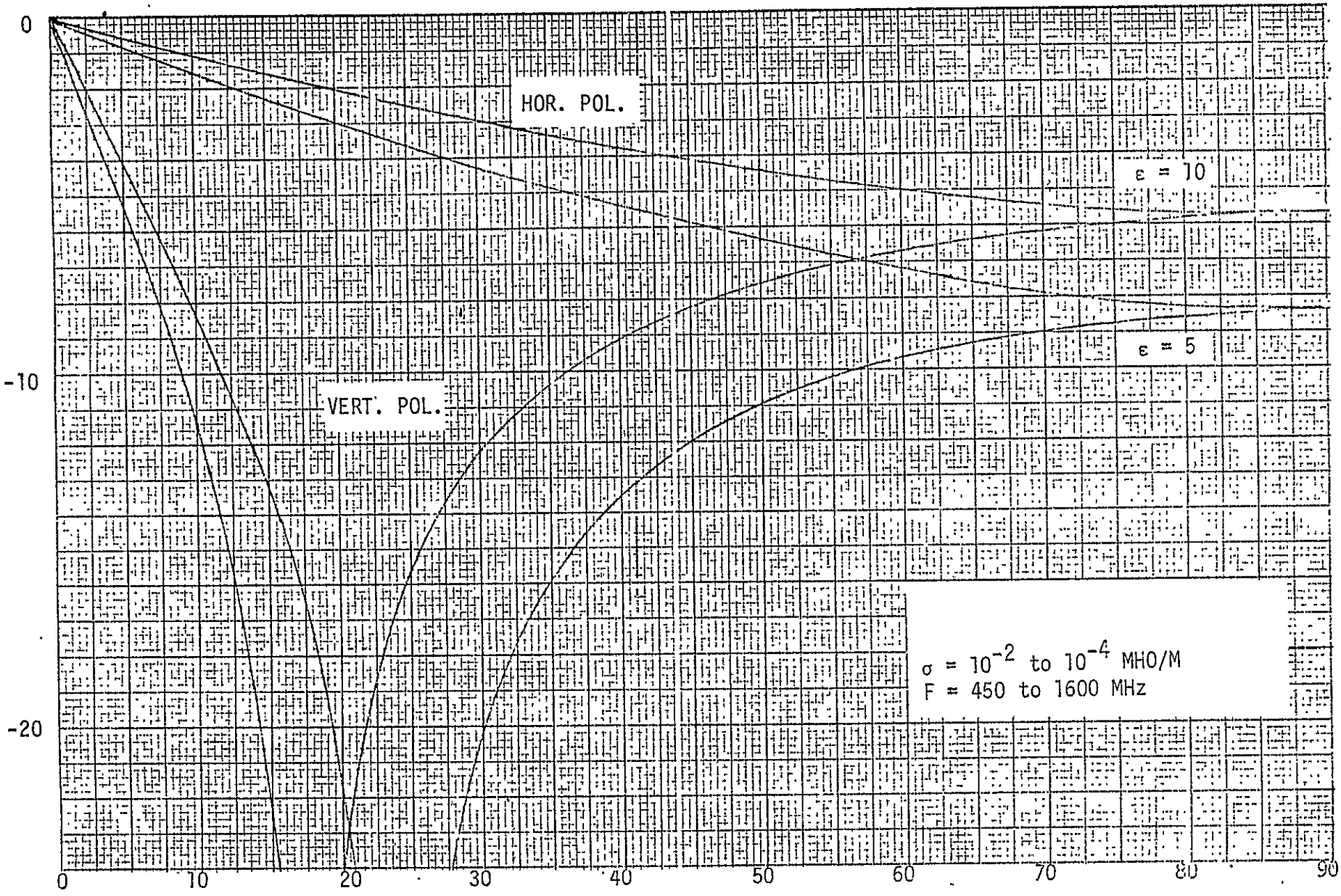

Figure G-1. Ground Reflection Coefficient

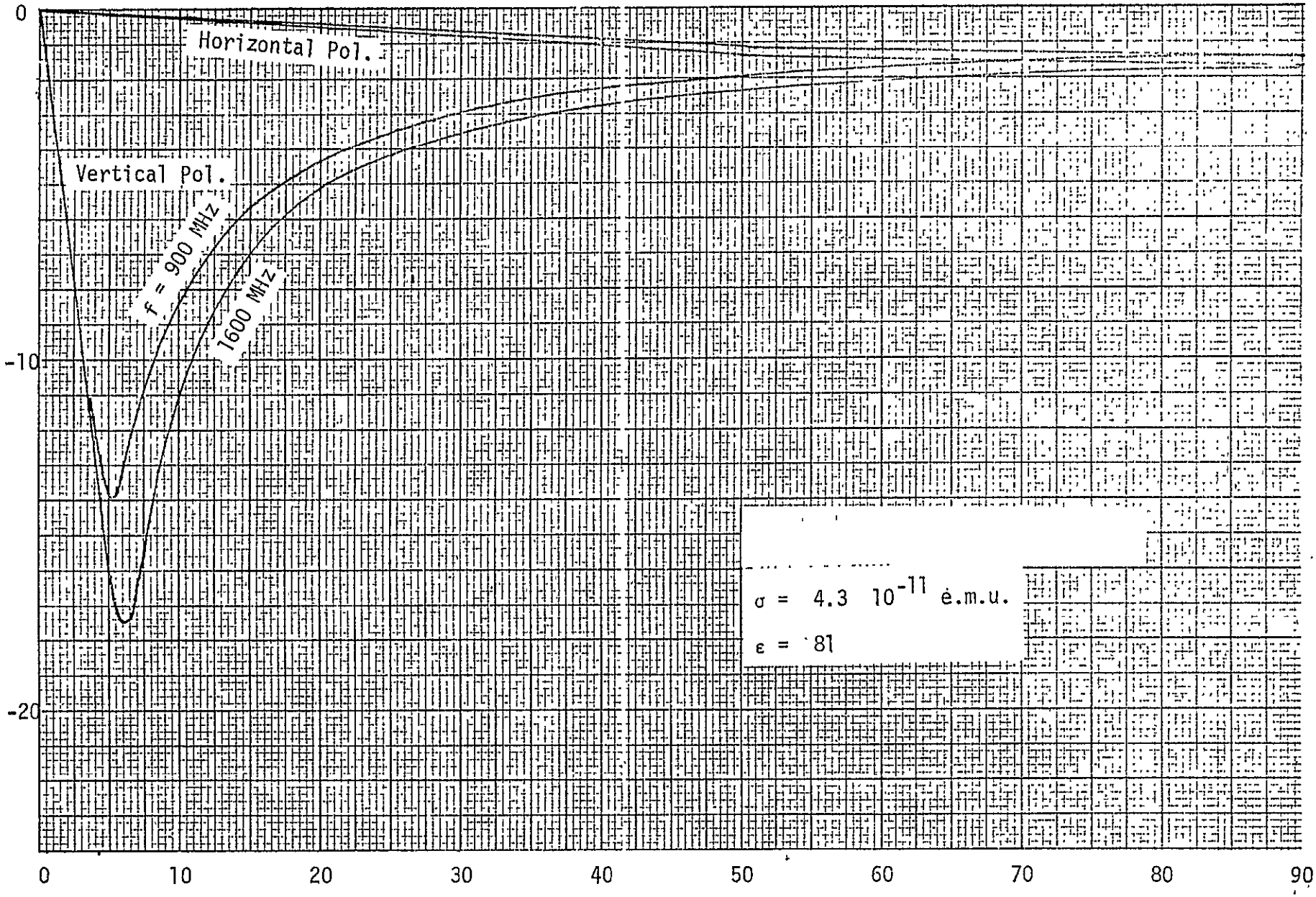

Figure G-2. Sea Water Reflection Coefficient

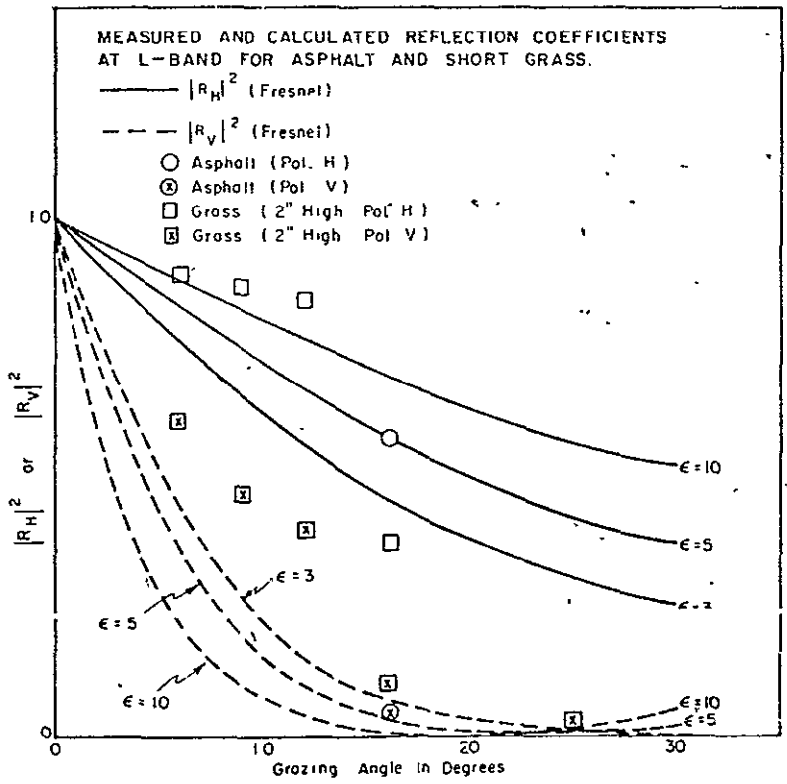

Figure G-3. Measured and Calculated Reflection Coefficients at L-Band for Asphalt and Short Grass

in terms of dielectric constant. Note that over the range 10 - 40^{o} elevation angle the reflection coefficient is generally below -10 db. At higher angles the aircraft antenna may be expected to afford significant multipath discrimination as will be discussed below. The sea water reflection coefficient is somewhat higher than land and frequency dependent. However, both cases clearly show the strong advantage of vertical polarization with regard to minimization of the ground return.

In Figure G-3 a number of the measurements have been interpreted in terms of a surface reflection coefficient. For comparison purposes, the Fresnel reflection coefficients for flat surfaces with dielectric constants of 3, 5, and 10 are provided on the same figure. It will be seen that although there is some scatter, due partly to the difficulties in allowing for antenna pattern effects, the results reinforce the conclusion that asphalt and grass surfaces at L-band act like smooth surfaces with a dielectric constant of about 5.

2.0 Combined Effect of Aircraft Antenna Directivity and Ground Reflection

In practice, the consideration of aircraft antenna directivity can hardly be separated from that of ground reflectivity because of the complex interaction in terms of wave polarization. In general, the aircraft antenna directivity depends markedly on the incident polarization. But for a given transmitted polarization, the polarization of the ground reflected wave depends on the electrical characteristics of the earth.

These factors are taken into account in a computer program called "MULS" (Ref. G-2). The program is illustrated in Figure G-4. For purposes of explanation, it is easiest to consider the satellite transmitting and the aircraft receiving although clearly by the reciprocity principle the direction of propagation makes no difference in the final calculation. The arbitrarily specified satellite polarization is first resolved into its vertical and horizontal components. The ordinary plan earth reflection coefficients for the H and V components are computed for the particular frequency, elevation angle and earth constants. The reflected H' and V' components are then recombined to compute the ground reflected wave amplitude and polarization.

The aircraft antenna is now subject to a direct incident wave of amplitude A_1 and polarization P_1 arriving from the direction azimuth θ_1 and E_1, and to an indirect wave A_2, P_2, θ_1, $-E_1$. To compute the antenna response to an arbitrary such wave requires measuring the actual (or scaled) antenna response to three or more suitably independent polarizations at each such incident angle. From these polarization measurements, it is possible to compute the response to an arbitrary polarization. This is done for the direct and indirect components yielding the multipath ratio at that particular look angle. Finally, this is repeated at a large number of azimuth angles for each elevation angle, and the results processed to yield a statistical distribution of the multipath ratio (indirect signal/direct signal) at the antenna terminals under the given condition.

The results reported herein are based on scale model antenna measurements for a curved arm turnstile antenna, nominally RHC polarized, mounted on an F-100 model aircraft at 1600 MHz. The statistical results are summarized in Figures 29, 30, 31, and 32 in Section 4.2.5.

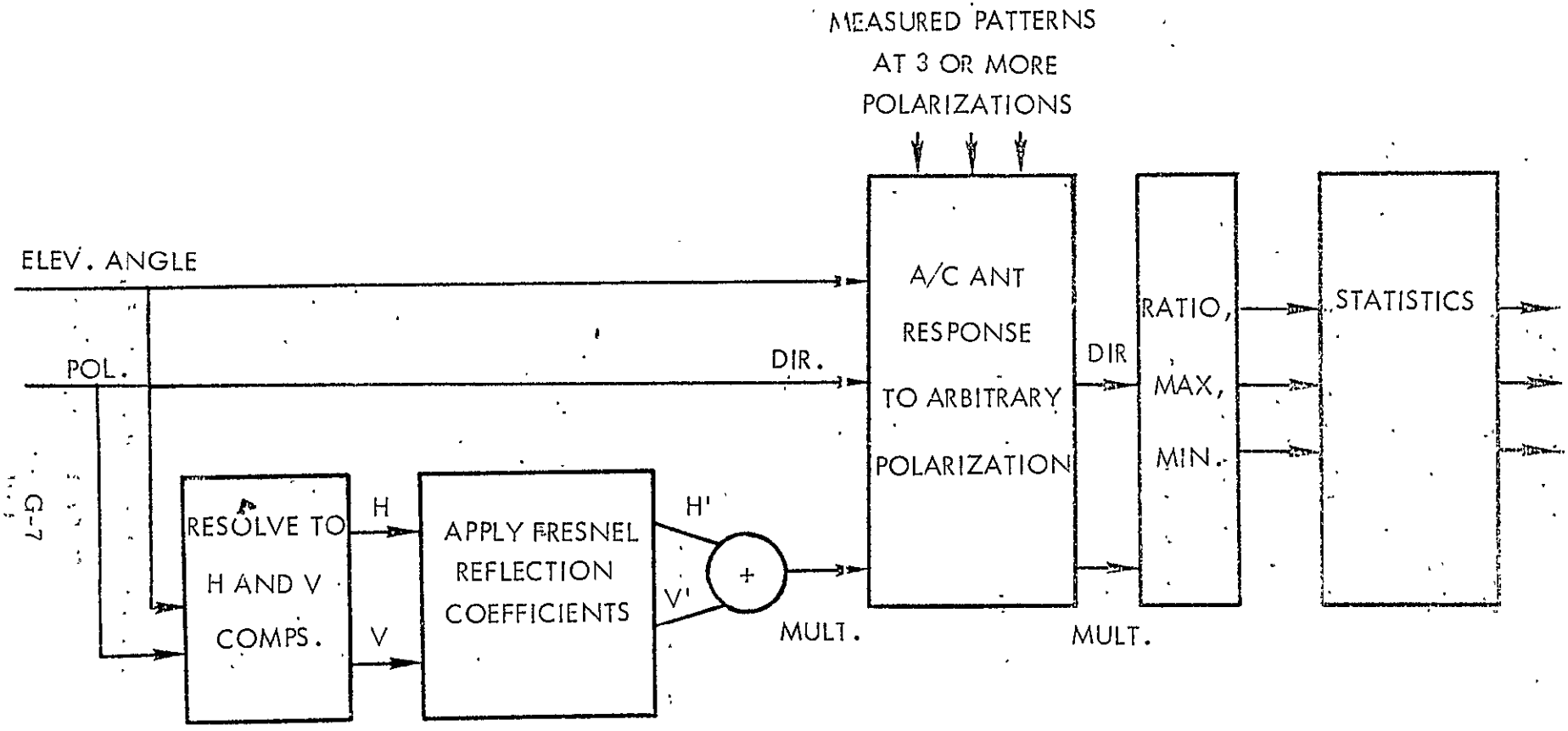

Figure G-4. Specular Multipath Analysis

Figures 30 and 32 show the effect of satellite righthand circular polarization over land and sea water while Figures 29 and 31 show the effect of satellite vertical polarization over land and sea water. At the lowest elevation angles (10^0) vertical satellite polarization performance is significantly better (about 7 - 10 db) than RHC satellite polarization. Of course, the disadvantage of vertical polarization is that the satellite gain reduces to zero directly overhead. However, it may be possible to use vertical polarization only at those times in orbit during which the elevation angles as seen from CONUS are low.

For RHC polarization, it can be confirmed by reference back to the original data that the occasional poor multipath ratio performance (5 - 7 db) at low elevation angles is occurring in the aircraft's fore and aft regions, particularly the latter. These are regions where the near horizontal radiation is most heavily shorted out by the ground plane effect of the aircraft skin, and in these directions considerable horizontal - vertical polarization mode conversion can be expected to occur. The patterns confirm that this is indeed happening. There is reason to believe that a tail cap mounting of a curved arm turnstile antenna would significantly reduce this worst case multipath response, although actual patterns of such an antenna have not been taken.

Using a combination of satellite vertical polarization at low elevation angles and aircraft antenna location, it is estimated that the multipath ratio would be less than -10 db at 10^0 elevation angle and less than -17 db at 20^0 elevation angle with high confidence (i.e., with very small probability ot exceeding these values).

3.0 Diffuse Return

The preceeding results pertain to the case of a perfectly smooth specular reflecting earth. In the case of a rough earth several significant

modifications of the preceding results occur. These modifications are due to the following first order effects:

1. The return signal is spread in time.
2. The return signal is spread in frequency.

However, the polarization and total reflected power are unchanged to first order (Ref. G-3). For much rougher surfaces, the reflection characteristics are modified but no satisfactory theory exists to describe them and one must rely solely on empirical data.

First let us consider what "rough" means quantitatively. This question is addressed by the classical Rayleigh criterion which says that reflection tends to be specular or diffuse according to whether the quantity

$$R \equiv \frac{\sigma \sin E}{\lambda}$$

is less than or greater than some constant.

Where

σ = rms surface roughness

λ = wavelength

E = elevation angle

This criterion has been made quantitative by Beckmann (Ref. G-3) and others who show that under reasonably assumed conditions the specular and diffuse power depend on R as

$$\text{specular power} = K\, e^{-(4\pi R)^2}$$

$$\text{diffuse power} = K\left[1 - e^{-(4\pi R)^2}\right]$$

where K = reflected power from a smooth surface.

Therefore, specular power will be down 4.3 db with respect to a smooth surface when $R = \pi/4$. This condition is called "critical" roughness,

$$\sigma_c = \frac{\lambda}{4\pi \sin E}$$

and is plotted in Figure G-5 for frequencies of 450, 900 and 1550 MHz.

At 900 MHz and E = 40^{o}, the critical roughness is only 0.13 feet which is exceptionally smooth. In order to estimate the rms roughness, σ, one must also specify the area of interest (e.g., must the area be large enough to encompass mountains or small enough to encompass a paved parking lot?) The answer is roughly that one must consider the first Fresnel zone, that is, the area of the surface around the specular reflection point over which if the surface were smooth, the total path length from aircraft to surface point to satellite is within 1/2 wavelength of the path length for the specular point. This is an elliptical area with half widths in the X (longitudinal) and Y (transverse) directions given by:

$$\Delta X = \sqrt{\frac{\lambda H_a}{\sin^3 E}}$$

$$\Delta Y = \sqrt{\frac{\lambda H_a}{\sin E}}$$

where H_a = aircraft altitude

λ = carrier wavelength

The Fresnel zone size is plotted in Figure G-6 for a few cases of interest to give an idea of magnitudes. For example, with an aircraft at 10,000 feet and typical elevation angles of 10 to 40^{o}, the dimensions are of the order of 50 to 100 feet transverse and 100 to 400 feet longitudinal. It seems clear from these considerations that diffuse conditions must generally prevail over land even at 450 MHz.

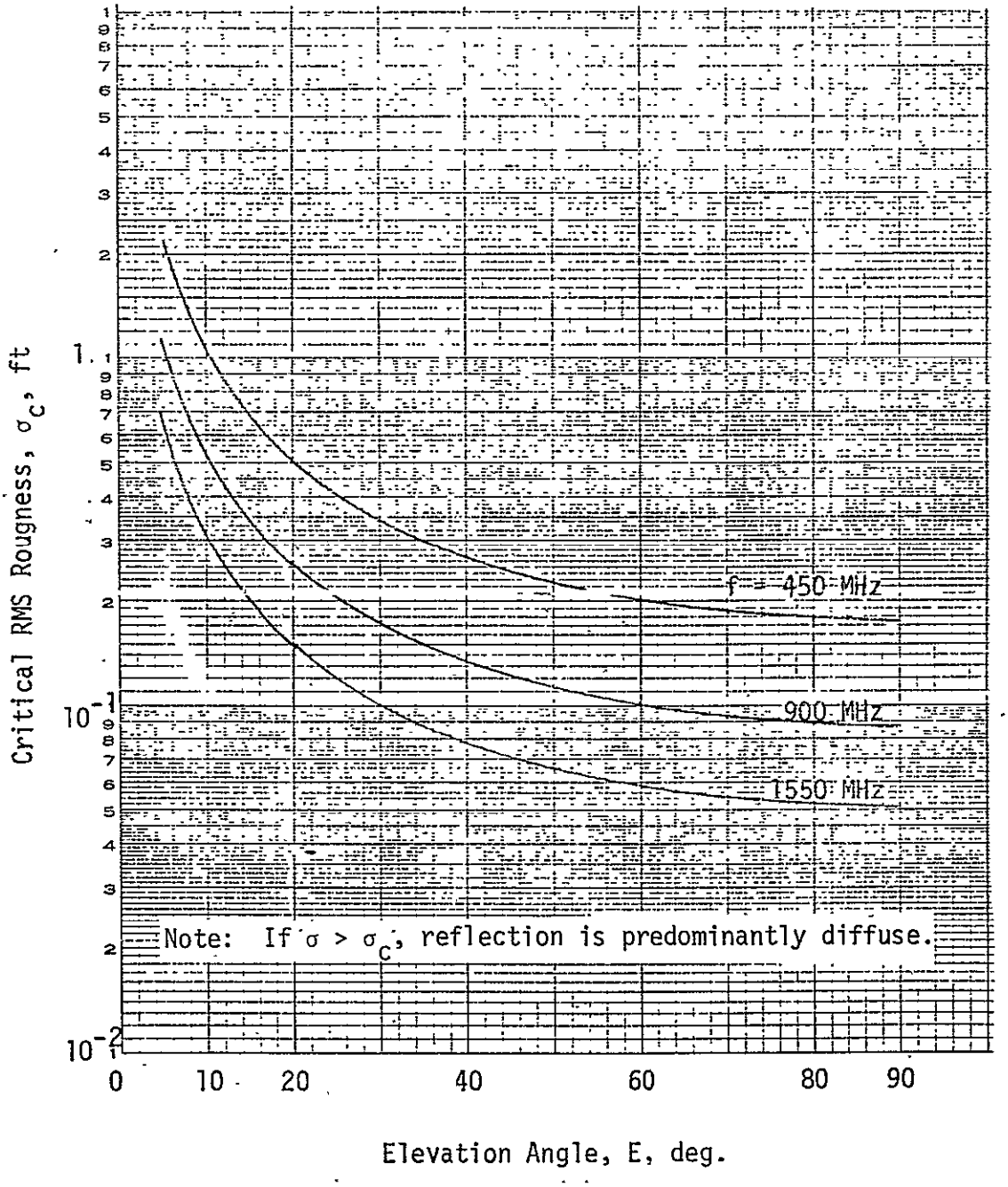

Figure G-5. Critical Roughness

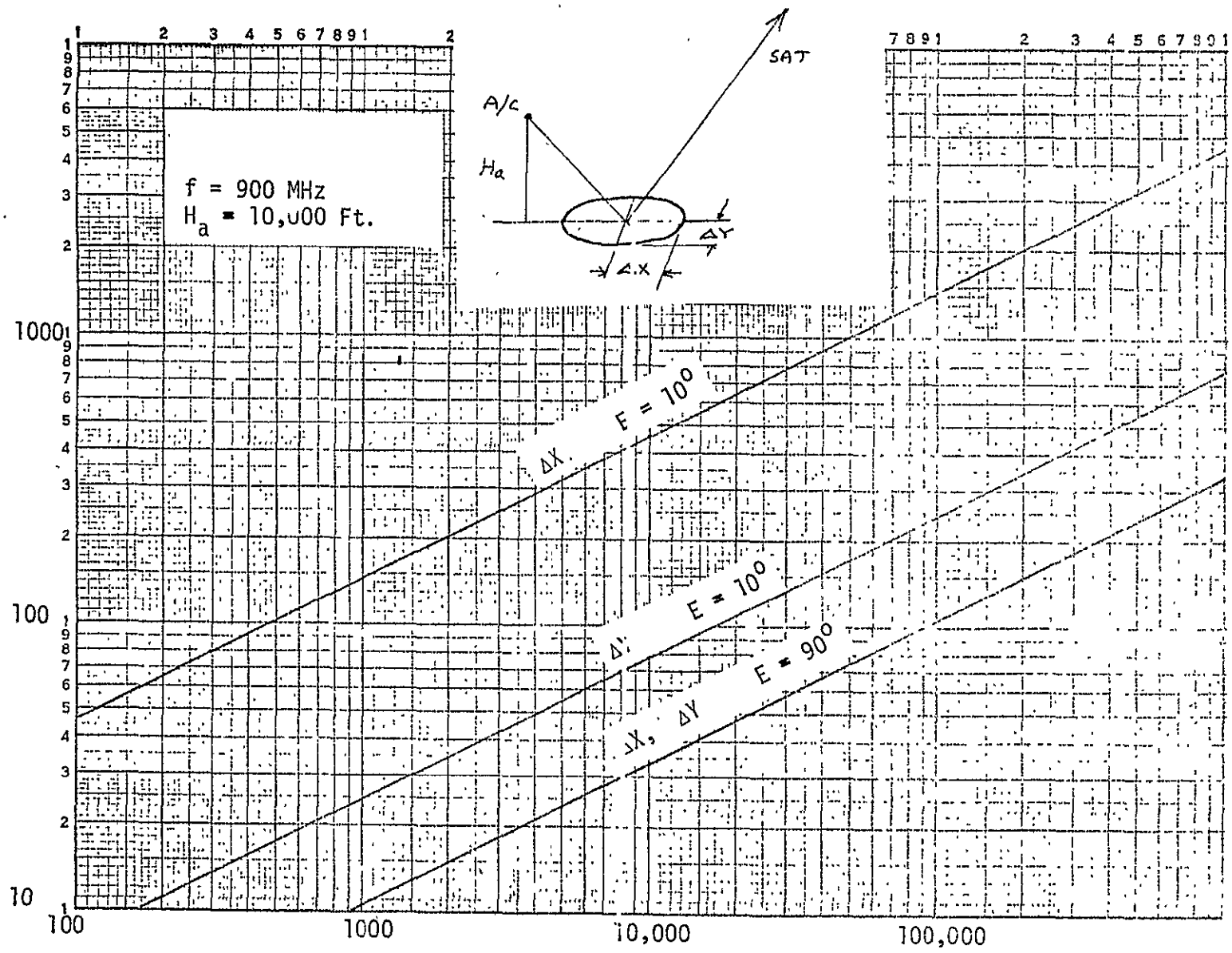

Figure G-6. Fresnel Zone Size

Given that diffuse scatter prevails, the extent of time and frequency spreading then depends on the rms slope of the surface through the relations (Ref. G-4):

$$\Delta f = 2\sqrt{2s}\ \text{Sin}\ E\ \frac{V_a}{\lambda}$$

$$\Delta t = 4s^2 \sqrt{\frac{3}{\text{Sin}^2 E} + 2 + 3\ \text{Sin}^2 E}\ \frac{H_a}{c}$$

where s = rms surface slope

V_a = aircraft speed - horizontal

c = velocity of light

If the receiving system has a narrow bandwidth, it may receive only part of the scatter due to frequency spread outside the band. Similarly if the receiver uses a narrow time gate it will reject part of the scatter due to time spread outside the gate. For orientation, with respect to these two effects, assume:

s = 0.2 (a moderate to high value for sea, but a low value for land)
f = 900 MHz
λ = 1.1 feet
V_a = 300 ft/sec.
H_a = 10,000 feet
E = 40^o

Then, the scatter in frequency and time are:

Δf = 156 Hz

Δt = 6.0 μsec

The LIT receiver system has an effective bandwidth of the order of the reciprocal integration time of the LIT pulse (51 μsec.) or about 20 KHz and an effective time gate of one chip width or 0.1 μsec. Under these circumstances, it is clear that the frequency spread is insignificant but the time spread may be very significant in reducing peak scattered pulse amplitude.

In order to evaluate the time-spread loss we can make use of the specific form of the time-spread function (i.e., the time wise scatter power density function or the impulse response function of the medium as derived in Ref. G-4 for the Gaussian random surface).

$$S(t) = \frac{c\rho}{\pi H_a (2s)^2} \exp\left[-\frac{(\mathrm{Csc}\ E + \mathrm{Sin}\ E)\ tc}{2(2s)^2\ H_a}\right] I_o \left[\frac{(\mathrm{Csc}\ E - \mathrm{Sin}\ E)\ tc}{2(2s)^2\ H_a}\right]$$

where ρ = specular reflection power coefficient

$I_o(\cdot)$ = modified Bessel function

Note that so long as

$$t << \frac{8s^2\ H_a}{c(\mathrm{Csc}\ E + \mathrm{Sin}\ E)}$$

both the exponential and the Bessel function are near unity and the scatter power density may be approximated by its value at $t = 0$ namely

$$S(t) \approx S(0)$$

$$= \frac{c\rho}{\pi H_a (2s)^2}$$

The total received power is the integral of this density over the time-wise aperture τ_c or to this approximation simply

$$P \approx S(0)\ \tau_c$$

$$= \frac{c\rho\ \tau_c}{\pi H_a (2s)^2}$$

where τ_c = LIT pulse chip width = 0.1 μsec

which represents a discrimination, relative to the specular case (where $P = \rho$) by the factor

$$F_\tau = \frac{c\ \tau_c}{\pi H_a (2s)^2}$$

This factor is plotted in Figure G-7 as a function of aircraft altitude for several different rms slopes, s, in the range 0.05 to 0.2, which is believed to cover the most probable values for average land. Obviously, the effective rms slope, s, plays a crucial role and it is of considerable importance to achieve better estimates of this factor.

The use of the term "effective" in connection with the rms slope is to be emphasized because what is really important is the angular beamwidth of the scatter from a particular surface. In the particular model of a

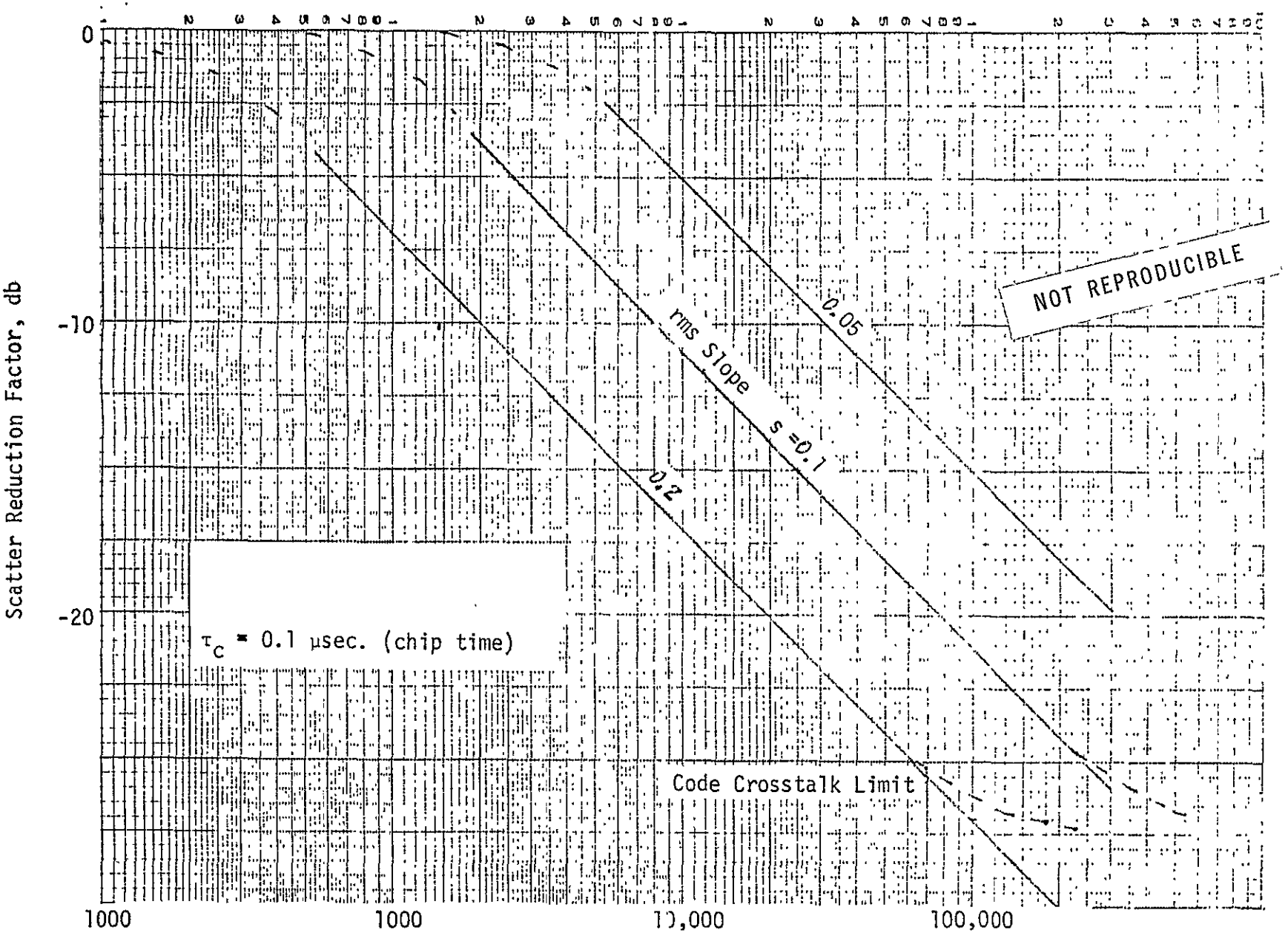

Figure G-7. Scatter Reduction Factor Due To Time

slightly rough surface such as the sea, this has a rather simple relation to the rms slope, but more generally it is the scatter beamwidth that is important. In cases such as forest, the effective rms slope may bear little relationship to physical slopes.

Indirect inferences of the effective slope, s, have been made (Ref. G-5) by comparison of near vertical incidence radar return pulse spread with the theoretical pulse spread from a Gaussian surface model (Refs. G-3 and G-6). Edison's experimentally determined parameter a/σ is related to effective rms slope, s, by

$$s = \frac{\sqrt{2}}{(a/\sigma)}$$

In these terms, his results are tabulated in Table G-1.

Table G-1. Effective Slope, s

	@ 415 MHz	@ 3800 MHz
Woods, Pine Island, Minn.	.24	.35
Snow covered farmland, Wahpteton, N.D.	.19	.19
Farmland, Cameron, Mo.	.18	.17
Industrial area, Minneapolis, Minn.	.18	.22
Residential area, Minneapolis, Minn.	.18	.20
Apartment buildings, Kansas City, Mo.	.18	.17
Desert Area, Salton Sea, California	.16	.18

Measurements of effective slope for the sea have been made by optical and by radar altimeter techniques. Katzin (Ref. G-7) reports optical measuremen of total rms slope of 0.16 and 0.25 for winds of 10 and 20 knots respectively. Dye (Ref. G-8, p. 140) reports earlier radar altimeter measurements by Katzin as follows:

Wind Velocity (Kts)	rms
3	.043
6	.059
25	.117

The lower radar values are consistent with the observation that the radar will tend to ignore the very small but steep ripple facets seen optically. In summary, it appears that the range from 0.05 to 0.2 pretty well brackets the effective rms slope leading to diffuse peak return pulse reduction factors as indicated in Figure G-7.

Of course, it must be pointed out that in the diffuse case the peak return pulse amplitude is a random variable, with mean about as indicated but with some distribution of values above and below the mean. The nature of this distribution will be a complex function of the nature of the terrain and of the pulse compression parameters of the LIT system. As Beckmann (Ref. G-3) has indicated and as has been confirmed experimentally, a simple Rayleigh model is not generally adequate to express this distribution. There does not appear to be a satisfactory way to estimate the distribution at this time for the LIT system; ultimately this will have to be the subject of flight test experiments.

4.0 Inferences from Back Scatter Measurements

Unfortunately, there has been very little in the way of forward scattering data in the frequency range of interest, and what data there is has been mostly measured on CW signals (Ref. G-1), thus disguising the time spread which is an important factor for the LIT pulses. On the other hand, there has been a great deal of data reported on the near vertical back scattering ground return for pulse altimeters. Within broad limits this data can be considered indicative of the forward scatter to be expected for oblique incidence in the LIT system.

Dye (Ref G-8) has summarized diverse measurements of this type by extrapolating them according to experimentally confirmed theoretical scaling laws to the case of a 4200 MHz, 0.1 μsec. pulse altimeter at 50,000 feet altitude. Expressed in terms of the multipath ratio for a satellite (peak scatter return/specular return) his results are given in Table G-2.

These scatter ratios of course include the effects of both CW reflection and pulse diffusion at normal incidence. The estimated CW reflection coefficient for a smooth surface of the same constituent characteristics is indicated in the first column of the table. For oblique incidence forward scatter, as in the LIT multipath case, one can show from the simple scattering theory, that the pulse diffusion effect is essentially independent of angle of incidence. On the other hand, the CW reflection coefficient will vary with incidence angle, becoming smaller (more favorable) at oblique incidence for vertically polarized waves and larger (less favorable) for horizontal polarized waves.

Table G-2. Measured and Extrapolated Scatter Coefficients 4200-MHz 0.1-μsec. Pulse (Ref. G-8)

Type of Surface	Scatter Direct, db	Estimated Specular Reflection Coefficient, db	Estimated Diffuse Time-Spread Attenuation db
Water, 7 knot wind	-8	-1.7	6.3
Water, 11 knot wind	-11	-1.7	9.3
Water, 3 knot wind	-6	-1.7	4.3
Water, 6 knot wind	-9	-1.7	7.3
Water, 25 knot wind	-15	-1.7	13.3
City	-8	-5.6	2.4
Residential Area	-10	-5.6	4.4
Countryside	-11	-5.6	5.4
Cultivated Land	-14	-5.6	8.4
Flat Field, dry grass	-17	-5.6	11.4
High grass, cornfield	-17	-5.6	11.4
Wooded land	-15	-5.6	9.4
Dry Woods, leaves	-16	-5.6	10.4
Heavy Woods, dry leaves	-18	-5.6	12.4
Woods, no leaves	-19	-5.6	13.4
Desert	-20	-5.6	14.4
Frozen snow covered forest	-25	-2.5	22.5

While it is difficult to generalize on such diverse data, it is seen that the observed peak scatter coefficient is generally from 3 to 20 db less than the estimated specular return.

5.0 Inferences from ILS Multipath

One of the principal problems of present Instrument Landing Systems is the so-called beam-bending errors that occur due to irregularities in the local terrain, buildings, and even other aircraft in the area. Category II (i.e., low visibility) accuracy standards, for glide slope and localizer beam bends due to all causes, are on the order of 0.06 to 0.1 degrees at runway threshold, whereas errors on the order of 0.5 degree are not unusual in the present system. Widespread awareness of these very serious errors has led the aircraft community to a healthy concern for multipath errors in any proposed new system. However, one examines these errors in quantitative detail, the very serious errors in ILS are seen to arise largely from the extreme error sensitivity of ILS to relatively weak multipath signals and that actually interpreted in terms of multipath ratio (indirect/direct signal voltage ratio), the implications on a more "multipath-rugged" system such as LIT are quite optimistic.

Both the localizer and glide slope systems are arranged to measure the algebraic (sense carrying) difference pattern of an antenna array which has an S-shaped pattern as shown below, and which may be approximated in the vicinity of the landing path by

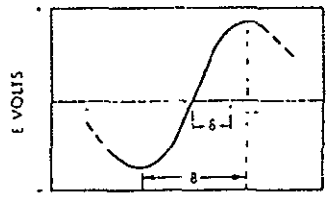

$$E(\delta) \approx \sin\left(\frac{\pi\delta}{B}\right)$$

$$\approx \frac{\pi\delta}{B} \quad \delta << B$$

where δ is the angular deviation from glide path or runway center and B the beamwidth. Then, having measured a given E* one infers

$$\delta^* = \frac{BE^*}{\pi}$$

where the asterisked quantities refer to measured values of the parameters.

For a scatterer of relative signal strength ρ, at angle δ_i the error multipath difference signal voltage is

$$E^* = r \text{ Sin } \phi$$

and the inferred angle error is

$$\delta^* = \frac{B}{\pi} r \text{ Sin } \phi$$

where $r = \rho E^2(\delta_i)$ = multipath signal power ratio including antenna directivity

ϕ = the r.f. phase corresponding to the excess path length between the multipath signal and the direct carrier reference signal.

Since ϕ is a rapidly varying function of either scatterer or receiver location, it can generally be assumed that in any dynamic situation δ will tend to be oscillatory with envelope

$$|\delta^*| = \frac{Br}{\pi}$$

This relation in turn can be used to infer the multipath ratio corresponding to any such ILS multipath error patterns. For the conventional glide slope and localizer

$$B_{LOC} \approx 10.0^{o} \quad \text{(15 element array)}$$

$$B_{GS} \approx 2.5^{o} \quad \text{(Same as glide slope angle)}$$

Figure G-8 illustrates typical "worst case" localizer bends of the order of 0.5 degree and glide slope bends of the order of 0.1 degree implying

$$\rho \geq 0.16 \quad \text{(Localizer, aircraft interference)}$$

$$\geq 0.125 \quad \text{(Glide slope, ground multipath)}$$

That is, in both cases, indirect/direct signal strength ratios of -16 to -18 db are experienced and lead to intolerable errors with the present ILS system. However, such multipath ratios would be quite negligible in LIT from the viewpoint of either errors or false alarms.

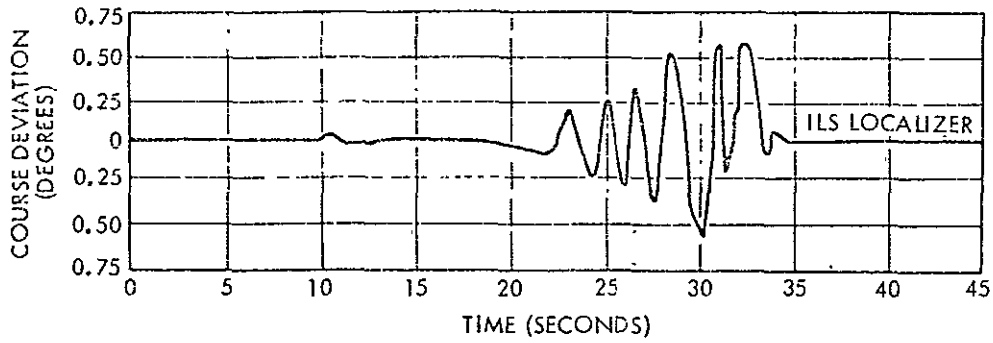

LOCALIZER BENDS AT FIXED LOCATION
T-29 EXECUTING TOUCH AND GO

(REFERENCE G-9)

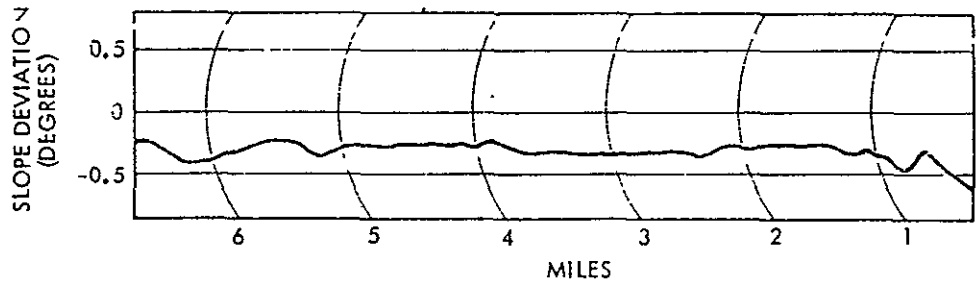

GLIDE SLOPE BENDS DUE TO BAD TERRAIN
McCHORD AFB

(REFERENCE G-10)

Figure G-8. Examples of ILS Bends Due to Multipath

REFERENCES

G-1 Cosgriff, Peake, and Taylor, "Terrain Scattering Properties for Sensor System Design", Bulletin No. 181, Antenna Laboratory, Ohio State University (May 1960).

G-2 A. J. Mallinckrodt, "Multipath Program Description", TRW IOC 7222.1-364 (5 December 1967).

G-3 P. Beckmann, A. Spizzichino, The Scattering of Electromagnetic Waves from Rough Surfaces, Pergamon Press (1963).

G-4 A. J. Mallinckrodt, "Propagation Errors", Course Notes on Short Course in Satellite Based Navigation Traffic Control and Communications to Mobil Terminals, UCLA (August 1969).

G-5 Edison, Moore, and Warner, "Radar Terrain Return Measured at Near Vertical Incidence", IRE Trans. A. P. (May 1960) p. 246.

G-6 H. Davies, "The Reflection of Electromagnetic Waves from a Rough Surface", IEEE Monograph No. 90, Journal IEE, Part IV, 101 (1954) p. 209.

G-7 M. Katzin, E. A. Wolff, and J. C. Katzin, "Investigations of Ground Clutter and Ground Scattering", Electromagnetic Research Corp., Report No. CRC-5198-4, Contract AF19(604)-5198 (15 March 1960).

G-8 J. E. Dye, "Ground and Sea Return Signal Characteristics of Microwave Pulse Altimeters", Trans. Symposium on Radar Return (1959) pp. 111-114; University of New Mexico, USNOTS, NOTS TP 2338 (11-12 May 1959).

APPENDIX H

SATELLITE LIT ANTENNA OPTIMIZATION

The problem is to determine optimized antenna beamwidths for a satellite which illuminates the contiguous United States. The satellite is in an elliptical, 16^{0} inclined, 24 hour orbit which has a roughly circular ground track centered at 0^{0} latitude and 100^{0} West longitude. There were two optimization criteria considered. The first was that the time-independent received power density or net gain at any U.S. location should be maximized under the constraint that the net gain variation between any two U.S. locations be less than or equal to 4 db. The other criteria was that the minimum net gain was to be absolutely maximized, thereby accepting the resulting variation of net gain that occurred over the U.S. These two optimization criteria were used for both circular and elliptical beam antennas. The optimized antenna beamwidths and corresponding reflector dimensions obtained are listed in Table H-1.

The net gain at any U.S. location is a function of satellite range to that location and antenna gain in that location direction (Friis transmission formula, Equation 1 below). Since the satellite is in an elliptical orbit, the range and direction to any U.S. location is a function of time. Range and angular location to five U.S. locations were computed as a function of time, The five locations chosen were Nebraska (40^{0} North latitude and 100^{0} West longitude); Seattle, Washington; Miami, Florida; Bangor, Maine; and Brownsville, Texas. The angular locations were

Table H-1. OPTIMIZED PARAMETERS

	3 db Total Beamwidth	Net Gain Variation	Net Gain* Minimum	Antenna Peak Gain	Reflector Diameters at 1.6 GHz	Reflector Diameters at 0.9 GHz
Optimized Circular Beams	8.8^{o}	4.0 db	21.1 db	24.3 db	4.5'	8.1'
	6.5^{o}	5.5 db	22.2 db	26.9 db	6.1'	10.9'
Optimized Elliptical Beams	$9.4^{o} \times 6.5^{o}$	4.0 db	22.1 db	25.3 db	4.2' x 6.1'	7.5' x 10.9'
	$6.8^{o} \times 4.8^{o}$	5.9 db	22.9 db	28.0 db	5.9' x 8.3'	10.4' x 14.7'

*Range Reference (R_o) = 120 x 10^6 feet

with respect to Nebraska, the direction in which the antenna beam would always be pointed. The following analysis then relates the range and angle information and net gain at the above five locations. Since the beam is pointed toward the central U.S. and the five locations chosen are on the U.S. perimeter, it is assumed that the perimeter locations will experience the lowest net gain and have the greatest net gain variation during the satellite orbit as compared with interior U.S. locations. For this reason, if the antenna beam is optimized for U.S. perimeter location it is assumed to be optimized for the entire contiguous United States.

If the Friis Transmission Formula

$$P_r = \frac{G_r G_t \lambda^2 P_t}{(4\pi)^2 R^2} \tag{1}$$

where

P_r = received power
P_t = transmitted power
G_r = gain of receiving antenna
G_t = gain of transmitting antenna
λ = wavelength of radiation
R = range between transmitting and receiving antennas

is converted to db and the constant 20 log R_o is added and subtracted from the right hand side of the equation, then:

$$P_r\,(db) = 10 \log \left(\frac{G_t \lambda^2 P_t}{(4\pi R_o)^2} \right) + G_r(db) - 20 \log \left(\frac{R}{R_o}\right) \tag{2}$$

where

R_o is a range reference

If the gain of the transmitting antenna (remembering that the satellite antenna is receiving), wavelength and transmit power are constant then the first term of Equation 2 is constant and the variation in received power is only due to the second and third terms (the sum of which are defined to be the net gain). Since the gain of the receive antenna can be written as the sum of peak antenna gain (in db) and pattern loss (in db) the net gain can be written as follows:

$$G_{Net}(db) = 10 \log \left(\frac{41,253(.5)}{B_x B_y} \right) - 12 \left(\frac{\theta^2 \cos^2 \phi}{B_x^2} + \frac{\theta^2 \sin^2 \phi}{B_y^2} \right) - 20 \log \left(\frac{R}{R_o} \right) \quad (3)$$

where

$G_{Net}(db)$ = net gain at a specific location

1st term is peak antenna gain (50% antenna efficiency assumed)

2nd term is antenna pattern loss for an elliptical beam with a Gaussian voltage characteristics

3rd term is range loss

B_x = total 3 db beamwidth in x or east-west direction across U.S.

B_y = total 3 db beamwidth in y or north-south direction across

R = range from satellite to location calculating net gain

R_o = range reference (an arbitrary constant)

θ and ϕ = defined in Figure H-1.

The range reference value was chosen to be 120×10^6 feet (synchronous orbit altitude is 117.41×10^6 feet). The circular beamwidth optimization curves in Figure H-2 indicate that in order to achieve a 4 db net gain variation over the U.S. for a circular symmetric antenna beam that the 3 db beamwidth of the antenna should be 8.8 degrees. The corresponding net gain minimum is 21.1 db. Figure H-3 shows this result graphically in the

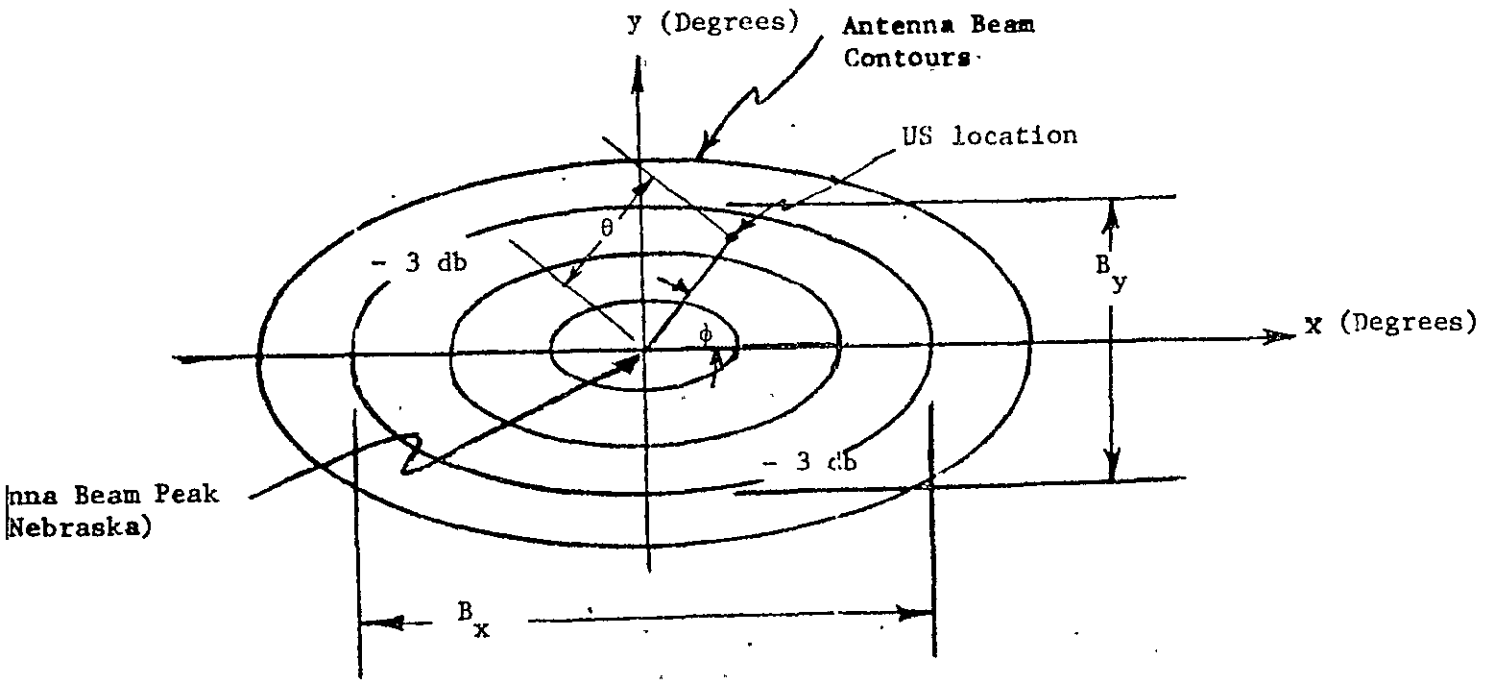

Figure H-1. Definition of Angles θ and ϕ

form of a net gain history or a plot of net gain versus time for the five locations considered. For the other optimization criteria, i.e., absolute maximum of smallest net gain value for any of the five locations, Figure H-2 indicates a minimum net gain maximum of 22.2 db with a 5.5 db variation for a 6.5 degree beamwidth antenna. This optimization criteria's gain history is shown in Figure H-4.

The same two criteria as above were applied to an elliptical beam. The problem here was to optimize the beamwidth in both the x and y planes in order to comply with the criteria. The notation $B_x \times B_y$ was adopted to indicate the beam orientation relative to the U.S. The curves on Figure H-5 illustrate the variations in net gain variation and net gain minimum versus B_y with B_x as a parameter. It is seen on Figure H-5 in regions A and C that a beam of the shape $9.4^0 \times 6.5^0$ optimizes the first criteria giving a net

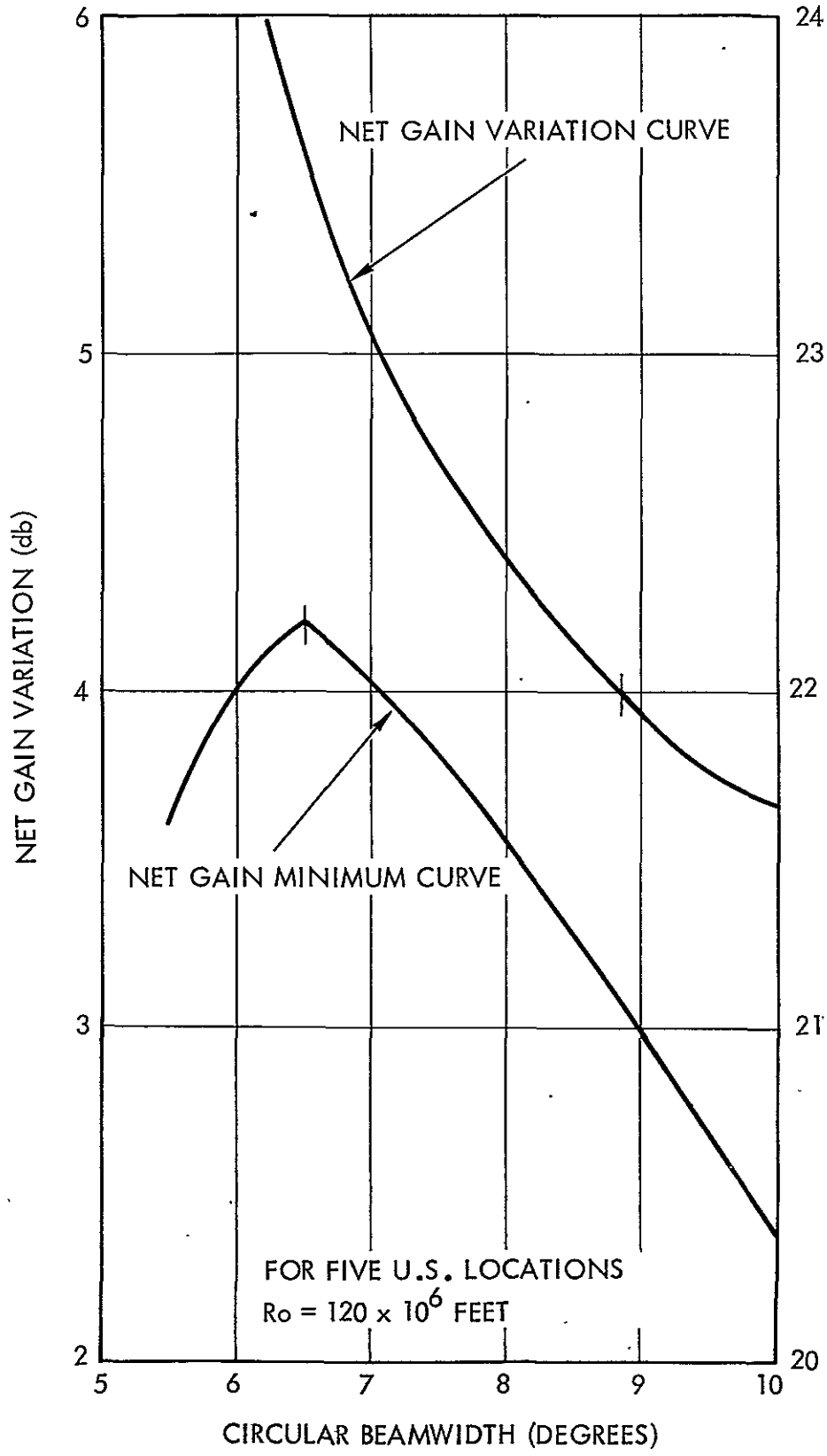

Figure H-2. Circular Beamwidth Optimization Curve

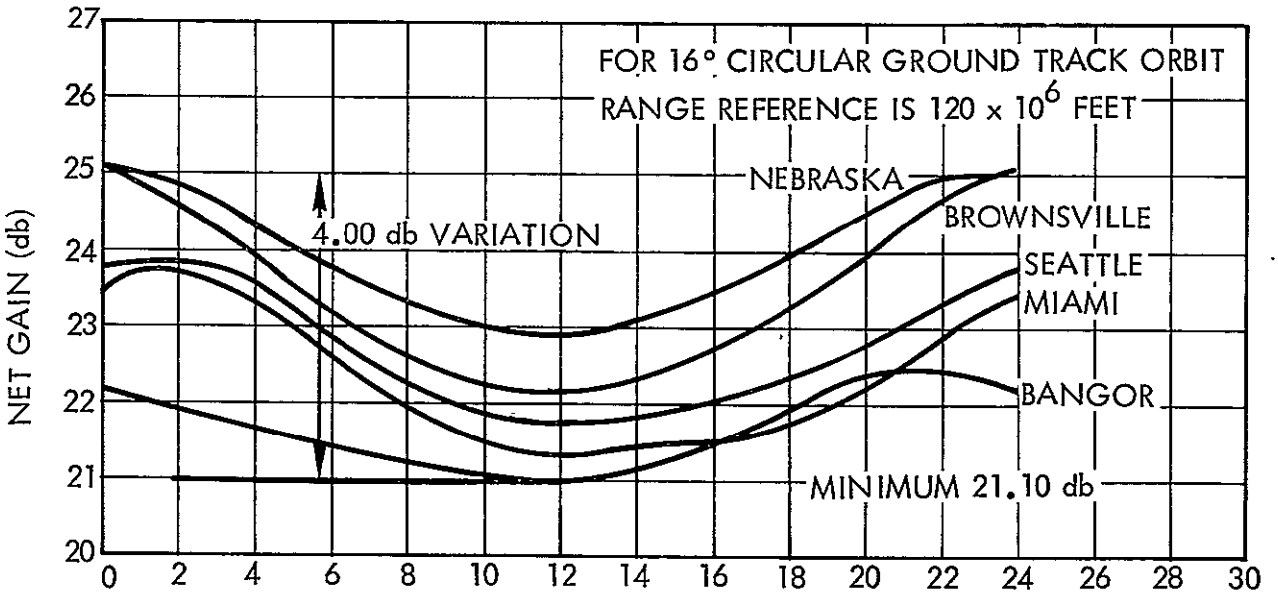

CIRCULAR BEAMED ANTENNA WITH BEAMWIDTH OF 8.8°
AND AN ON-AXIS GAIN OF 24.25 db

Figure H-3. Gain History - Net Gain Versus Time

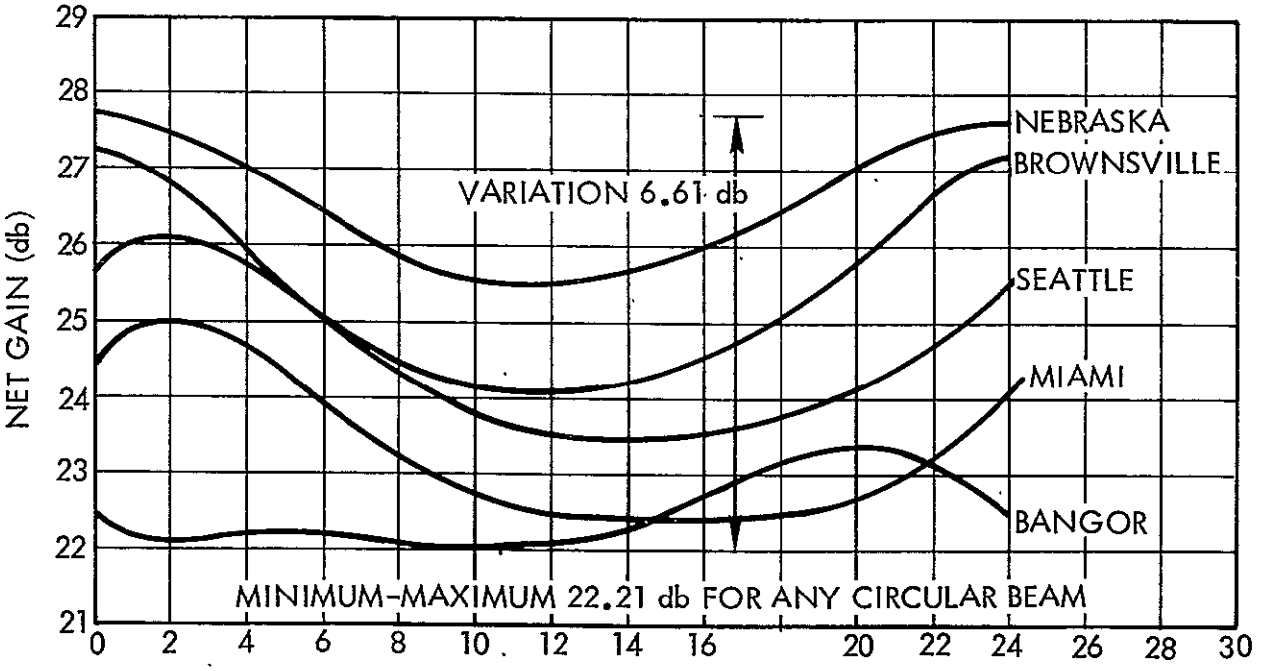

OPTIMIZED CIRCULAR BEAMED ANTENNA WITH BEAMWIDTH OF 6.5° AND
AN ON-AXIS GAIN OF 26.88 db

Figure H-4. Gain History - Net Gain Versus Time

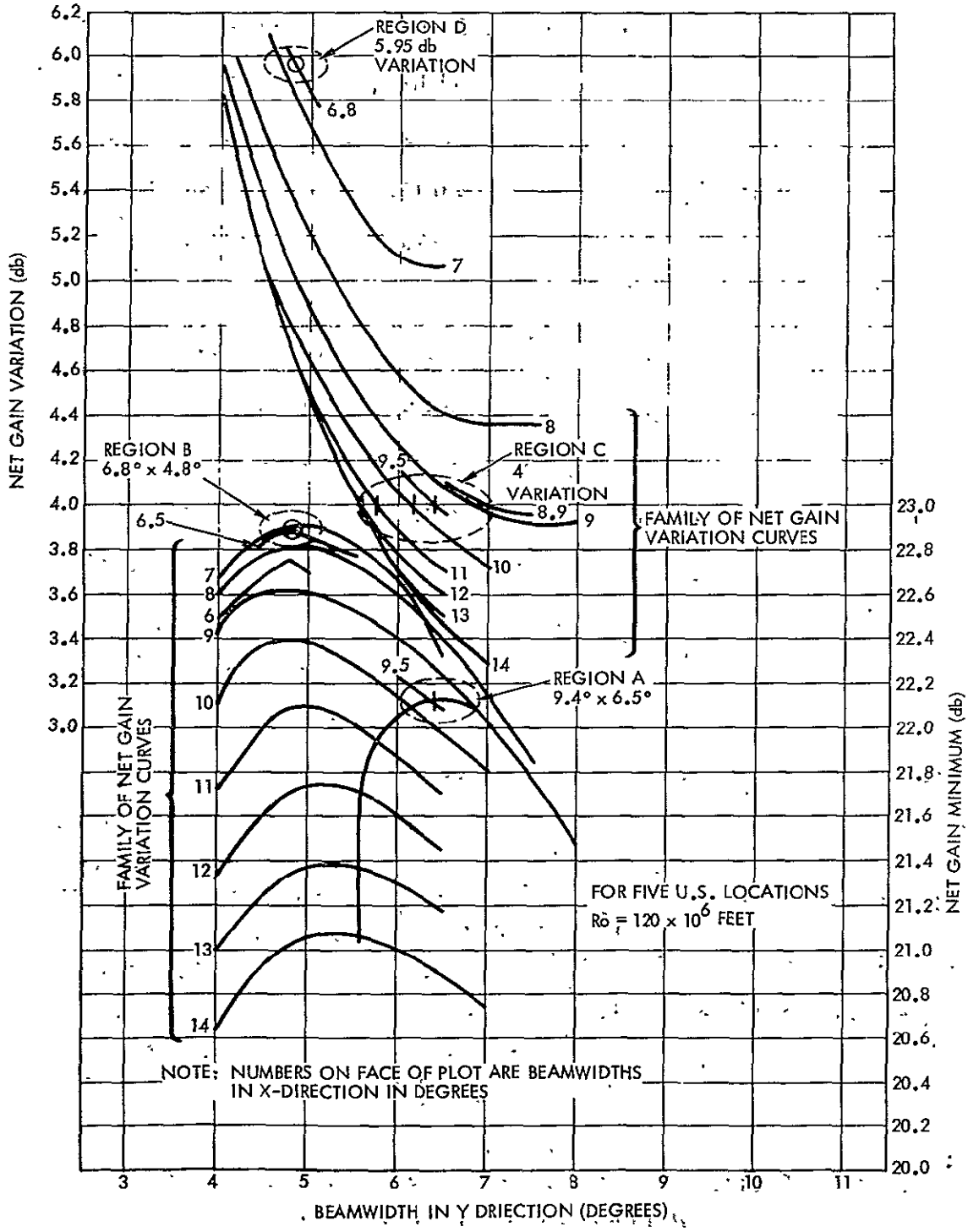

Figure H-5. Elliptical Beamwidth Optimization Curves

gain minimum of 22.1 db for a 4 db variation. Also it is seen at Regions B and D that a beam of the shape $6.8^{o} \times 4.8^{o}$ optimizes the second criteria giving a net gain minimum maximum of 22.9 db with a corresponding net gain variation of 5.9 db. Figures H-6 and H-7 give the net gain histories for these two optimized beams. Table H-1 summarizes all the optimized beamwidths, net gain minimums, net gain variations, and parabolic reflector sizes at 1.6 GHz and 0.9 GHz needed for the air traffic control satellites.

For the ATC application, the antenna chosen was the elliptical beam with the 4 db net gain variation. This antenna results in a lower net gain than the other elliptical beam, but is more desirable because of the lower net variation. The minimization of this variation is important to keep the dynamic range of LIT pulses from different aircraft to a minimum.

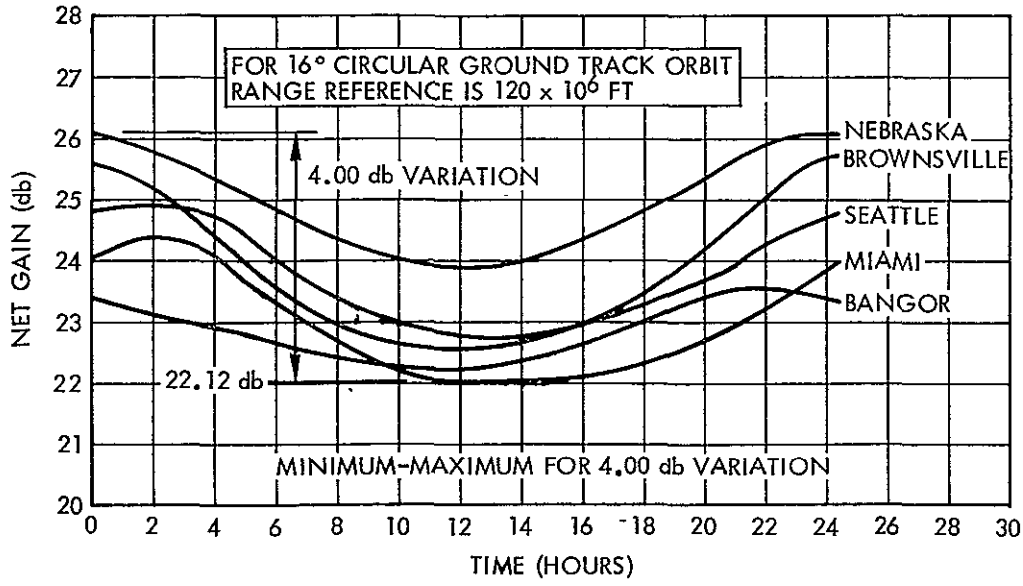

OPTIMIZED ANTENNA WITH 9.4° x 6.5° ELLIPTICAL BEAMWIDTHS
AND AN ON-AXIS GAIN OF 25.28 db

Figure H-6. Gain History - Net Gain Versus Time

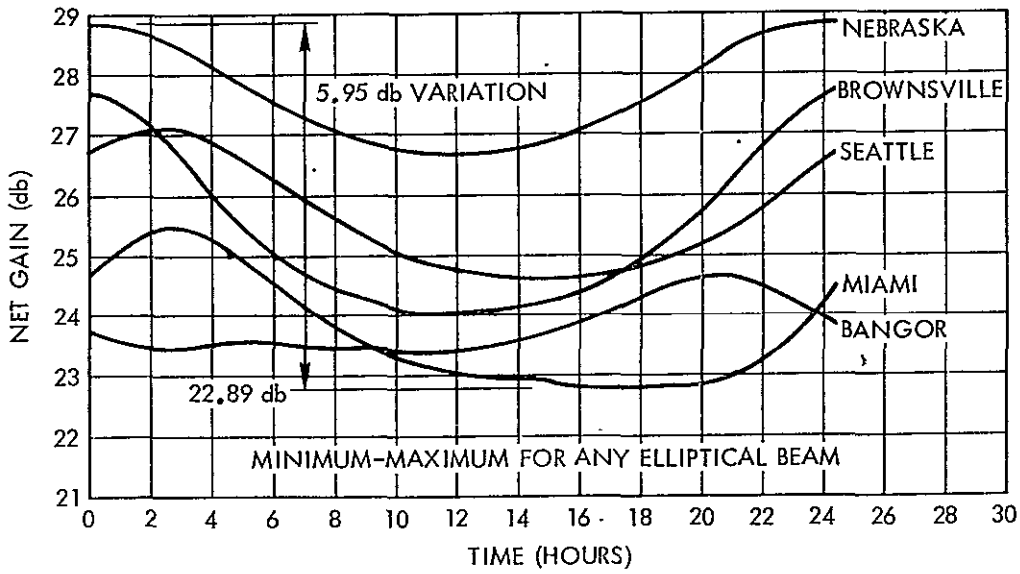

OPTIMIZED ANTENNA WITH 6.8° x 4.8° ELLIPTICAL BEAMWIDTHS
AND AN ON-AXIS GAIN OF 28.01 db

Figure H-7. Gain History - Net Gain Versus Time

APPENDIX I

COMPUTATION OF SATELLITE TRANSMITTER LINEAR RANGE REQUIREMENTS FOR LIT

In the LIT system, the input to the satellite transponder consists of the sum of signals from all equipped aircraft. Since the number of simultaneous signals and their phase and amplitude are random variables the question arises, what signal dynamic range occurs at the satellites?

To compute the cumulative probability distribution of the amplitude at the input, the following assumptions are made:

1. The input signal to the transponder = $mC + N$

   where N = transponder thermal noise
   C = sinusoidal signal of fixed frequency, f_o
   m = number of signals, C, present at any instant

2. The signals C are uniformly distributed in amplitude within the range 1.0 to 4.35 volts rms (12.8 db range).

3. The thermal noise is Gaussian distributed, and has an rms level of 2.6 volts.

4. The number of signals, m, is distributed in some unknown fashion, but it is assumed that it can be approximated by a Poisson distribution.

5. Two cases are considered. In the first case, the average number of pulses per second is 10^5, and in the second the average number is 5×10^4. With a 51 μsec. pulse duration, this corresponds to an average number of simultaneous signals of 5.1 and 2.55, respectively.

6. The phase of each signal is random with a uniform probability distribution from $-\pi$ to π. The phase and amplitude of all signals are independent and modulation is ignored.

1. Computation Procedure

Since the number of signals, m, present at any instant is random, the procedure for finding the cumulative distribution is first, to compute the conditional distribution for each fixed value of m, and then to form the cumulative distribution by suming all conditional distributions each multipled by the probability of the assumed value of m. In principle this could be done analytically; however, the integration of the composite conditional probability density of the m signals plus noise, laborously obtained by (m+1)-fold convolutions, would invariably require numerical integration. Since recourse to computer evaluation appears to be necessary in any case, a Monte Carlo procedure seemed to be the most direct means of obtaining results.

Three separate time share programs were used in obtaining the cumulative distribution. The first, the "Dynamic Range Program", accepts as inputs the number of signals, m, the number of Monte Carlo's, N, (i.e., the number of times the calculation is repeated), and the standard deviation for the Gaussian noise distribution. In the program, a pair of uniformly distributed random numbers are selected and appropriately scaled to the specified range for the phase and amplitude and a value for C $\sin\phi$ is computed. This procedure is repeated m times. Each time a different pair of random numbers is selected, C $\sin\phi$ computed, and the result added to the sum of the previous values. To add the noise component, a Gaussian distributed random number is generated using a conventional procedure based on the

Central Limit Theorem, scaled by the input value of the standard deviation, and added to the sum of the m signal components. The resulting random number is used to designate a memory location. The value 1/N is added to the contents of the designated location. After the Monte Carlo procedure has been repeated N times, the contents of the various memory locations represent a histogram of the m signals plus noise. The histogram is written on magnetic tape. At the same time, the conditional probability distribution (dependent on m) is computed and selected values of the conditional density and distribution are printed. Since the histogram is computed with as many as 1000 points, it is necessary to limit the volume of print out to values corresponding to the 2% and 98% points, all multiples of 5%, and the extreme points of the probability distribution.

A second program is used to combine the histograms obtained by the "Dynamic Range" program. The "Combine" program reads a set of histogram values, multiplies them by a given input value of probability and stores the values in the memory. A second set of histogram values is then read, multiplied by a second input value of probability, and added term by term to the first set of histogram values. The resulting combined histogram is then written on magnetic tape, and extreme values of the distribution are printed so that the program action can be monitored.

The determination of the signal cumulative probability distribution requires three steps. First, the "Dynamic Range" program is run M times to obtain the M conditional probability densities. Truncation of the maximum number of signals present to M=15 for the case with 10^5 user aircraft

and M=12 for the case of 5×10^4 aircraft corresponds to ignoring events with probability less than 10^{-4}.

Next, the "Combine" program is used to determine the cumulative distribution. The conditional densities for m = 0 and m = 1 are multiplied, respectively, by P(0) and P(1), where P(m) is the Poisson distributed value of the probability for the indicated value of m; the resulting combined density then is written on magnetic tape. The "Combine" program is used a second time to take the combined m = 0 and m = 1 density, multiply it by 1.0 and add it to the conditional density for m = 2 multiplied by P(2); the resulting combined density for m = 0,1,2 again is written on magnetic tape. For the case of 10^5 user aircraft, the "Combine" program was repeated 15 times to obtain a magnetic tape containing the cumulative density for all significant values of m.

The final step was to use the "Output" program to read in the cumulative density, compute the cumulative distribution, and printout the distribution values corresponding to 0.1%, 2%, 98%, 99.9% and all multiples of 5%.

2. Results

To obtain accurate results using the Monte Carlo method, the number of trials, N, must be made large. A practical limitation on N is imposed by the computer time required for each run. N = 10,000 was chosen as a compromise between cost and accuracy.

For the m = 0 case (no signal), the standard deviation of the Gaussian distribution was 2.56 instead of the 2.60 specified indicating an error of about 1.5%; the mean showed an equivalent error. For non-zero values of m, the standard deviation is unknown. However, the mean

should always be zero since neither the sinusoidal signals nor the noise present an offset. The computed values of the mean are all close to zero with accuracy improving from 1.5% to 0.3% as m ranges from 0 to 15.

Since the input to the satellite transponder consists of the sum of several signals plus noise, one might expect that the cumulative distribution would be approximately Gaussian. To estimate the variance of the signal, one might make the admittedly crude approximation that the variance of the sum is equal to the sum of the signal average variance times the expected number of signals plus the noise variance. For the case of 10^5 users, this becomes:

$$\sigma_T^2 = 5.1\bar{\sigma}_S^2 + \sigma_n^2$$

where σ_T^2 is the variance of sum of signals plus noise

$\bar{\sigma}_S^2$ is the average variance of a single signal

σ_n^2 is the noise variance

Taking $\bar{\sigma}_S^2 = 7.15$ and $\sigma_n^2 = (2.6)^2 = 6.76$, we have $\sigma_T^2 = 43.2$ and $\sigma_T = 6.59$. This compares with $\sigma_T = 6.92$ computed by Monte Carlo. For the case of $5x10^4$ user aircraft, the estimated σ_T is 5.01 compared to the computed value of 5.23. In both cases, the crude estimate for σ_T is about 4.5% lower than the computed value.

The distributions for the two cases are plotted on probability paper in Figure I-1, from which it may be seen that both plots are fairly linear in the 5% to 95% region. The case for 10^5 users with $\bar{m} = 5.1$ is more linear (i.e., closer to being Gaussian) than the base for 5×10^4 users with $\bar{m} = 2.55$ as would be expected from the Central Limit Theorem.

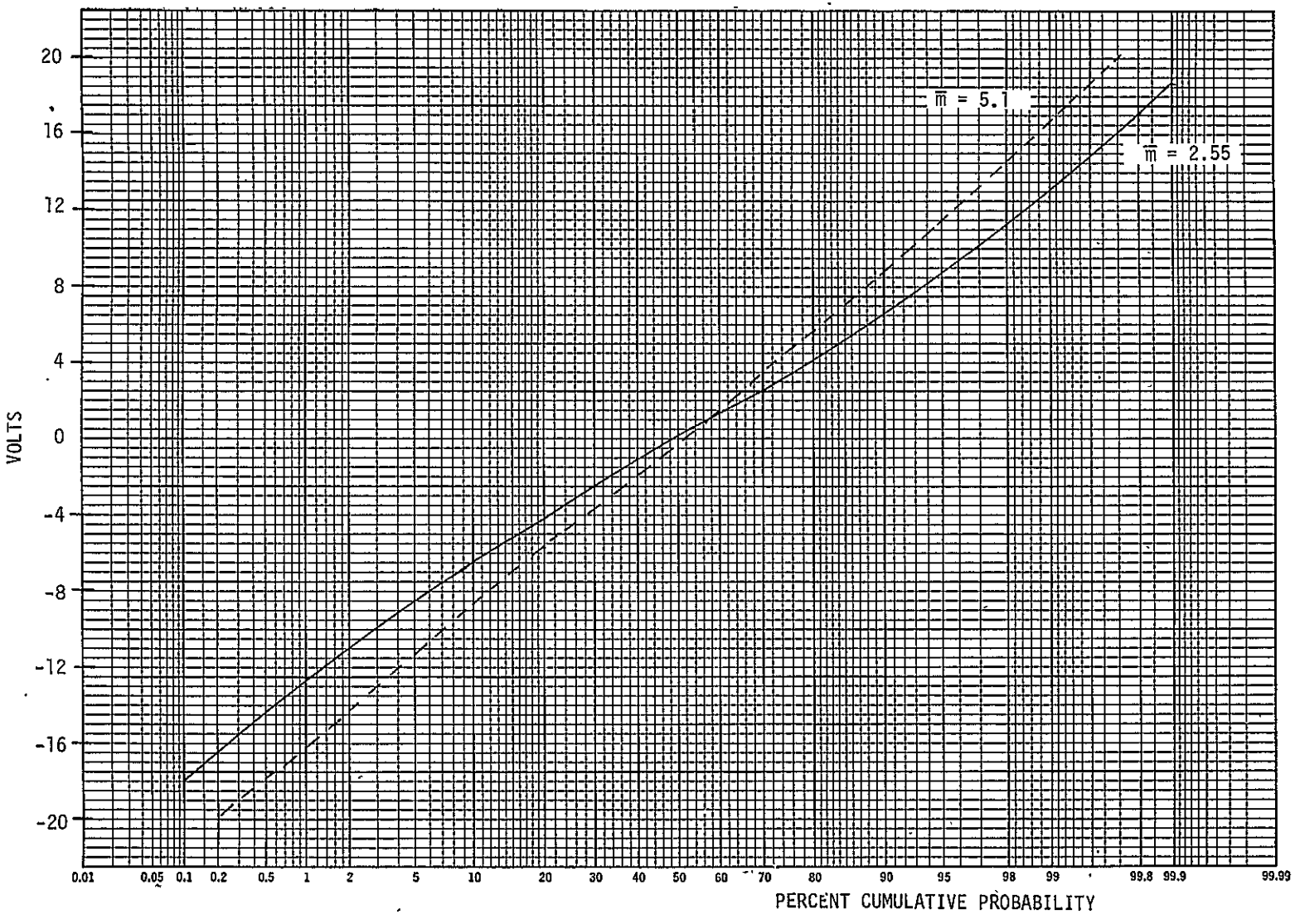

Figure I-1. Probability Distributions of Signal Plus Noise

The downlink C-band power budget (Ref. Section 4.2.6) requires two watts of RF output power for the case of five simultaneous signals of the weakest level (1.0 volt rms) and noise (2.6 volts rms) at the transponder input. Therefore, the corresponding rms voltage of the signal is:

$$\sigma_T = \sqrt{\sigma_s^2 + \sigma_n^2} = \sqrt{5^2 + 2.6^2} = 3.43 \text{ volts.}$$

This voltage then corresponds to 2 watts RF power. For the case of 50,000 users ($\bar{m} = 2.55$), the rms voltage for the total signal is 5.23 volts and the 98% peak value is 11.0 volts. These voltages correspond to an RF output power of 4.65 watts average and a 98% peak power of 20.6 watts.

APPENDIX J

ALTERNATE DESIGN APPROACHES FOR THE LOCATION IDENTIFICATION TRANSMITTER

In the design and costing studies for the transmitter, it became apparent that the main area in which a significant cost and/or design savings might be made would be in reducing or eliminating the multiplier-amplifier chain from which the required carrier frequency stability is derived. A number of possible approaches were investigated, the more salient of which are discussed briefly below.

1. 100 MHz Crystal Oscillator

In this approach, a 100 MHz crystal source could be used to replace the 10 MHz oscillator and X10 multiplier. A divide-by 10 flip-flop circuit would also be required as a clock source for the code generator.

This approach would be used provided the cost savings of the X10 multiplier and amplifier offset the cost of a ÷10 register. However, the X10 multiplier is a very simple snap recovery diode circuit and the amplifier quite simple and inexpensive. However, commercial integrated circuits or flip-flops that operate at 100 MHz (TTL, SUHL, etc.) are more costly at present than the circuitry removed. Since IC prices are continually going down, this approach may eventually become cost competitive with the multiplier-amplifier circuitry. Also, the required 2 ppm oscillator stability at 100 MHz is slightly more costly than at 10 MHz, but not so much as to preclude the use of a frequency divider if the IC ÷10 function cost less than it does at present.

2. Two Separate Oscillators

It is technically quite feasible to use two oscillators, one at 100 MHz to generate the RF, the other at 10 MHz to provide a clock source for the code generator. Since the bi-phase modulation 180° phase reversals should occur ideally at an RF sinewave zero crossing, or at very least at the same phase point on the RF waveform each time, synchronization between the two oscillators is implicit. Fortunately, this is a simple requirement to meet. If the frequencies of two crystal oscillators are very close to an integer multiple of each other, then by simply coupling a small amount of energy from the output of one to the input of the other and likewise from the output to input in the other direction, the two oscillators will both pull in phase and remain phase locked. This has the additional advantage that only one oscillator need meet the 2 ppm stability requirement since the other oscillator is phase locked. Thus the frequency stability is determined by the most stable oscillator and the other may be considerably less stable with no effect upon the system.

Unfortunately, this configuration, though relatively inexpensive, does not appear cost competitive with the present proposed oscillator multiplier chain at this time.

3. High Level Oscillator at the Output Frequency

This is probably the approach that would be taken for the design of a piece of military equipment. An avalanche transit-time oscillator (ATTO) can easily provide over a watt of power in the GHz frequency range. Basic stability is rather poor, however, so the ATTO would have to be injection locked through a multiplier chain to the 10 MHz crystal oscillator. This is easy to do and costs very little to implement, as relatively low power from the multiplier chain output is usually sufficient to phase lock the ATTO. Hence, the multiplier chain may be a very simple series of several inexpensive snap recovery diodes. But this approach, though yielding the most efficient design, smallest package, least weight, and perhaps even the most reliable system, had one insurmountable obstacle for this

application: it would more than double the parts cost of the present transmitter design due to the price of the ATTO.

4. High Power Cavity Oscillator Locked to Crystal Source

This technique is one which shows great promise for being both technically competitive and cost competitive with the present approach.

It has been but a short while since transistors capable of several watts output in the GHz region have become commercially available. Now that these devices are available, it is possible to utilize a technique formerly reserved only for much lower frequencies. The high power, GHz frequency device may be used to create a simple self-excited high power oscillator consisting of the transistor, one or two simple passive components, and an easily constructed tuned cavity for the collector circuit. In practice, the transistor is mounted in an easily-constructed box having dimensions providing a resonant cavity for the collector, with the emitter grounded and the base biased just slightly into forward conduction. Ample feedback usually exists in the base-collector path to cause oscillation. Cavity tuning may be accomplished in several ways, either by a simple piston plunger, variable end plate, or a stripline inductance in the collector surrounded by the fixed cavity. Since stability is poor, the oscillator must be locked to the 10 MHz crystal oscillator, but as in the case of the ATTO this may be accomplished by a simple and inexpensive multiplier chain providing a small amount of power to a cavity probe located near the transistor base. This approach could yield the least expensive system capable of doing the required job provided the price of the required transistor is reasonably low in quantity. One minor problem results in that the biphase modulation must

now be done at a higher power level and higher frequency than previously, but obtaining an adequate modulator does not seem difficult.
If the power oscillator were tuned to half the output frequency and the first pulsed amplifier operated as a frequency doubler the maximum frequency at which the biphase modulator would operate is 800 MHz, which is within the upper limits of commercially available circuits.

As appealing as it seems to be, the primary reason this technique cannot be unreservedly recommended is a lack of essential data regarding the oscillator. Questions which still require definition are, for example; can the free running oscillator power be easily regulated within some limits over temperature extremes, or will this require expensive ancillary circuitry? Will the feedback path be sufficiently controllable that mass produced oscillators will be reasonably uniform in electrical characteristics, or will a lot of manhours be consumed in tuning and testing? Is injection locking as simple as it seems or does it take a more expensive multiplier chain than is competitive with the present approach?

APPENDIX K

AIRCRAFT ANTENNA PATTERN MEASUREMENTS

Aircraft antennas for general aviation were experimentally studied to determine their coverage capabilities for a Cessna 172 type of aircraft. The antenna configurations selected for experimental evaluation were the curved turnstile and curved dipole antennas. The antennas were tested on separate ground planes and their dimensions were sized to represent the wing of the Cessna 172 aircraft. The pattern test frequencies were 1550 MHz for the turnstile design and 2200 MHz for the curved dipole. These scale model tests were designed to verify the coverage requirements of -3 db to +4 db near hemispherical coverage gain for a 900 MHz antenna.

The rectangular metal surface ground plane used for pattern studies of the curved turnstile antenna is shown in Figure K-1, and the antenna model in Figure K-2. The metal surface was fabricated to represent a 1/1.7 scale of the wing of the Cessna 172 aircraft. The metal surface measures 28" x 80" which represents full scale wing dimensions of 48" x 136". Although the actual length of the wing span is substantially longer, the selected surface was adequate for pattern performance evaluation. The antenna was illuminated by a circularly polarized source.

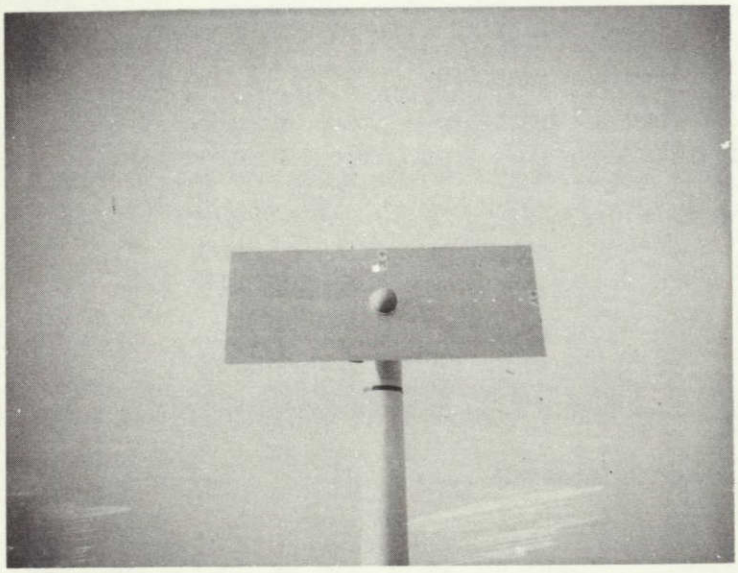

Figure K-1. Curved Turnstile Antenna with Randome on Ground Plane

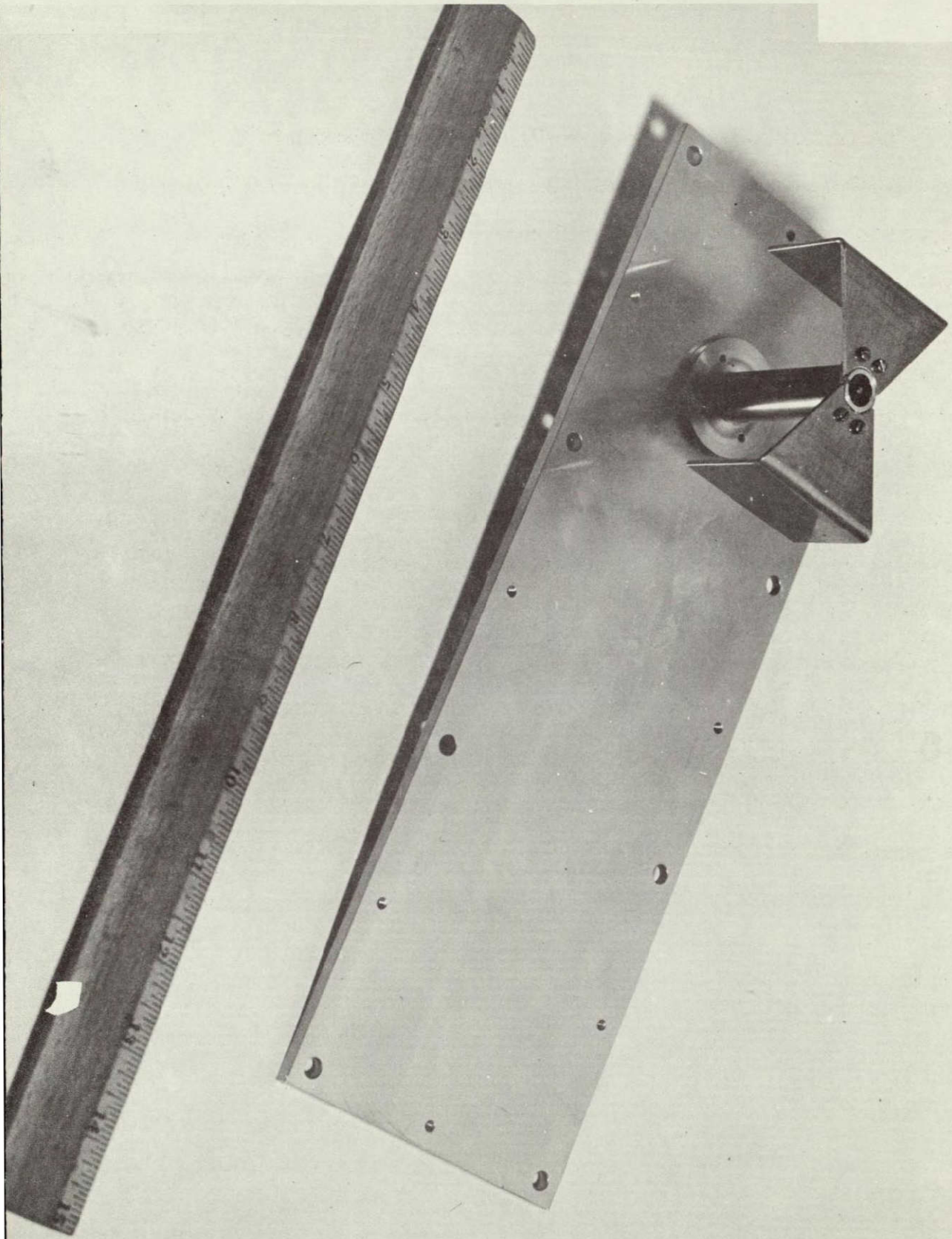

Figure K-2. Curved Dipole Antenna Test Model

The test results are given in Figures K-3(1) through K-3(3). The results given in Figures K-3 to K-8 show excellent uniformity over the required coverage cone of 160^{o}.* The antenna gain distribution is within -3 db to +4 db with respect to a circularly polarized isotropic source. However, the major portion of the coverage area is at gain levels of 0 dbi to 4 dbi.

The minimum gain coverage pattern is shown in Figure K-8. This pattern would normally be affected by the aircraft vertical stabilizer due to mutual interactions and shadowing effects with the antenna. With reduced coverage in this direction, the effect of the vertical stabilizer on the pattern would be minimized.

The test results of the curved dipole antenna are shown in Figures K-9 through K-15. The physical dimensions of the ground plane used for the pattern tests was 20" x 60". The antenna was mounted with its long dimensions along width dimensions of the ground plane. The gain of this antenna is seen to be generally lower than the turnstile. Peak gain is only +1 dbi.

---

*The angles ϕ and θ refer to the directions shown in Figure 45 Section 5.2.1.4.

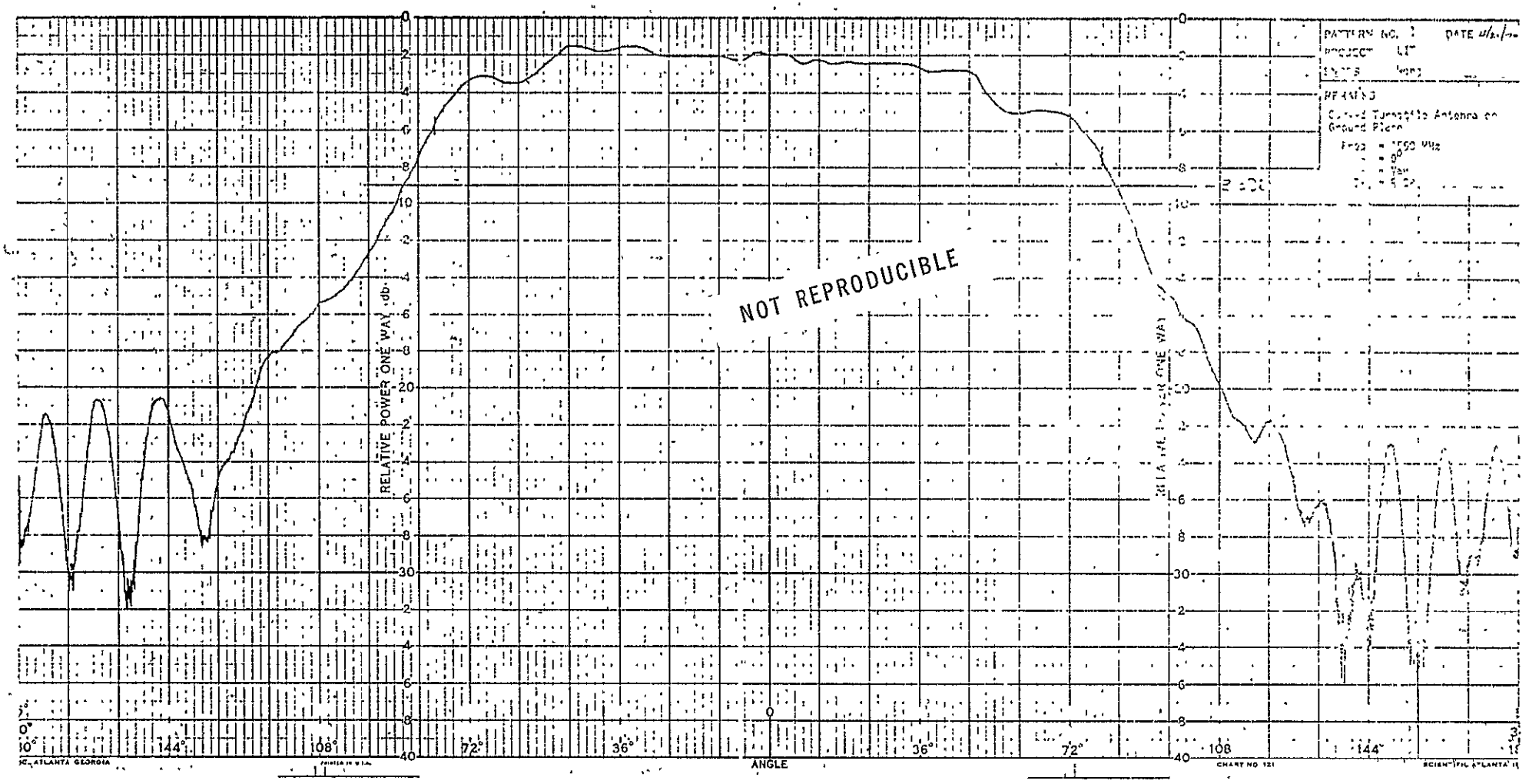

Figure K-3. Test Pattern No.

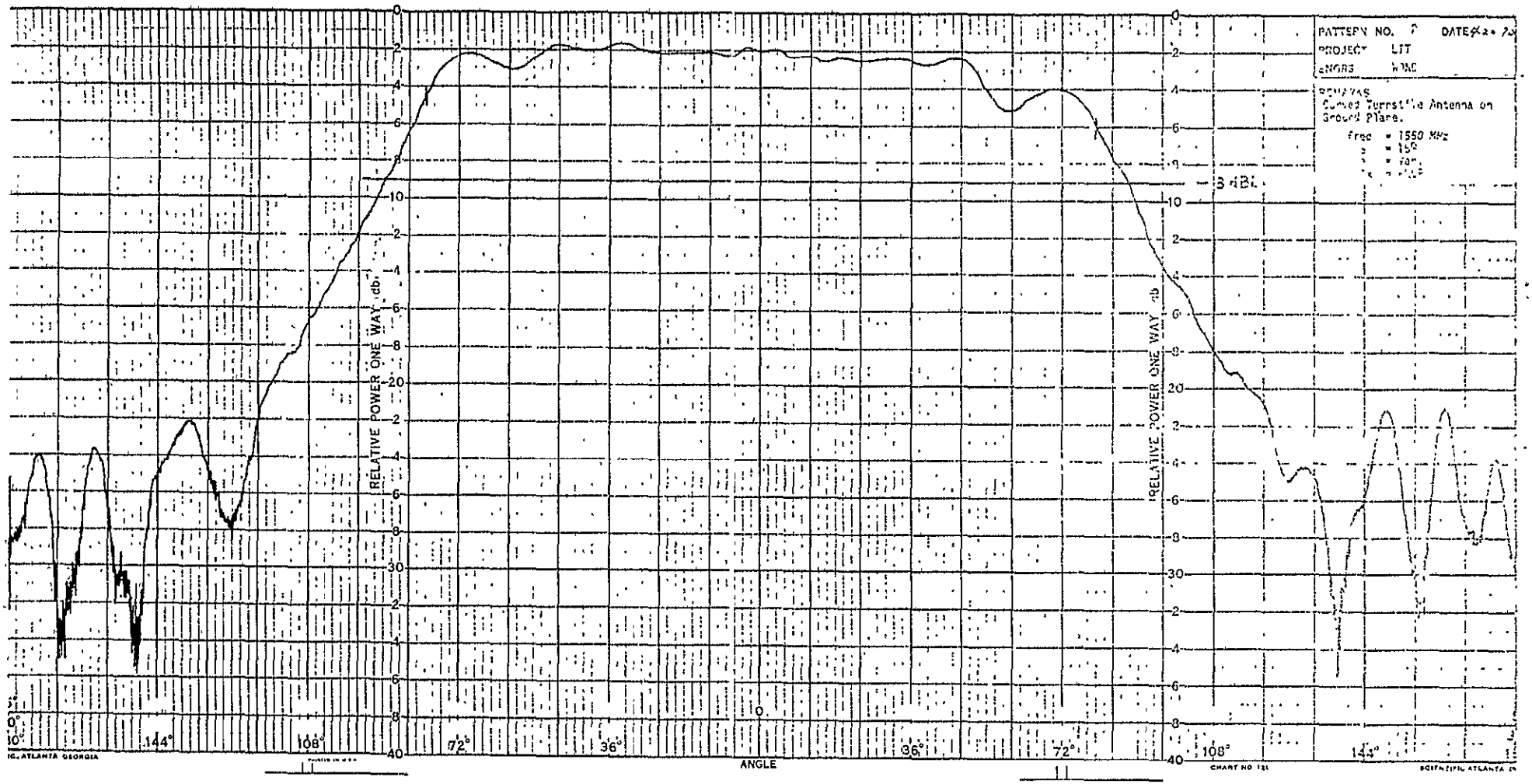

Figure K-3. Test Pattern No. 2

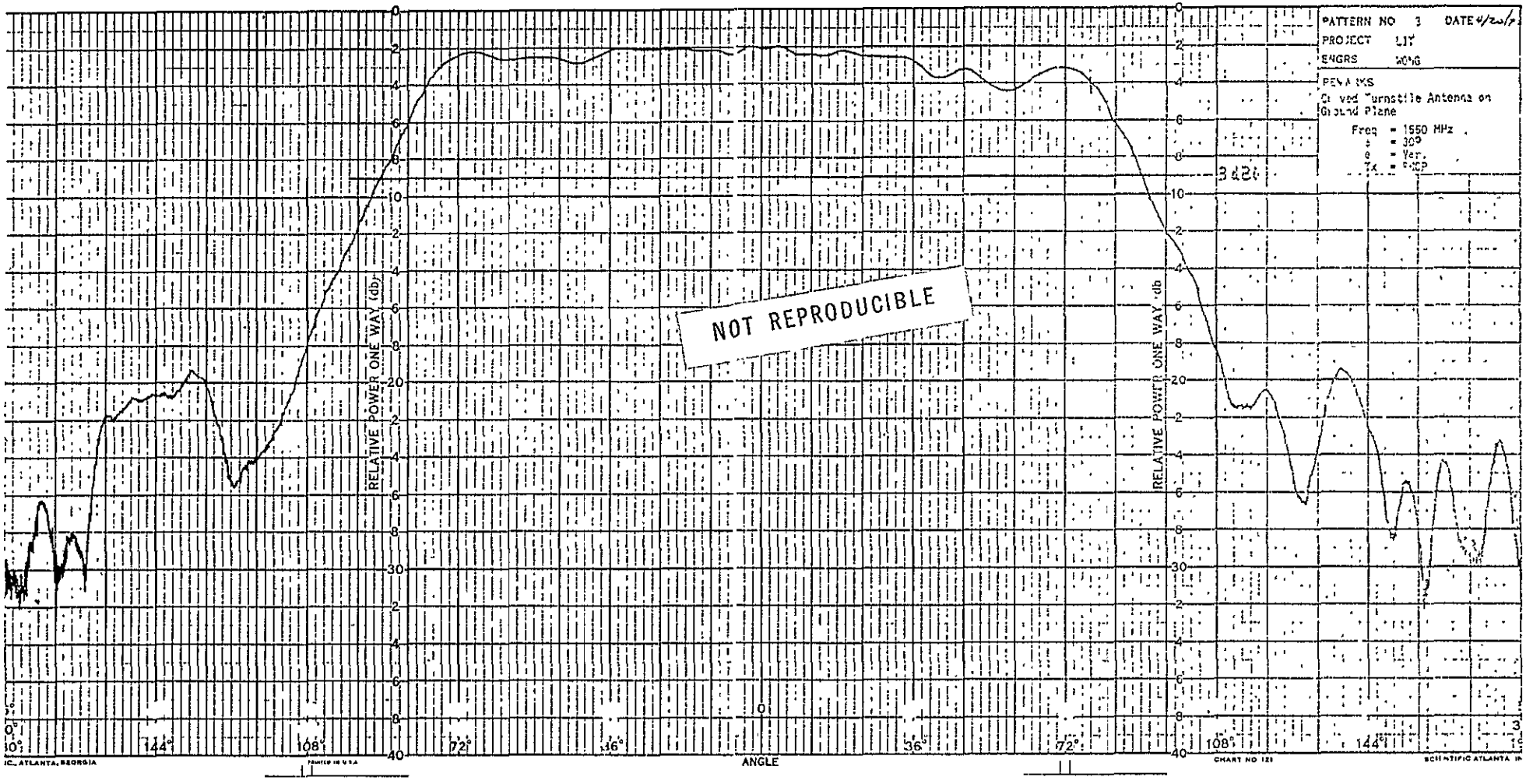

Figure K-3. Test Pattern No. 3

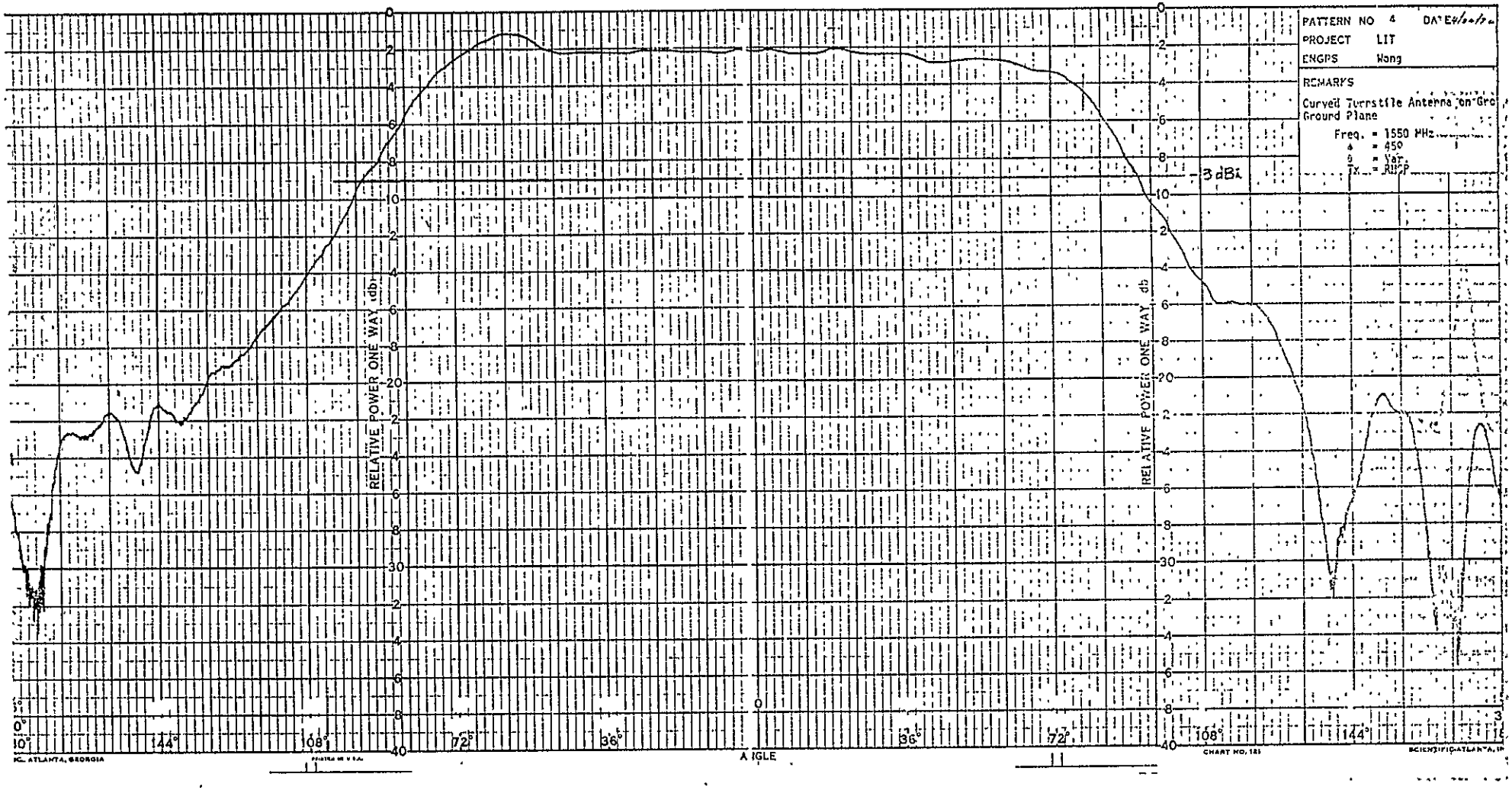

Figure K-3. Test Pattern No. 4

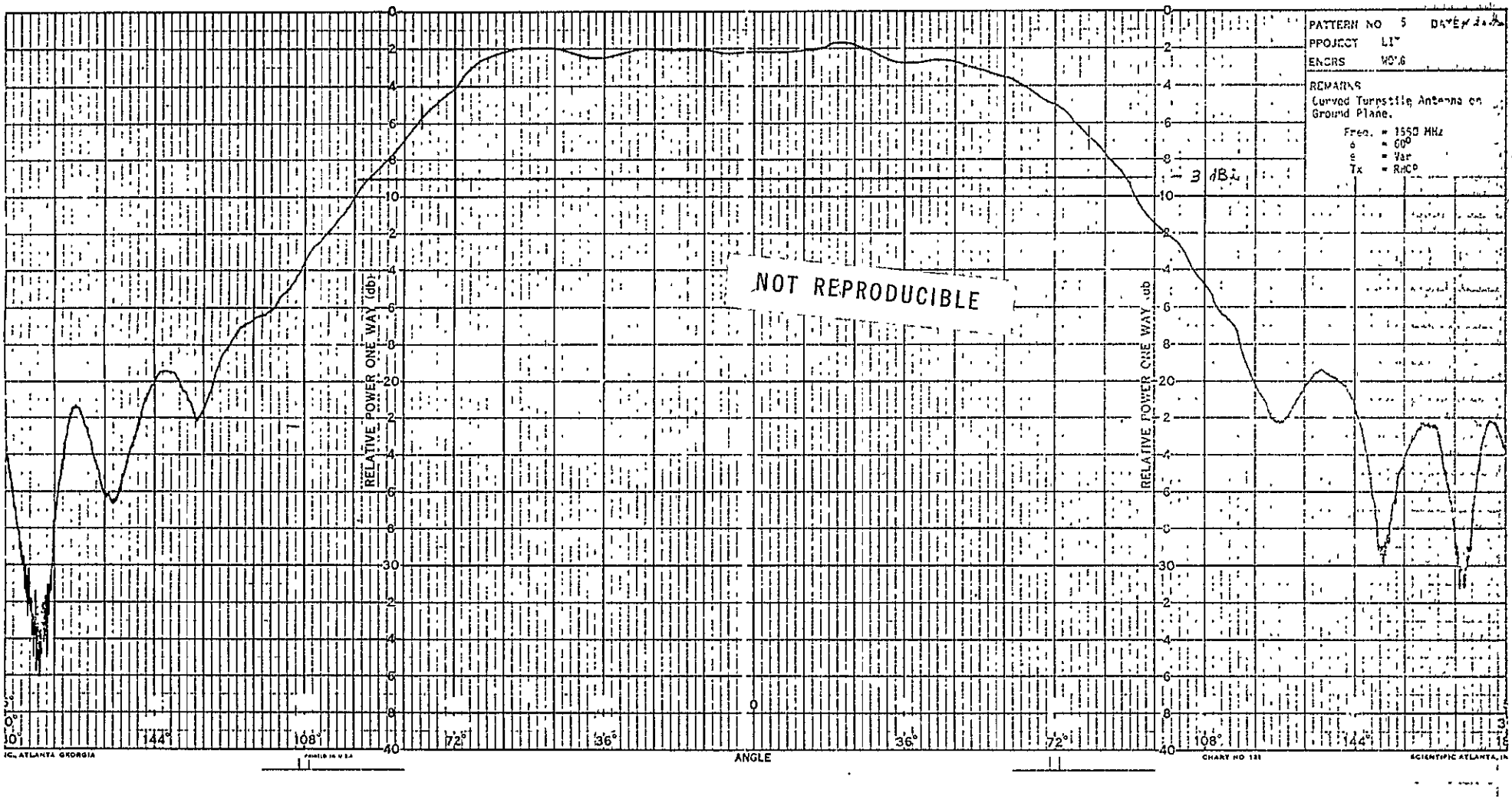

Figure K-3. Test Pattern No. 5

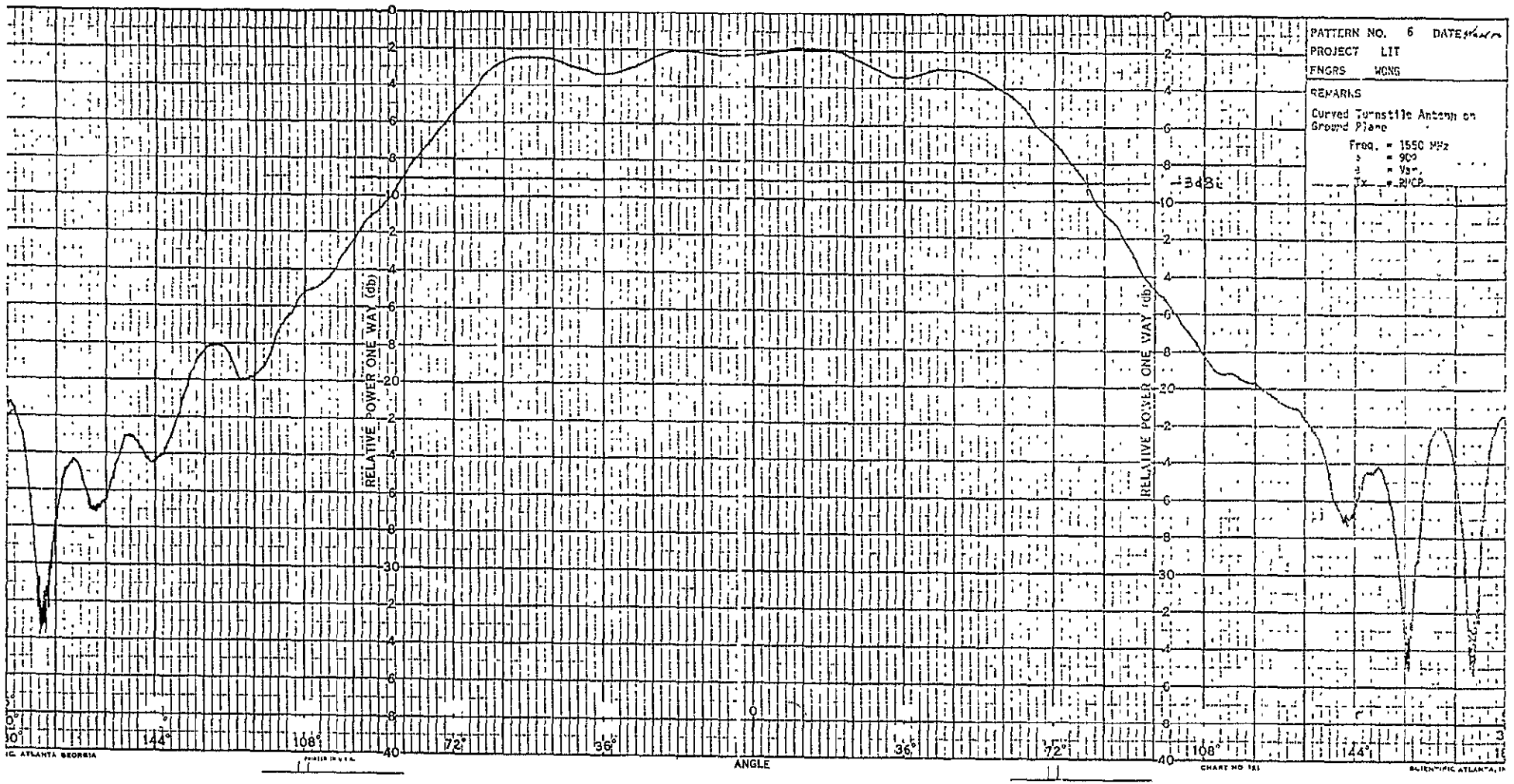

Figure K-3. Test Pattern No. 6

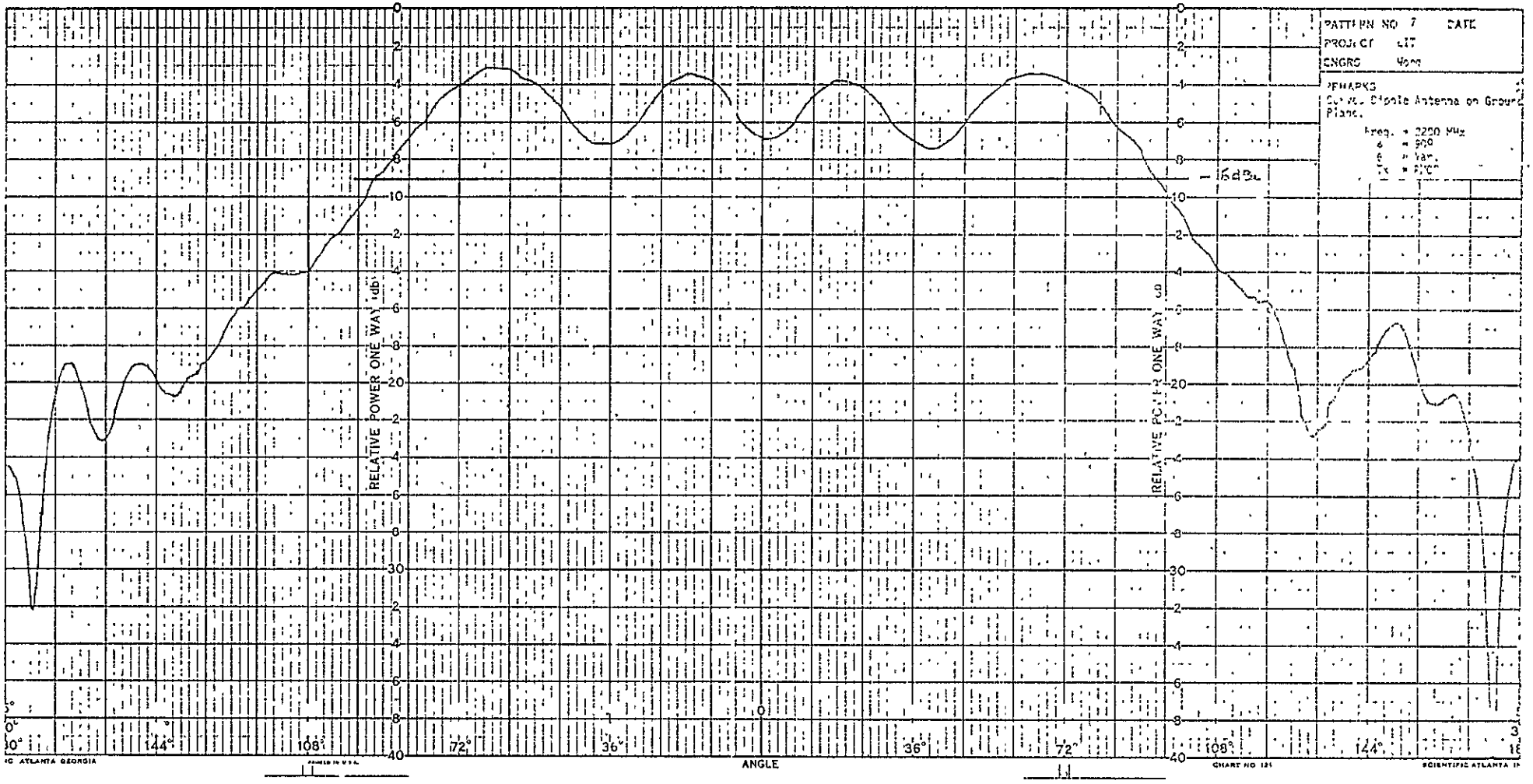

Figure K-3. Test Pattern No. 7

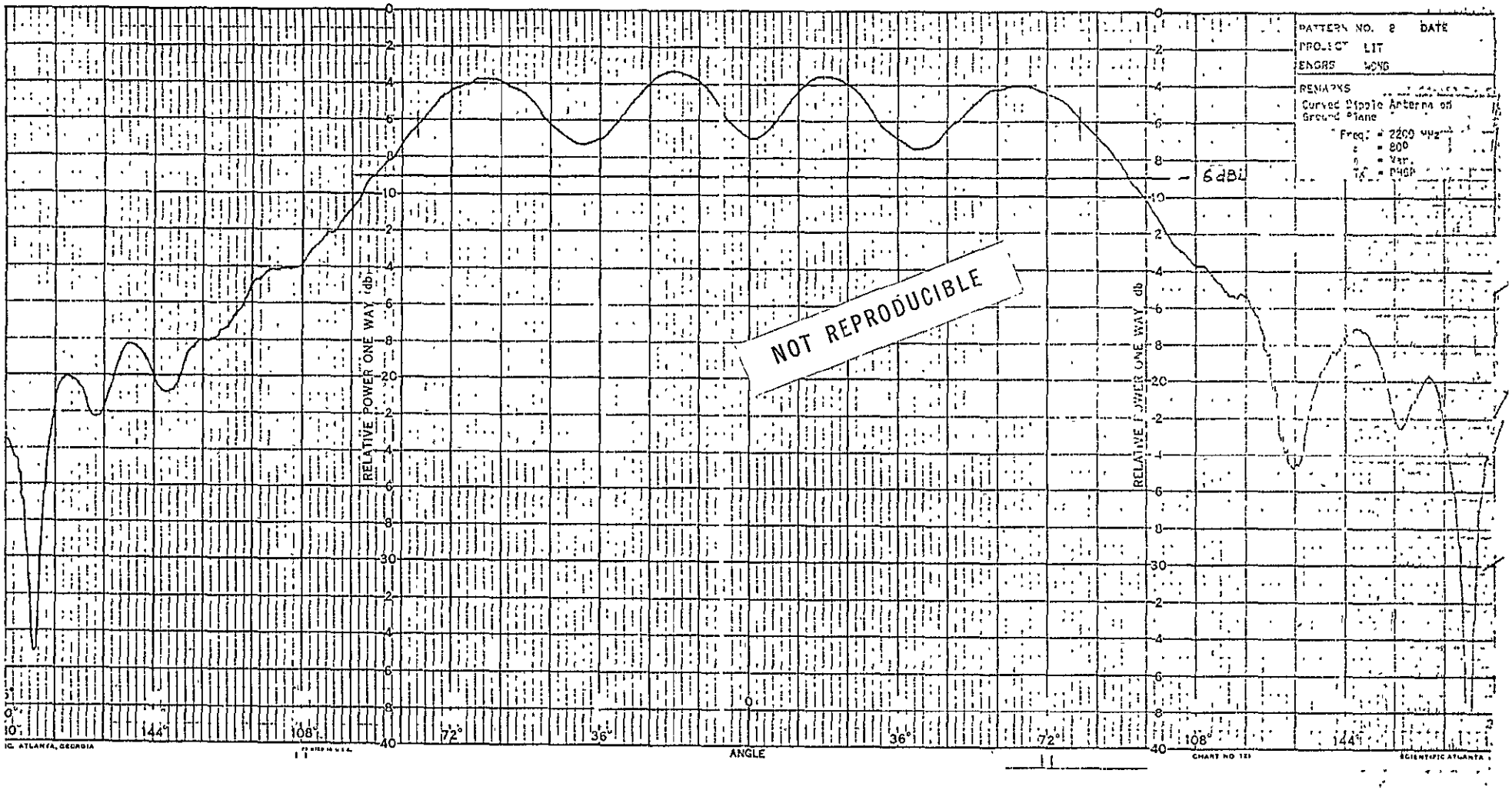

Figure K-3. Test Pattern No. 8

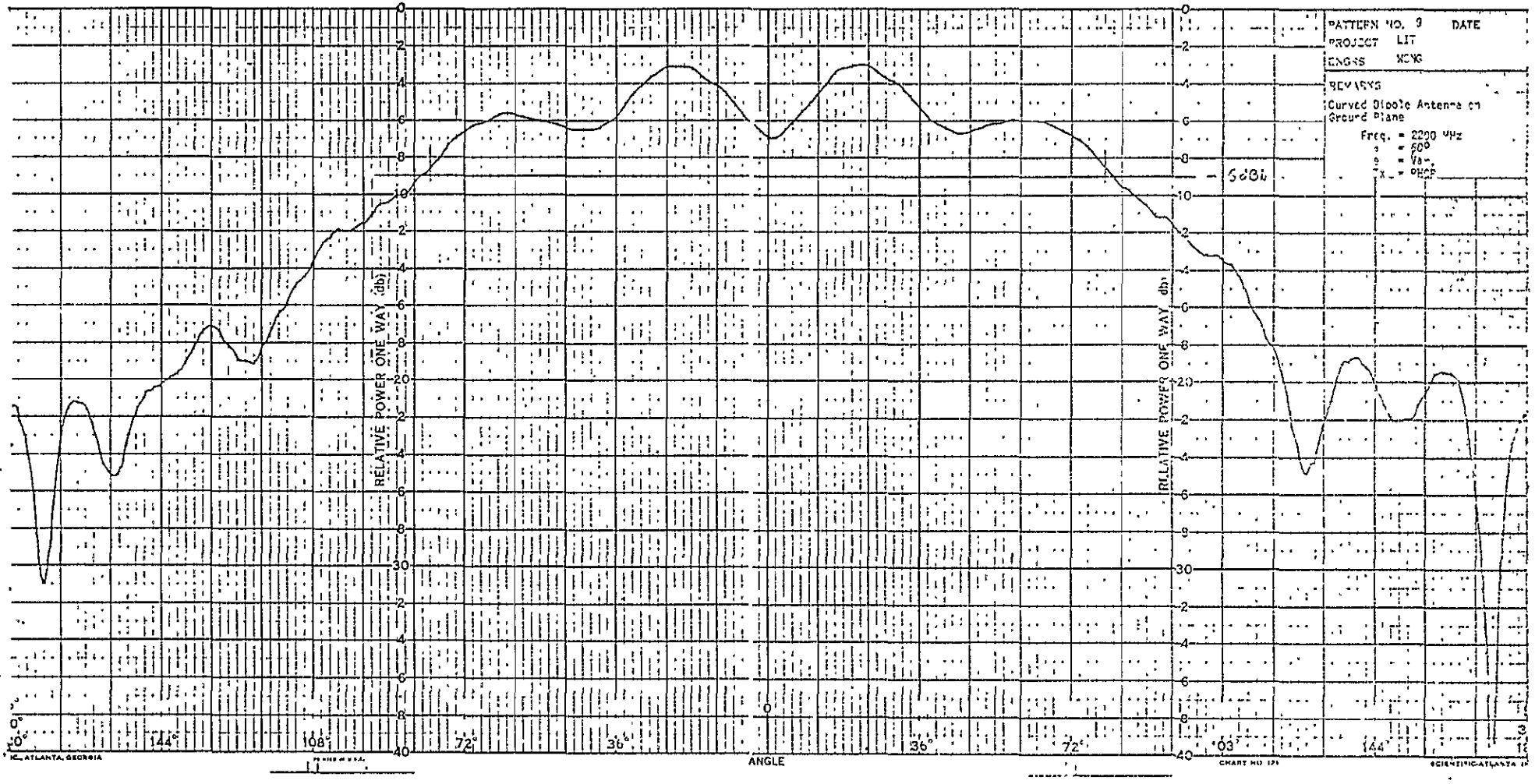

Figure K-3. Test Pattern No. 9

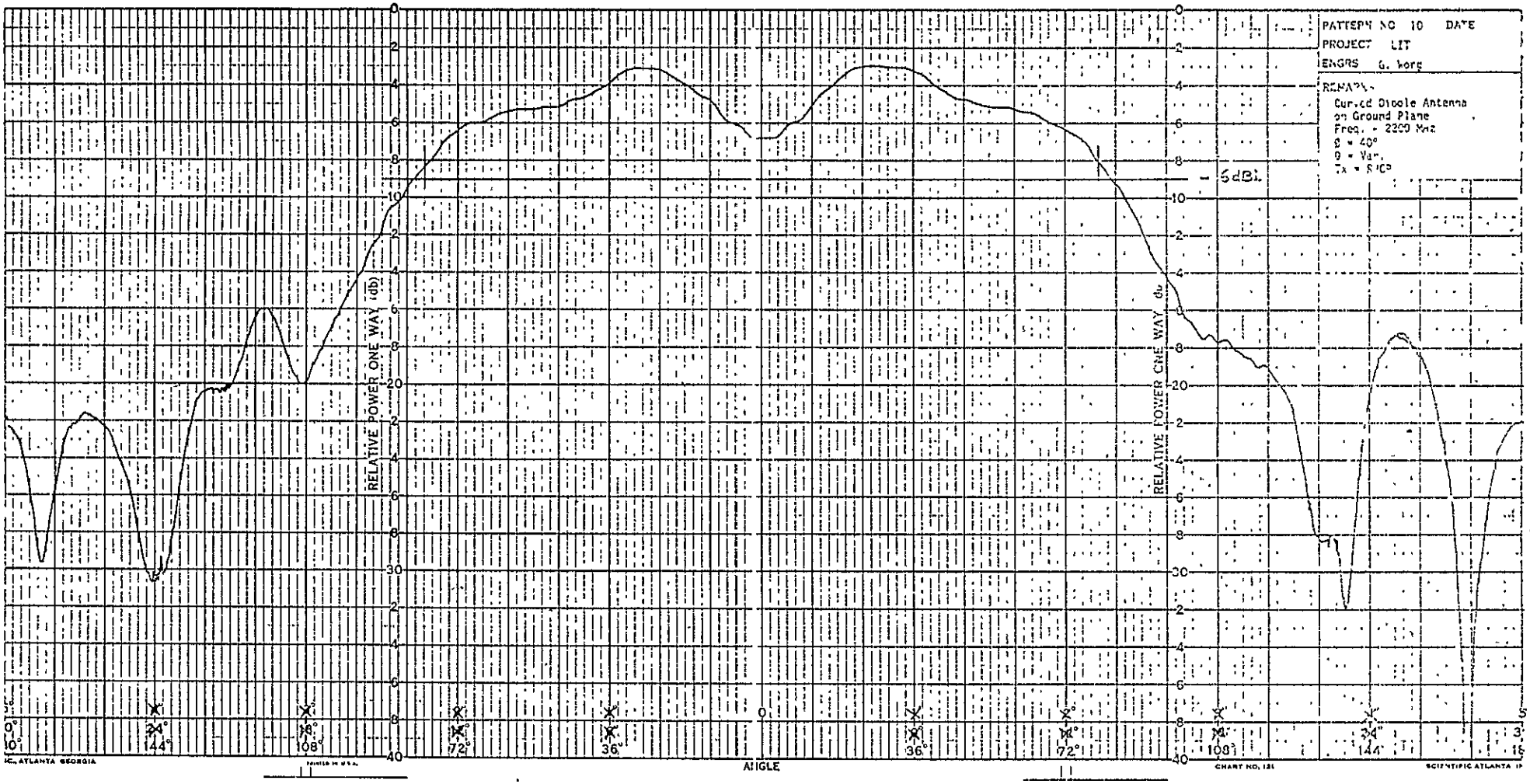

Figure K-3. Test Pattern No. 10

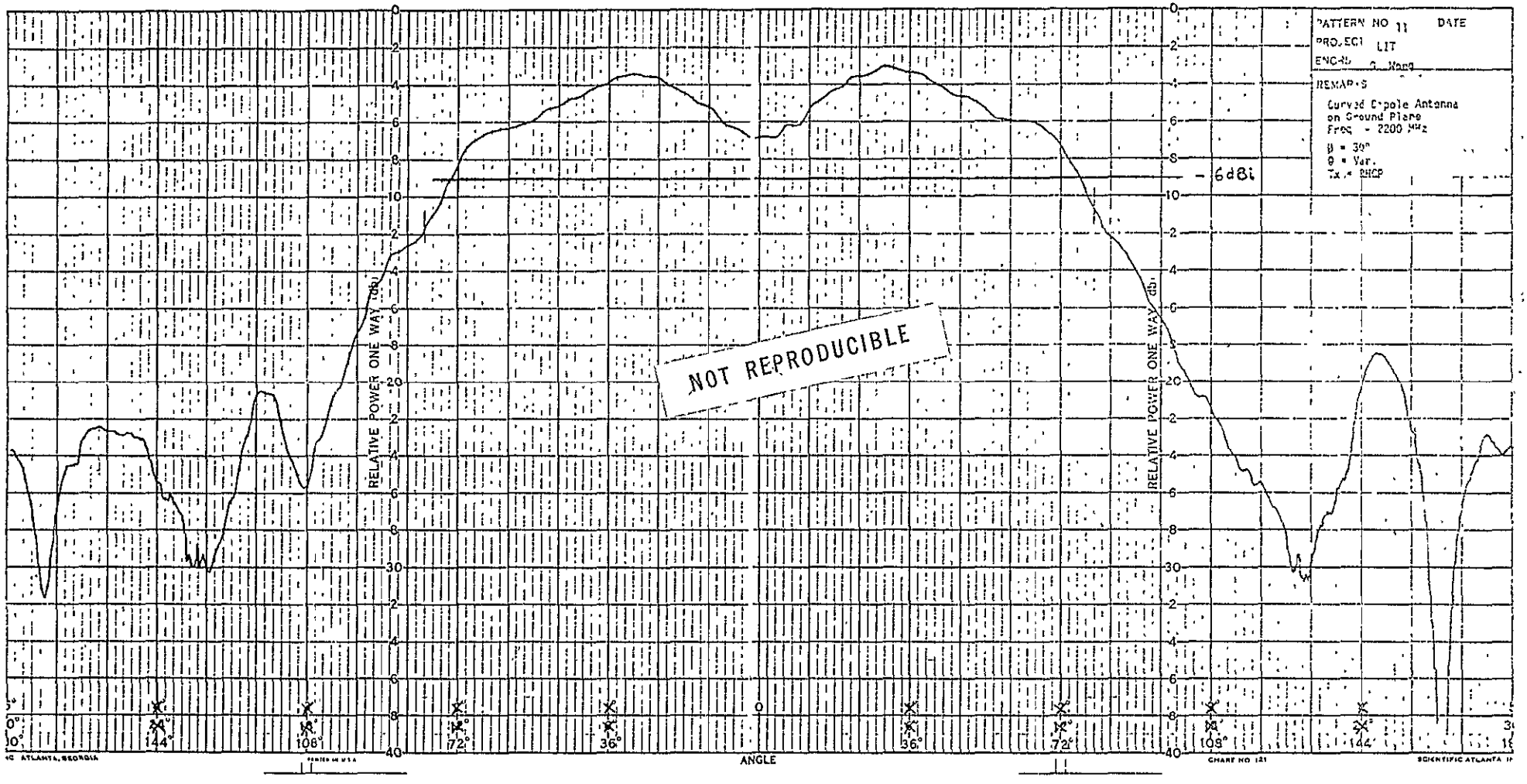

Figure K-3. Test Pattern No. 11

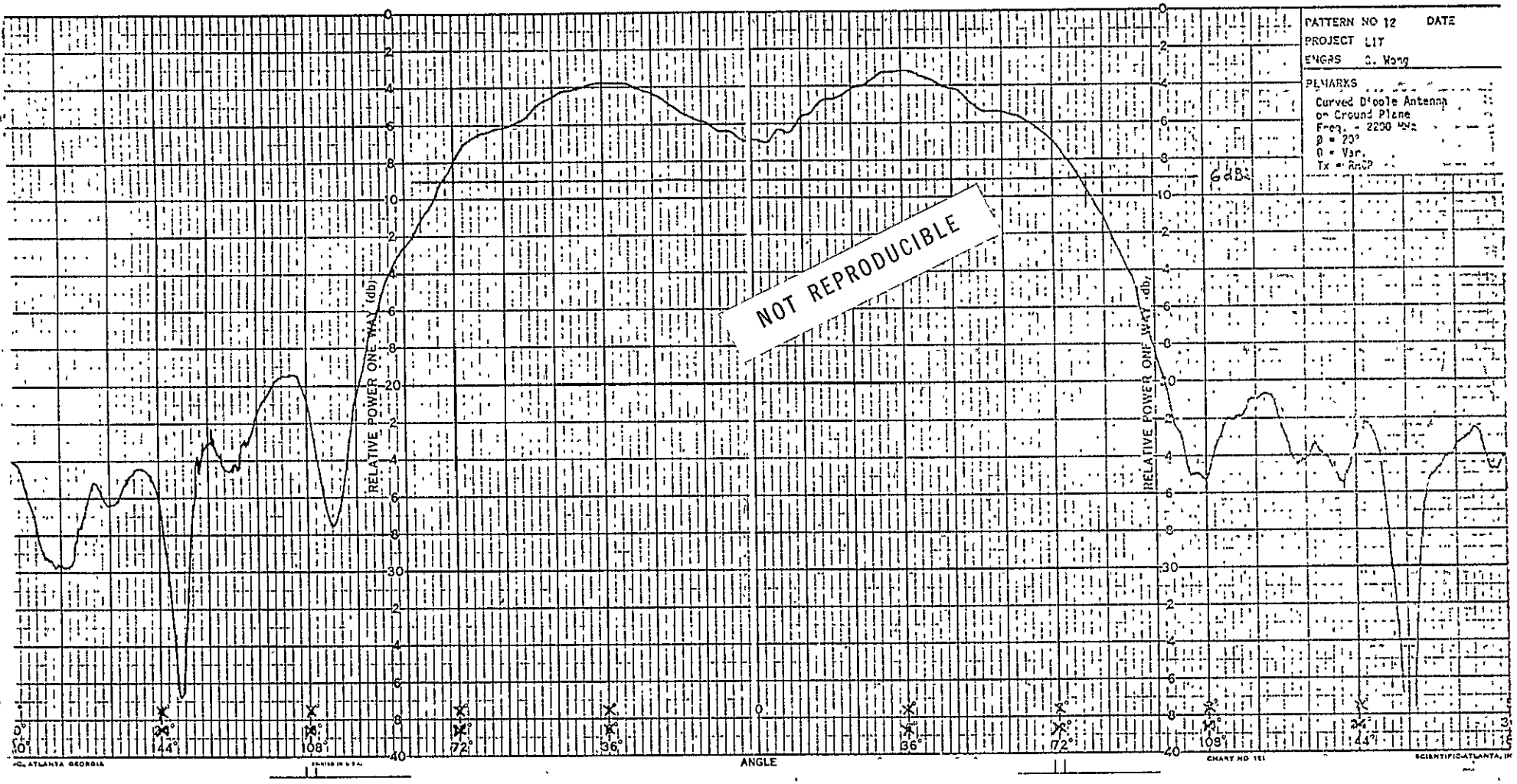

Figure K-3. Test Pattern No. 12

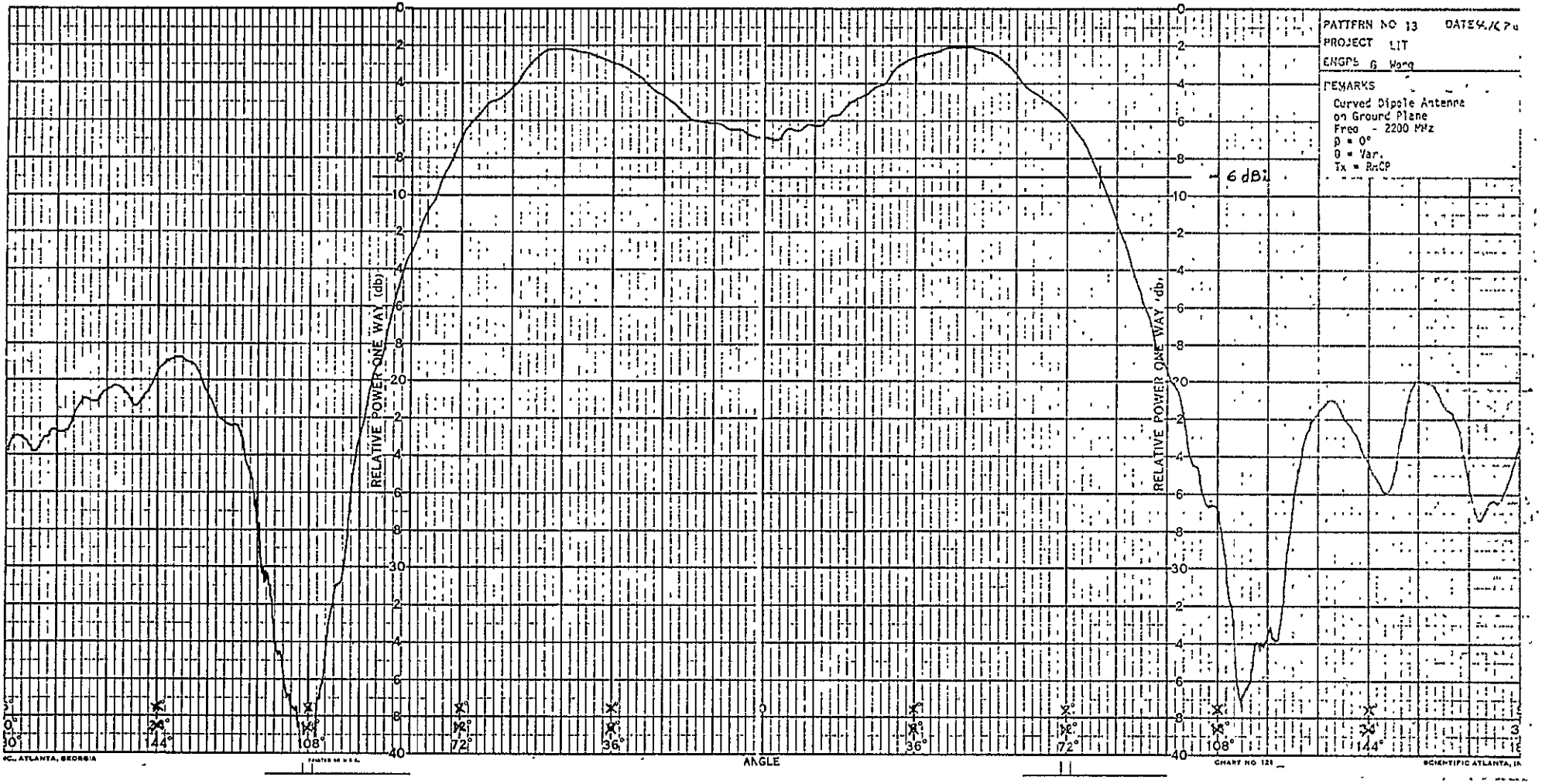

Figure K-3. Test Pattern No. 13

APPENDIX L

Copy of Attachment to North American Rockwell Autonetics Proposal to TRW Systems on Multiple Tap Surface Wave Delay Line, dated June 16, 1970.

Attachment to
Autonetics Letter
70AN14878
AN70-1153

Exhibit A. MULTIPLE TAP SURFACE WAVE DELAY LINE

I. OBJECTIVE

The objective is to conduct a feasibility demonstration program with the goal of producing and delivering a surface acoustic wave tapped delay line with 511 taps with 100 nsec spacing between taps. This line will be designed with a 10 MHz bandwidth and operated as an analog matched filter for a repetitive maximal length sequence of pseudo-random noise code--presumably a code generated by a 9-bit shift register--with a 10 MHz chip rate of biphase information. The tap coding of the line will be accomplished either by a laser burn out technique or by etching using a photolithographic mask.

II. BACKGROUND

The feasibility of surface acoustic wave multiple tapped delay lines was first demonstrated by Autonetics in 1969[1,2,3] and the design principles and fabrication techniques are well established at Autonetics. Tapped delay lines with 50 taps at 200 nsec intervals with a center frequency of 120 MHz were designed and fabricated for use as analog matched filters for 63-bit maximal length codes with 5 MHz chip rates. These lines were made with Y-cut, X-propagating quartz and used a 1.5 inch length of single crystal quartz for the delay medium. Delay lines have also been made at Autonetics with lithium niobate, bismuth germanium oxide $Bi_{12}GeO_{20}$ and other special materials grown at Autonetics such as zinc oxide on sapphire, aluminum nitride on sapphire, beryllium oxide. These lines have been fabricated on programs directed towards evaluating a variety of different piezoelectric materials for their suitability for advanced devices capable of operating as time domain or frequency domain filters in system applications.

III. TECHNICAL APPROACH

The material to be used for the 511-tap delay line is bismuth germanium oxide $Bi_{12}GeO_{20}$ and the center frequency will be 80 MHz. These choices are dictated by the following considerations.

a. Bandwidth

The 100 nsec between taps means a line with a 10 MHz input bandwidth is required. For an interdigital transducer the fractional bandwidth is 1/N where N is the number of finger pairs in the structure--assuming a transducer with a constant periodicity. For any piezoelectric material there is an effective electromechanical coupling factor k which determines the efficiency of coupling between electromagnetic energy and acoustic energy. For coupling using interdigital transducers this constant k in combination with the dielectric constant of the material dictates the geometry of the interdigital transducer used to convert the incoming signal to an acoustic surface wave signal if optimum conversion (lowest insertion loss coupled with maximum bandwidth) is required. The result is that for an interdigital transducer deposited on a particular material cut and orientation there is an optimum number of finger pairs in the transducer structure (N_{opt}) for which minimum conversion loss and maximum bandwidth are simultaneously obtained. For quartz N_{opt} is 19 which gives an optimum bandwidth of approximately 5% which means the center frequency will be 200 MHz for a 10 MHz bandwidth. Bismuth germanium oxide has an N_{opt} of 7.5 for an optimum bandwidth of 13.5% which gives a center frequency of approximately 80 MHz for a 10 MHz bandwidth. This lower center frequency is desirable since attenuation increases with frequency as also does dispersion introduced by the mass loading of the metal interdigital finger structures on the piezoelectric material. This a major reason for the choice of bismuth germanium oxide for the delay medium.

b. Size

The total time delay of the line is determined by the total number of taps (511) multiplied by the time between taps (100 nsec) plus a small extra time due to the input transducer and the spaced required to apply an acoustic absorber on the piezoelectric material outside the active line length. The actual physical length of the line is given by the total time delay multiplied by the acoustic surface wave velocity in the propagating direction. This velocity

is 3.15×10^5 cm/sec for YX quartz and 1.68×10^5 cm/sec for bismuth germanium oxide. The length of the piezoelectric bar required for the 511-tap line is approximately 6.5 inches for quartz and 3.5 inches for bismuth germanium oxide. Bismuth germanium oxide therefore allows a size reduction over quartz in addition to the lowering of the center frequency requirement. The smaller length for bismuth germanium oxide will also reduce in magnitude one problem associated with long delay lines--beam steering effects caused by a tendency for the acoustic energy to propagate down a particular crystallographic direction which may not be perpendicular to the interdigital transducer fingers.

c. Tap Placement Accuracy

For optimum device performance represented by all taps adding in phase at the required time interval the absolute placement of the individual taps must be highly accurate. For example, a tap placement error of 1 micron corresponds to a phase deviation of 18° from the required phase of the signal from that tap for an 80 MHz center frequency, and a phase deviation of 47° for a 200 MHz center frequency--another advantage for the lower frequency possible with bismuth germanium oxide. The main point however is that the photolithographic masks have to be fabricated on the highest accuracy mask making equipment available. This equipment is the OPTOMECHANISMS machine which is laser controlled and which is capable of giving an accuracy of tap placement of 3 microinches corresponding to a phase accuracy of less than 1° at 80 MHz. In addition, this accuracy is only achievable over a 4 inch by 4 inch area which means masks for bismuth germanium oxide can be made to this accuracy but masks for a quartz line would have to be made on less precise equipment with a maximum attainable accuracy of 2.5 microinches corresponding to a phase deviation of 60° at 200 MHz--an error which would lead to considerably less than optimum performance being obtained.

IV. SUMMARY

For the reasons cited above bismuth germanium oxide will be used for the delay medium and center frequency will be 80 MHz. The device to be delivered will be contained in a package approximately 4 in. x 3/4 in. x

3/4 in. excluding coaxial connector extensions. The chances of obtaining a tapped delay line with a minimum of 490 good taps out of 511 possible is considered excellent and if, as expected, lost taps occur in a random manner then time sidelobes greater than 30 dB down should be obtained. Dynamic range requirement of 40 dB without processing gain is not considered to be a problem since individual tap outputs will be designed for -40 dB with respect to the input signal and with a noise level at 10 MHz bandwidth of -104 dBm the line will have an input dynamic range between -64 dBm (40 dB above noise level) and +30 dBm (input transducer maximum input power level) for a better than 90 dB dynamic range after allowing for a 3 dB bidirectional loss in the input transducer and a few more dB in the matching circuit. The bandwidth of the correlation peak--when all taps add coherently--will be ~20 KHz. A shift in this peak with temperature over the 20 - 60°C range for YX quartz will be ~2.8 KHz/°C-- experimentally determined for 50-tap lines. No data is currently available on temperature coefficients for bismuth germanium oxide but experimental results will be available within the next two weeks as a result of evaluations in progress at North American Rockwell Science Center.

REFERENCES

1. S. T. Costanza, P. J. Hagon, L. A. MacNevin, "Analog Matched Filter Using Tapped Acoustic Surface Wave Delay Line," IEEE Transactions on Microwave Theory and Techniques, MTT-17, p. 1043 (November 1969).

2. J. H. Collins and P. J. Hagon, "Surface Wave Delay Lines Promise Filters for Radar, Flat Tubes for TV's, and Faster Computers," Electronics 43, pp. 110-122 (19 January 1970).

3. L. R. Adkins, T. W. Bristol, P. J. Hagon and A. J. Hughes, "Surface Acoustic Waves--Device Applications and Signal Routing Techniques for VHF and UHF," Microwave Journal 13, pp. 87-94 (March 1970).

Exhibit B. MULTIPLE TAP SURFACE WAVE DELAY LINE

The B&P estimate covers five fixed coded tapped delay lines of the type described in Exhibit A with specified codes and reflects a reduced price consistent with the rate of learning expected in the Exhibit A program.

Work on programmable tapped delay lines is in progress at Autonetics. This work is directed toward using microelectronic switching devices to electronically change the coding of a tapped delay line within a time equal to the total delay through the line - in this case within 51.1 μsec.

However, this program is in too early a stage to be considered for this estimate but the results will be available in about 6 - 12 months for future consideration.

APPENDIX M

LIT SURVEILLANCE COMPUTER PROGRAM

The computer program has four major blocks. There is one program P1 which takes the observed pulse times and compares them with predicted pulse times for all the aircraft with known PRP's and codes. This program outputs the identified pulses to the position calculation program P3 which computes aircraft position from the pulse times and sends these positions to the appropriate air traffic control centers. All unidentified pulses are sent to the deinterleaver program P2. These unidentified pulses will typically represent either new aircraft or extraneous pulses. The deinterleaver program will unscramble the various PRP's and send the data which it has identified to the position calculation program. Any pulses which are still not identified will be sent to the executive program P4 which will collect and display various statistics on unidentified pulses. The comparison program also sends data on missing pulses to the executive program. An aircraft will be considered dropped from the system whenever a number - say three in a row - of its predicted pulses are missing.

1. Pulse Comparison Program (P1)

In the steady state operation of the system the computer has a list of predicted pulse times T_1, T_2, ... Each pulse time has a pointer to a group of data about the aircraft. This data group would include the aircraft identification, the LIT code identifier, the nominal PRP, the current estimate of the observed PRP, the time interval between position calculations required, and a counter to indicate how long it has been since the last position update, the number (normally zero) of consecutive missing pulses which have occurred.

The computer also has a list of observed pulse times and LIT code identifiers. The times are denoted by t_1, t_2, ...

The predicted pulse times T_i will probably be kept in separate groups for separate LIT codes. The observed pulse times may be stored in the same way, or they might all be stored in time order with the code identifier attached to each time.

The basic operations are the following. Find the next observed pulse time t_i. For the code associated with this pulse, find the next predicted time T_j. If t_i is close to T_j, i.e., if $|t_i - T_j| < \varepsilon$, the computer decides that the pulse is associated with the aircraft whose predicted time is T_j. If it is time to compute the position of this aircraft, the computer sends the time t_i to the appropriate place in the block of data required by the position calculation program. If it is not time to compute this aircraft's position, the position calculation counter is simply updated. In either case, the estimate of PRP is updated. The new estimate P' is given by $P' = t_i - T_j + P$, where P was the last estimate of PRP. The next pulse for this aircraft will be expected at $\tau = t_i + P'$. The time τ is computed and merged into the sorted list of predicted pulse times. Conservatively, 50 instructions per pulse will handle the P1 computing task.

The above paragraphs describe a very simple algorithm for updating. The next predicted pulse time is computed by linearly extrapolating from the current and past pulse times. One might in fact use a more sophisticated algorithm, e.g., one might use a prediction based on a quadratic least squares fit to the last few pulse times. It is also likely that one would not merge the new predicted times into the sorted list one at a time as in the above algorithm. It would be more efficient to collect a buffer full of predicted pulse times and merge the entire buffer into the list at once. For purposes of computer sizing, however, the methods described above are probably sufficiently good.

The computer load for this program turns out to be fairly light. The program must compare each observed pulse with the corresponding predicted pulse and determine whether to associate the predicted pulse with the measured pulse. It must also check a counter to determine if a position is to be calculated. The number of instructions will depend on the particular computer involved, but it is probably safe to say that 30 instructions per pulse would do the job. With 10^5 pulses per second, this gives 12 MIPS to handle all of the aircraft from four satellites.

2. Deinterleaver Program (P2)

This program unscrambles the various PRP's which identify the aircraft. This is a heavy computer load and, consequently, a fairly lengthy discussion of this program will be given.

One algorithm for solving this problem and a rough estimate of the computer load have already been developed (Ref. M-1). In this section, a more careful estimate will be made. Also, a different algorithm will be described and the time required by this routine will be estimated. This will involve the worst case, namely, all of the pulses are unidentified. This would be the case, for example, after a computer failure in which all the aircraft identifications are lost.

The problem of identifying an aircraft from the pulse data is illustrated graphically in Figure M-1. The time axis is divided into one second segments and plotted with the segments stacked as in the figure. If one can draw a straight line (as illustrated) through a group of pulses, an aircraft has been identified.

Two different kinds of algorithms will be considered - one in which each pulse time is represented by a number in the computer, and one in which each pulse time is represented by a one in a string of zeros and ones.

2.1 First Algorithm

For the first algorithm, it was shown (Ref. M-1) that for each satellite the total number of instructions is about $\frac{1}{2} N^2/C$ instructions, where N is the total number of aircraft and C is the number of codes. This makes the assumption that it requires about 10 computer instructions to determine whether a particular pair of pulses are associated. The assumption was made that there were 10,000 PRP's instead of 32,500. This paragraph will address the problem of determining whether 10 instructions are enough.

The two pulse times are denoted by t_i and t_j. Figure M-2 illustrates the algorithm graphically. The program must compute $2t_i - t_j = T$. It must then find out whether the predicted pulse time T is near any observed pulse time (3 instructions). The number of operations to do this depends on how the table of pulse times is organized. It is a good idea to divide the time axis into discrete times with step size H and then list the indices of the pulses which immediately follow each discrete time.

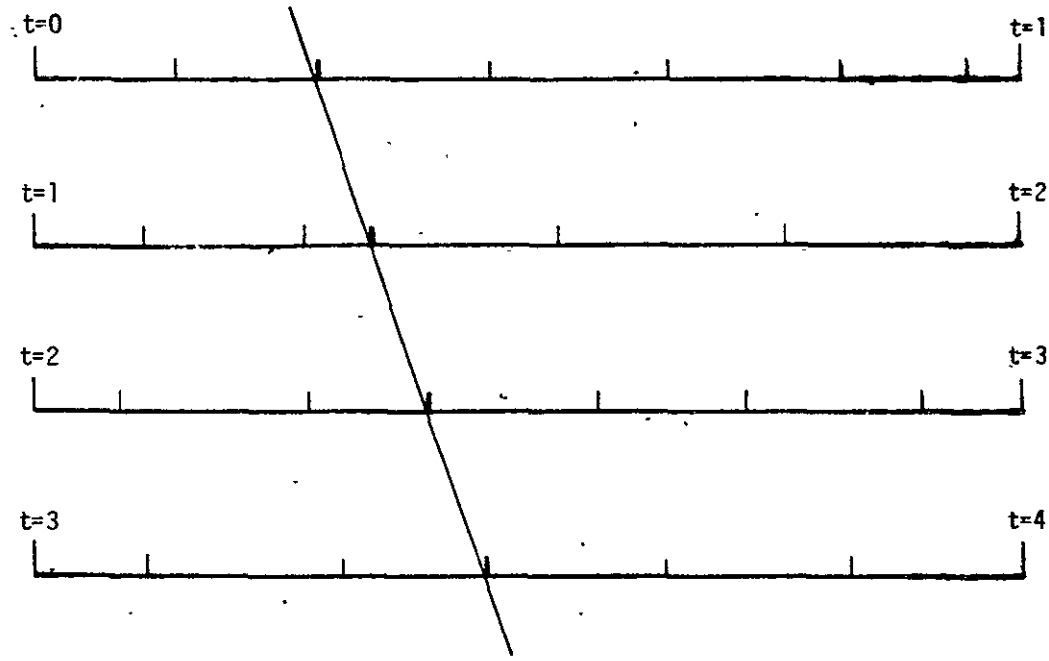

Figure M-1. Identification of PRP

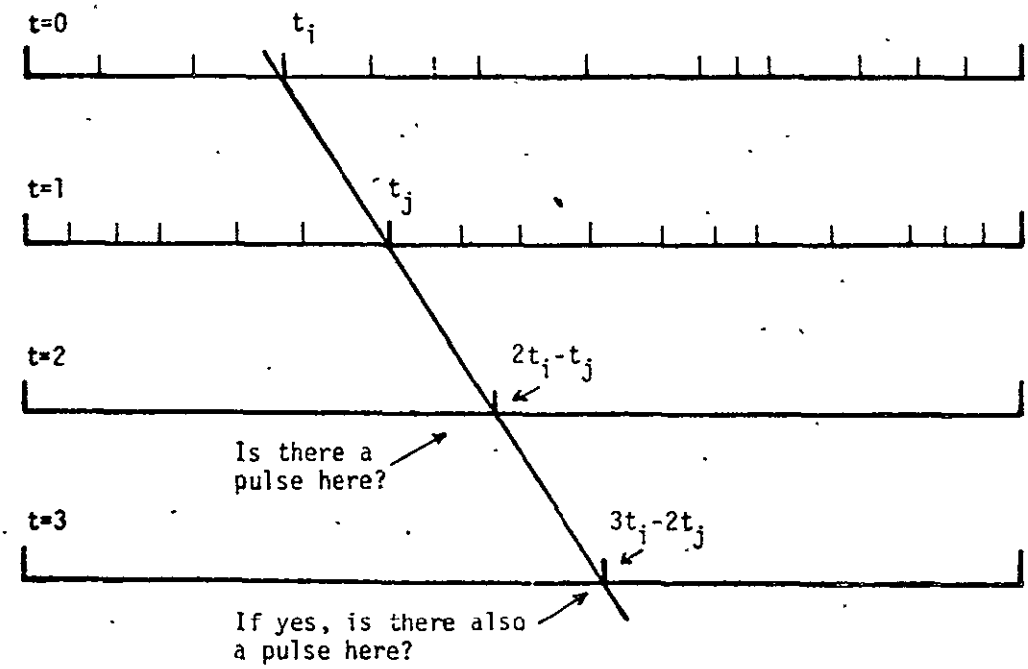

Aircraft has been identified if N equally spaced pulses have been identified.

Figure M-2. PRP Sort Algorithm

That is, a set of indices j(k) is stored such that $t_{j(k)}$ is the pulse which immediately follows time kH. The program computes T/H and throws away the fractional part, i.e., K = [T/H]. (This can be done particularly fast if H is an integral power of 2.) The program then compares T with each of the times $t_{j(k)}$, $t_{j(k)+1}$, ..., $t_{j(k+1)-1}$; i.e., the program looks at each of the times in an interval of size H. There are N/C pulses in an interval of one second and hence an average of HN/C pulses in an interval of size H. Hence, on the average, the time T must be compared with about HN/C pulses. If one would like to have an average of only about one pulse to look at, one would choose H = C/N. This cuts down on the computer time at the expense of computer storage since it requires 1/H words of data to store the indices of j(k) for one second of data. If H = C/N, then it would usually be only necessary to compare T with $t_j(k)$, and it would require about 6 computer instructions to compute k, find j(k), find $t_j(k)$, and compare T with $t_j(k)$. (The exact number of instructions depends on the instruction set of the particular computer used.) Now, if T does not compare with any of the observed pulse times, the particular pair (t_i, t_j) is finished.

If it is necessary to look at the next predicted time $(3/2)\ T - 1/2t_i$, the process must be repeated. If we assume that the process must be repeated about three times on the average, then the total number of computer operations would be about 30 for each pair (t_i, t_j) of pulse times.

If we use 30 instructions per pair instead of 10, consider 32,000 PRP's instead of 10,000, and consider 6 satellites, the total instruction count is about 27N/C instructions. In the steady state of operation, the computer load is light. For example, suppose that new aircraft appear at a rate of 100 aircraft per second. The program will collect the data for a certain time, say, 5 seconds, before starting computations to identify the aircraft. It then has N = 500 aircraft. If C = 16, the computations can be done in about 4.2×10^5 instructions. Since five seconds can be used, the computing load is only .1 MIPS.

There would be, of course, a very significant load if all of the aircraft had to be identified at once. As mentioned earlier, this would have to be performed in the event of a total but temporary computational or satellite downlink outage.

With $N = 10^5$, $C = 16$, there are about 5.6×10^9 instructions. A Computer operating at 20 MIPS could identify all the aircraft in 840 seconds, for example. Note that this estimate is conservative and could be reduced by using certain tricks. For example, once the PRP's have been identified for one satellite it is not necessary to completely repeat the process for the other satellites. The conservative estimate does demonstrate the feasibility of the process.

In the worst case, it appears that the above algorithm would impose a large computer load. This is one of the reasons for examining the alternate algorithm in which pulse times are represented by a string of zeros and ones. The advantage of this algorithm is that the computer time is proportional to N instead of N^2, and it is to be preferred for very large values of N. The remainder of this section describes the alternate algorithm.

2.2 Second Algorithm

Instead of representing the pulse times as numbers, the time axis is divided into small steps of size h and a long binary word is formed to indicate which steps includes pulses as shown in Figure M-3. The basic idea is to eliminate arithmetic operations like adding and subtracting pulse times and use instead logical operations, like boolean sums and products. These operations are performed extremely fast on a computer.

A "word" will be defined as a sequence of zeros and ones in the computer. These words might be very long, say 10^6 bits. Most computers can only do operations directly on smaller units, of length 48 bits, for example. These shorter units will be called "computer words." Thus a "word" may consist of a string of thousands of "computer words." If a word is denoted by ω, the individual bits will be denoted by ω_j (i.e., ω_7 is the 7th bit in the word ω).

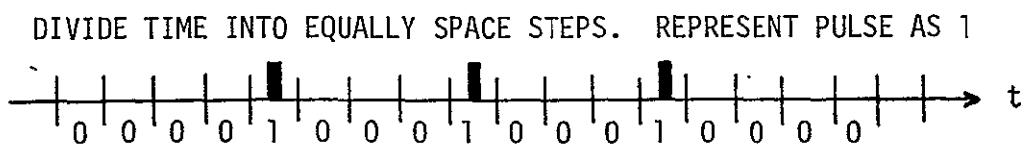

Figure M-3. Second Algorithm Concept

A convenient reference time is chosen and called t = 0. A step size h is chosen. For sizing purposes we will take $h = 10^{-6}$ (i.e., time is divided into microsecond units). Let $N = \frac{1}{h}$. Then N is the number of steps in one second. The data word is denoted by ω and is defined by

$$\omega_j = \begin{cases} 1, \text{ if there is a pulse in the interval } (jh - \frac{h}{2},\ jh + \frac{h}{2}) \\ 0, \text{ otherwise .} \end{cases}$$

Note that ω is 10^7 bits long if 10 seconds of data is kept. If we consider a computer with 100 bit "computer words", this is 10^5 computer words of storage. We assume that the data is in high speed storage (e.g., core storage)

The computer has a list of possible PRP's in its memory. If there is no a priori information, this list contains all possible values, namely all values $P = 1 + k \cdot 10^{-5}$, where $k = 0, 1, 2, \cdots, 32{,}000$. Let S be the set of possible nominal PRP values (assumed to be integral multiplies of h). There is a maximum error associated with each PRP, and we assume that this error is εh. In other words P is a possible value for a PRP if and only if

$$|P - P^*| < \varepsilon h$$

where P* belongs to S. The value ε is taken to be an integer. (Typically $\varepsilon = 4$)

Two pulses are said to be "associated" if they come from the same aircraft.

The idea behind the algorithm is illustrated in Figure M-4. The main problem is that one does not know exactly where the pulse lies within an interval of size δ. As shown in the figure, there are sometimes three possible intervals in which the following pulse can occur. When the possible locations of the next pulses are known, a "mask" is formed and compared with the observed data to see if a match is found. The following discussion concerns the construction and use of this mask.

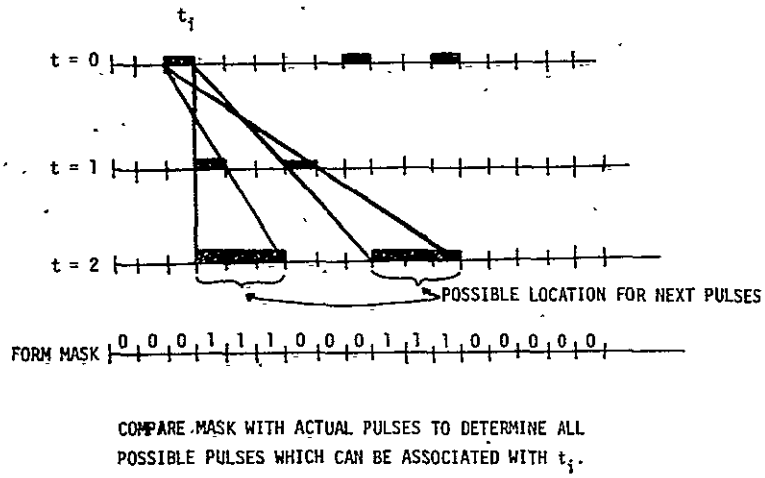

Figure M-4. Binary Word Algorithm

The program starts by finding the first pulse in the sequence. Suppose that this pulse is indicated by a one in bit k: i.e., the first pulse t_o is in the interval $(kh - \frac{h}{2}, kh + \frac{h}{2})$. This is called the reference pulse.

The problem is to find the pulses which are associated with the reference pulse.

From the set of possible PRP's, the computer forms a "mask". This is a word ϕ defined by

$$\phi_i = \begin{cases} 1, \text{ if there are any possible PRP's in the interval} \\ \quad (1 + (i-1)h,\ 1 + (i+1)h) \\ 0, \text{ otherwise .} \end{cases}$$

Now consider the word ψ which is a part of the data word ω and is defined by

$$\psi_j = \omega_{j+N+k},$$

(In other words, ψ, will cover the data starting exactly one second after the reference pulse and continuing for the period Kh which is 0.1 sec.)

The logical product of two words ψ and ϕ is denoted by $\psi^*\phi$. (That is, $\psi^*\phi$ is a word whose k^{th} bit is one if and only if both ψ and ϕ have a one as their k^{th} bits.)

The computer takes the logical product of ψ and ϕ and places the result into a word $\bar{\omega}$: $\psi * \phi \rightarrow \bar{\omega}$. Then $\bar{\omega}$ has the property that a one bit in the j^{th} position of $\bar{\omega}$ indicates that there is a pulse in the interval $((k+j)h + 1 - \frac{h}{2}, (k+j)h + 1 + \frac{h}{2}))$ and that pulse is a candidate for association with the reference pulse. (Proof: A one in the j^{th} bit of ψ indicates that there is a one in the $(j + N + k)^{th}$ bit of ω. This means that there is a pulse at some time T in the interval $(1 + (j+k)h - \frac{h}{2}, 1 + (j+k)h + \frac{h}{2})$. If this pulse can be associated with the reference pulse at time t_o which lies in the interval $(kh - \frac{h}{2}, kh + \frac{h}{2})$ then the PRP is $T - t_o$ and must lie in the interval $(1 + jh - h, 1 + jh + h)$. This is a possible PRP if $\phi_j = 1$.)

If there is only a single one bit in the word $\bar{\omega}$, the PRP for the reference pulse has been identified. Generally this will not happen and it is necessary to look at subsequent times.

Suppose that a set of candidates for association with the reference pulse have been identified. The pulses just identified are R periods after the first pulse. That is, each candidate pulse time t is related to the initial pulse time t_o by $t = t_o + RP$, where P is a possible value of a PRP. To start with, $R = 1$. These candidate pulses are represented by a word $\bar{\omega}$. If $\bar{\omega}_j = 1$, then there is a candidate pulse in the interval $(R + (j+k)h + \frac{h}{2}, R + (j+k)h - \frac{h}{2})$, and that pulse is a candidate for association with the reference pulse.

From the word $\bar{\omega}$, a mask word ϕ is formed as follows. If $\bar{\omega}_i = 1$ and i is a multiple of R, set $\phi_q = \phi_{q+1} = \phi_{q+2} = 1$, where $q = \frac{i}{R} + i - 1$. If $\bar{\omega}_i = 1$ and i is not a multiple of R, set $\phi_q = \phi_{q+1} = 1$, where $q = [\frac{i}{R}] + i$ Any bit of ϕ not set to one is defined to be zero. Now let ψ be the word defined by

$$\psi_i = \omega_{j+k+(R+1)N}.$$

Then let

$$\phi * \psi = \gamma .$$

If this new word γ has only one bit, the PRP associated with the reference pulse has been identified. Otherwise, we let $R + 1 \rightarrow R$, $\gamma \rightarrow \bar{\omega}$, and try again.

2.3 Derivation of the Method.

The idea behind the method is simple. From each candidate pulses in period R, the idea is to compute the predicted position of the pulse which appears in period R + 1 and see whether an observed pulse is at the predicted time. The details are complicated by the fact that the exact times are not known - only the intervals which contain pulses are known.

The initial pulse satisfies

$$t_o = kh + \varepsilon_1 h$$

where $|\varepsilon_1| < h/2$. If $\bar{\omega}_j = 1$, then there is a candidate pulse τ which satisfies

$$\tau = (k + RN + j)\ h + \varepsilon_2 h,$$

where $|\varepsilon_2| < h/2$. If the pulses at t_o and τ come from the same aircraft, then the next pulse time for this aircraft will be at time t, where

$$t = t_o + \frac{R+1}{R}(\tau - t_o)$$

$$= \left[k + (R+1)\ N + \frac{R+1}{R}\ j\right] h + Eh.$$

Since it is known which intervals the times t_o and τ belong to, the problem is to determine which interval t belongs to. The solution is not unique; it will be found to be in one of two or three intervals depending on whether j is a multiple of R.

Consider the case where j is a multiple of R, say j = R. In this case, t becomes

$$t = (k + (R+1)N + (R+1)i)h + Eh$$

$$= (k + (R+1)N + q + 1)h + Eh$$

We will show that t must be in one of the three intervals I_q, I_{q+1}, I_{q+2}, where I_q is defined to be the interval

$$I_q = \left(\left[k + (R+1)N + q - \frac{1}{2}\right] h,\ \left[k + (R+1)N + q + \frac{1}{2}\right] h\right).$$

and where q is defined by $q = j + k - 1 = j + \frac{j}{R} - 1$.

This means that we must show that t satisfies

$$(k + (R+1)N + q)\, h - \frac{h}{2} \le t \le (k + (R+1)N + q + 2)h + \frac{h}{2} .$$

First note that

$$|E| = \left|\frac{R+1}{R}\,\varepsilon_2 - \frac{1}{R}\,\varepsilon_1\right| \le \frac{1}{2} + \frac{1}{R}$$

Then

$$1 + E \ge \frac{1}{2} - \frac{1}{R} \ge -\frac{1}{2}$$

and

$$E - 1 \le -\frac{1}{2} + \frac{1}{R} \le \frac{1}{2} .$$

Hence

$$t = (k + (R+1)\, N + q)\, h + (1 + E)\, h$$

$$\ge (k + (R+1) + q)\, h - \frac{h}{2} ,$$

and

$$t = (k + (R+1)\, N + q + 2)\, h + (E - 1)\, h$$

$$\le (k + (R+1)\, N + q + 2)\, h + \frac{h}{2} .$$

Thus the next possible candidate time must lie in one of the intervals I_q, I_{q+1}, I_{q+2} . This is the reason for setting $\phi_q = \phi_{q+1} = \phi_{q+2} = 1$ in the algorithm.

In case j is not a multiple of R, one can write $j = i\,R + m$, where $1 \le m \le R - 1$. In this case the algorithm sets $q = j + i + (R+1)\,i + m$. Then

$$t = h(k + (R+1)N + (\frac{R+1}{R})(i\,R + m)) + Eh$$

$$= h(k + (R+1)N + (R+1)\,i + m) + (\frac{m}{R} + E)h$$

$$= h(k + (R+1)N + q) + (\frac{m}{R} + E)h$$

It must be shown that t is in one of the intervals I_q or I_{q+1}. That is, it must be shown that

$$(k + (R+1)N + q)\,h - \frac{h}{2} \le t \le (k + (R+1)N + q + 1)\,h + \frac{h}{2}\,.$$

Note that

$$\frac{m}{R} + E \ge \frac{1}{R} - \frac{1}{R} - \frac{1}{2} = -\frac{1}{2}$$

and

$$\frac{m}{R} + E - 1 \le \frac{R-1}{R} + \frac{1}{2} + \frac{1}{R} - 1 = \frac{1}{2}\,.$$

Hence

$$t = (k + (R+1)N + q)\,h + (\frac{m}{R} + E)\,h$$

$$\ge (k + (R+1)N + q)\,h - \frac{h}{2}$$

and

$$t = (k + (R+1)N + q + 1)\,h + (\frac{m}{R} + E - 1)\,h$$

$$\le (k + (R+1)N + q + 1)\,h + \frac{h}{2}\,.$$

This shows that t must lie in one of the intervals I_q or I_{q+1}, which is why the algorithm sets $\phi_q = \phi_{q+1} = 1$ in this case.

To estimate the computer operations for this algorithm, consider a computer with a word size W. The time axis is divided with a step size of h. The basic operation involves taking a 'mask' word out of core, performing a logical product of this word with a portion of the pulse data word, and computing a new mask word. The basic operations (e.g., logical sum and product) are extremely simple and fast. The major source of the computer time will be taken up by the simple process of taking the data from core and storing it back in core.

The process involves, for each pulse in the first 1.31255 seconds, stepping through a number of periods until the pulse has been identified or until it is decided to list it as unidentified. Suppose that it requires five steps on the average to identify a pulse. Then the following basic step is performed for R = 1,2,3,4,5. A mask is extracted from core. The mask represents .3R seconds of time, which is described by .3R/h bits, or .3R/hW words. A portion of the data is extracted, the logical operations are performed, and the new mask stored back. There are three instructions involved. If the machine has a speed of p MIPs, three instructions are performed in $\frac{3}{p} \times 10^{-6}$ seconds. For a particular pulse at a particular step, the time required is $.9 \times 10^{-6}/$ hWp seconds. Since the operation is done for R = 1,2,3,4,5, the total time is 13.5×10^{-6}hWp for each pulse. Since there are 4N pulses for four satellites, the total time is

$$\frac{54 \times 10^{-6}}{hWp}.$$

With $h = 10^{-6}$, $N = 10^{5}$, W - 100, and p = 20, the total time is 3000 seconds.

3. Position Determination Program (P3)

This program will calculate the position of the aircraft from the pulse times. The method of calculation is a least squares solution if data from more than four satellites are used.

Let x, y, y_2, y_3, y_4 represent the position vectors of the aircraft and the four satellites in any convenient rectangular coordinate system. A pulse is sent from the aircraft at time T, received at the satellites at time t_j and received at the ground at time j; j = 1,2,3,4.

In the computer sizing estimates which follow an "operation" consists of an arithmetic operation (add, divide, etc.). The estimates are based on the assumption that measurements from 6 satellites are available.

The time τ_j are first converted to times t_j. If the range R_j to satellite j is known, this involves computing $t_j = \tau_j - R_j/c$. (12 operations).

Next the position vector x is computed from four of the times t_j. The steps in the process are as follows.

1. Form the matrix A with rows z_1^T, z_2^T, z_3^T
   where $Z_j = Y_{j+1} - Y_1$ (9 operations)
   Form the vector C with components $C_j = (t_{j+1} - t_1)$; j = 1,2,3. (3 operations). Form the vector b with components
   $b_j = 1/2\ (|Z_j|^2 - C_j^2)$ (24 operations)
2. Solve the equations A p = b and A q = c for p and q.
   If Gaussian elimination is used, this requires 43 operations.
3. Form $A = |q|^2 - 1$, $B = p \cdot q$, and $C = |p|^2$.
   (16 operations. Solve the equation $A\rho^2 + 2\ B\ \rho + C = 0$ for ρ (6 operations).
4. Compute the position vector $X = Y_1 + p + \rho q$ (9 operations).

If the measurements from only four satellites are available, the solution is finished. If data is available from five or six satellites, a least squares refinement is performed as follows.

The basic equations of condition are

$$|y_j - X| - c(t_j - T) = 0;\ j = 1, \ldots, 6.$$

These equations will be solved in the least squares sense for the four unknowns (X, T).

Let (X_o, T_o) be a first guess at the solution. Linearizing the equations of condition about X_o gives

$$\frac{(y_j - x_o) \cdot \delta x}{|y_j - x_o|} + c\delta T = C(t_j - T_o) - |y_i - x_o| + \text{higher order terms}$$

where $\delta x = x - x_o$. These linear equations are solved in the least squares sense for δx, δT. The operations required are the following.

a) Form the 6 x 4 matrix A with rows a_j given by

$$a_j = \left(\frac{(y_j - x_o)^T}{|y_j - x_o|} , c \right)$$

Forming A requires 12 operations per row, or 72 operations.

b) Form the residual vector b with components

$$b_j = c(t_j - T_o) - |y_j - x_o| .$$

Forming b requires 18 operations

c) Form the matrix $S + A^T A$ and $A^T b$. The matrix S is a constant 4 x 4 (usually diagonal) matrix which is used to reflect a priori data about the solution. This operation requires 158 operations.

d) Solve the equation

$$(S + A^T A)\ \psi = A^T b$$

for the vector ψ. If Gaussian elimination is used, this requires 62 operations.

e) Add the first three components of ψ to x_o. Add the last component to T_o (3 operations). The result is an improved approximation to the solution for x and T.

It is sometimes necessary in least squares problems to iterate (i.e., replace x_o and T_o by the improved values and repeat the above computations). Experience with this problem indicates that the equations are very linear and that no iterations are necessary. The total number of operations for the least squares solution is 313.

The total number of computer operations is 525. Generally, the number of instructions is about twice this number. The exact number of instructions depends on the particular set of instructions available on the computer; e.g., if an "add" and "store" are done in two instructions. A reasonable estimate is then 1,000 computer instructions to calculate the position vector.

The number of operations can be somewhat reduced by using the same matrix $(A^TA + S)^{-1}$ for all the aircraft in the vicinity of a particular point. It would be possible, for example, to divide the airspace into a number of distinct regions, compute a matrix for each region and use that matrix for any aircraft within the region. Before doing this it would be necessary to make a careful study of the errors involved in the process.

4. Executive Program (P4)

The executive program has the task of deciding what to do about unidentified pulses and missing pulses. The unidentified pulses are those which have not been associated with any aircraft, even after program P2 has attempted to match a PRP to the aircraft. The program will display the number and distribution of unidentified pulses so that the operator will know whether an unusual number of unidentified pulses are in the system. Normally there will be a small residual of unidentified pulses.

When a pulse is missing for three successive periods, the aircraft is probably no longer in the system. The code and PRP of the aircraft is then dropped from the list of expected codes and PRP's and a notice of termination is sent to the center(s) or terminal(s) which received the last position report.

The executive program also performs some bookkeeping functions on the list of aircraft identifications, etc. Because of the miscellaneous nature of the functions of this program, it is not possible to give a very good estimate of its running time. Although such programs tend to "grow" in scope, solving a number of additional tasks, it is probably safe to say that the running time remains small compared to the running time of the remainder of the program.

5. Reference

M-1 Proposal to study the applications of satellites to Communications, Navigation and Surveillance for Aircraft Operating over the Contiguous United States, Technical Proposal, 14671.000, 25 October 1969, Prepared for NASA Electronics Research Center under RFP No. ERC/R&D PS-066.

SATELLITE CNS SYSTEM - REFERENCE DATA

COMMUNICATIONS

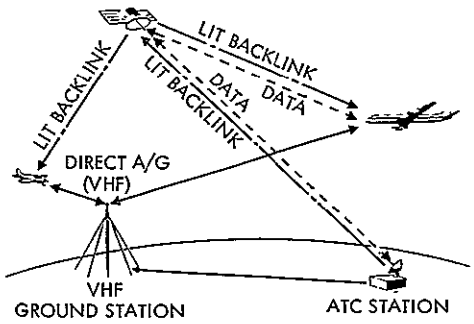

PARAMETER	DATA	LIT BACKLINK
CHANNELS	2/SAT.	2
CAPACITY/CH	1200 BPS FULL DUPLEX	100 MESSAGES/ SEC
CARRIER FREQ	5140-5170 MHz(Gnd) 950-980 MHz(A/C)	5050 MHz UP 940 MHz DOWN
BANDWIDTH	100 KHz/SAT	500 KHz

NAVIGATION

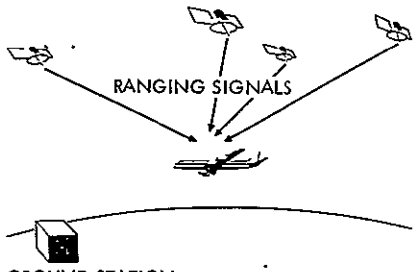

PARAMETER	RANGING
CHANNELS	1
CAPACITY	UNLIMITED
CARRIER FREQ	1550 MHz
BANDWIDTH	2 MHz

SURVEILLANCE

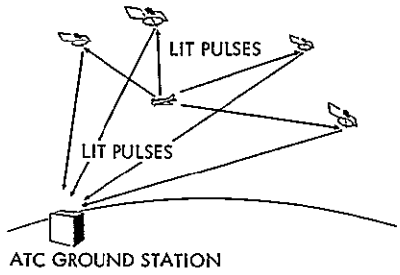

PARAMETER	RANGING
CHANNELS	2
CAPACITY/CH	50,000 UPDATES/
CARRIER FREQ	912.5 MHz UP 5087.5 MHz DOWN
BANDWIDTH	50 MHz

NOTE SAME SATELLITES FOR ALL THREE FUNCTIONS. CARRIER FREQUENCIES ARE TENTATIVE.

SYSTEM DATA

6-SATELLITE 16° X-CONFIGURATION
~200 FT ACCURACY (1σ ALT, HORIZONTAL CEP)
PROBABILITY OF OUTAGE, 30 YR LIFE ≅ 3.3%

SATELLITE DATA

PAYLOAD 2 LIT	100 W	20 LB
2 LIT BACKLINK	46 W	20 LB
1 NAVSTAR	25 W	25 LB
2 DATA LINK	60 W	20 LB
OTHER SATELLITE FUNCTIONS	100 W	637 (1146) LB
	331 W	722 (1231) LB

DESIGN LIFE/MTTF 7 YEARS/9.8 TO 12.5 YEARS
LAUNCH VEHICLE THOR DELTA 904

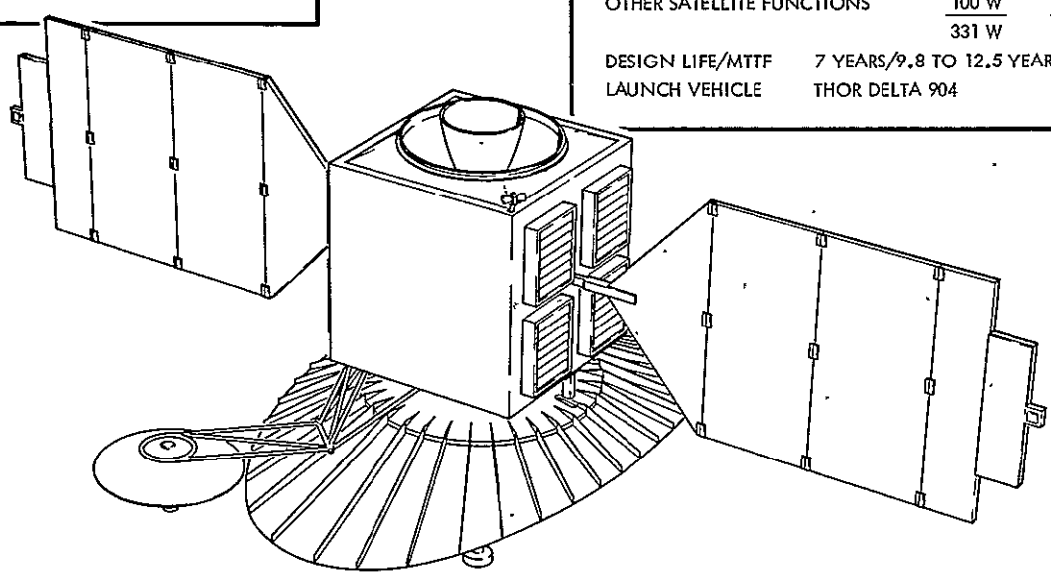

LIT SYSTEM CAPACITY

ATCAC AIRCRAFT POPULATION FORECAST
1995 - 54,000 PEAK AIRBORNE
525,000 REGISTERED

LIT CHANNEL CAPACITY (25 MHz BAND)
50,000 AIRCRAFT POSITION UPDATES/SEC
500,000 AIRCRAFT ID'S ASSIGNABLE *
* FROM PRODUCT OF 31,255 PRP'S AND 16 BIPHASE CODES

LIT MODULATION PARAMETERS

TRANSMITTED PULSE WIDTH	51.1 μSEC
PULSE REPETITION PERIOD (PRP)	BETWEEN 1.0 AND 1.31 SEC/PULSE
NUMBER OF DISCRETE PRP'S	31,255 - SPACED 10 μSEC APART
BIPHASE CODE LENGTH	511 BITS
BIT LENGTH	0.1 μSEC (COMPRESSED PULSE WIDTH)
NUMBER OF BIPHASE CODES	16